Onset of strongly non-linear energetic particle dynamics at ASDEX Upgrade

Ph. Lauber with input from
I. Chavdarovski, A. Biancalani, M. Schneller, G. Fu,
A. Bierwage, H. Wang, F. Palermo, P. Poloskei, G. Papp, M. Maraschek
and ASDEX Upgrade team

off-axis drive, high beam energy (93keV)

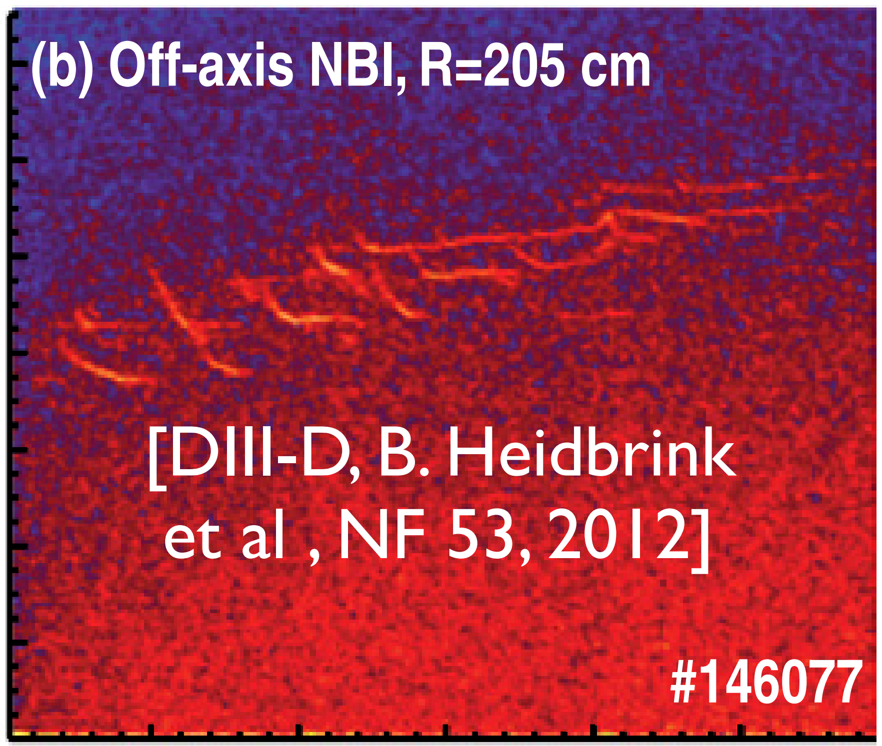

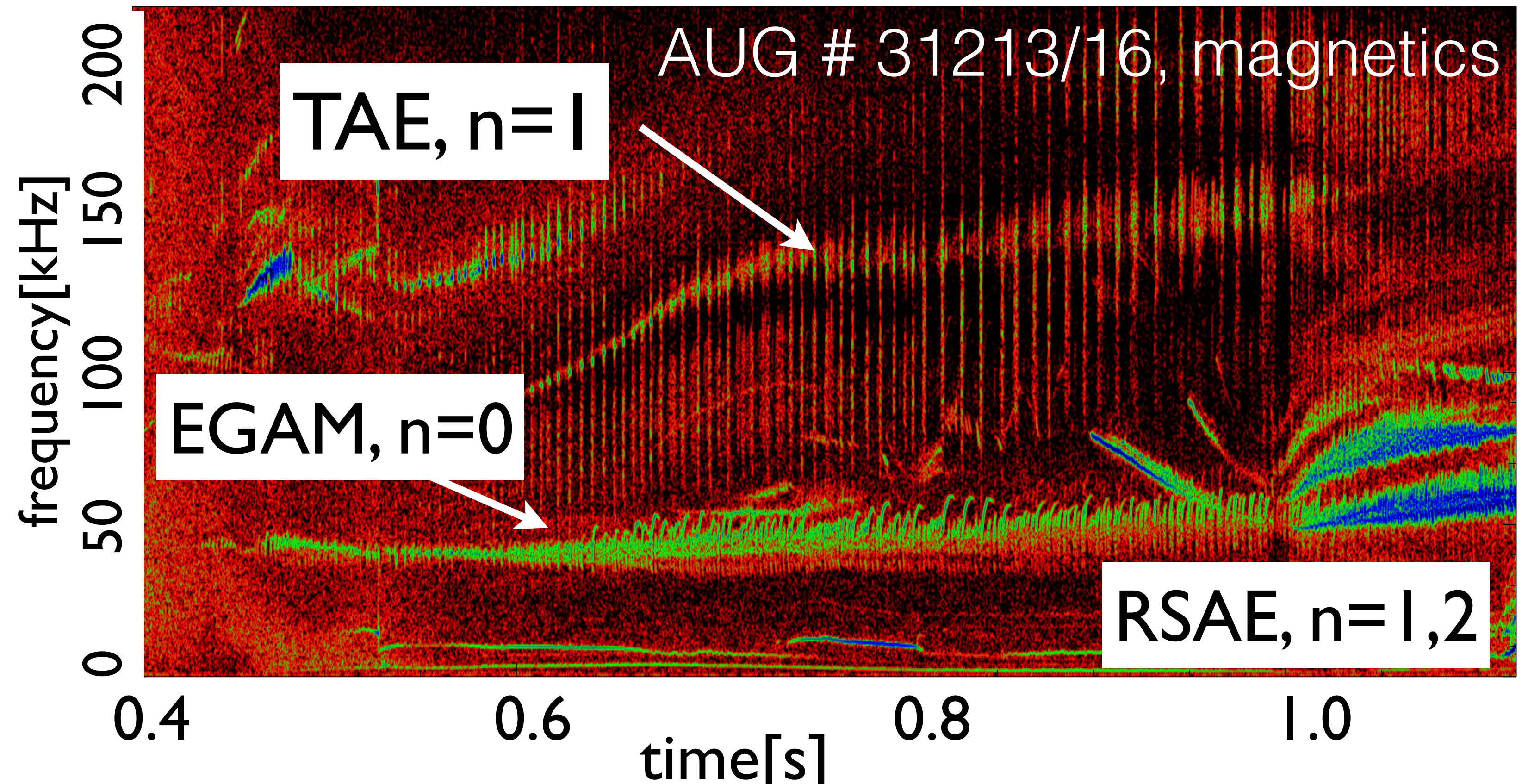

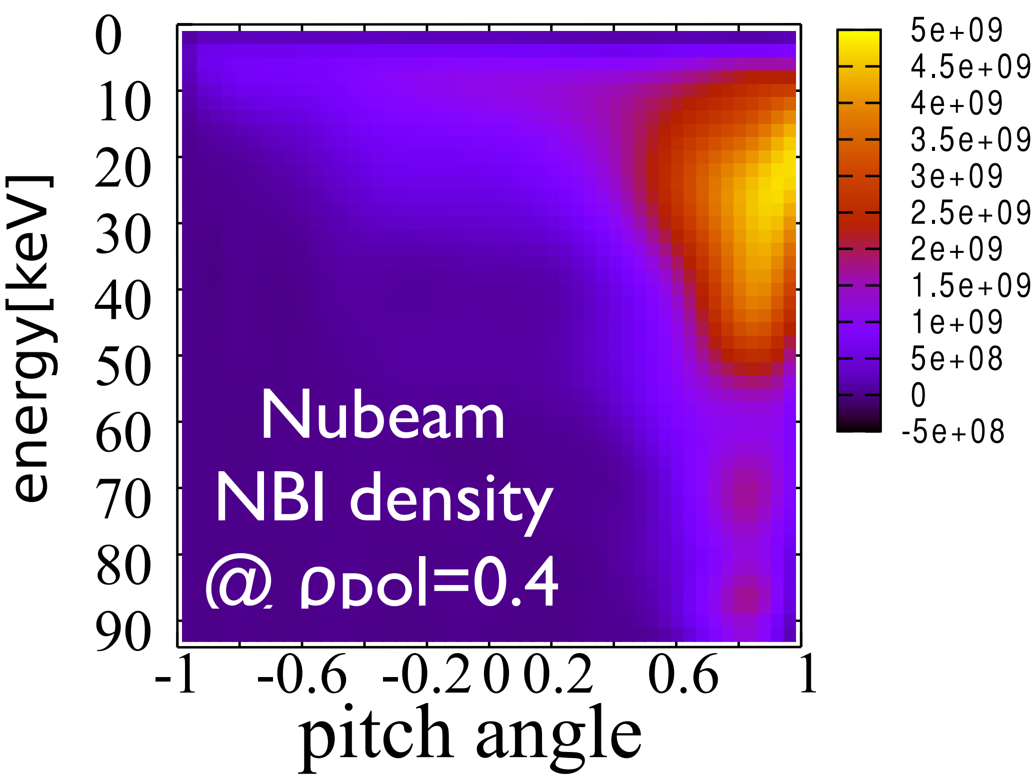

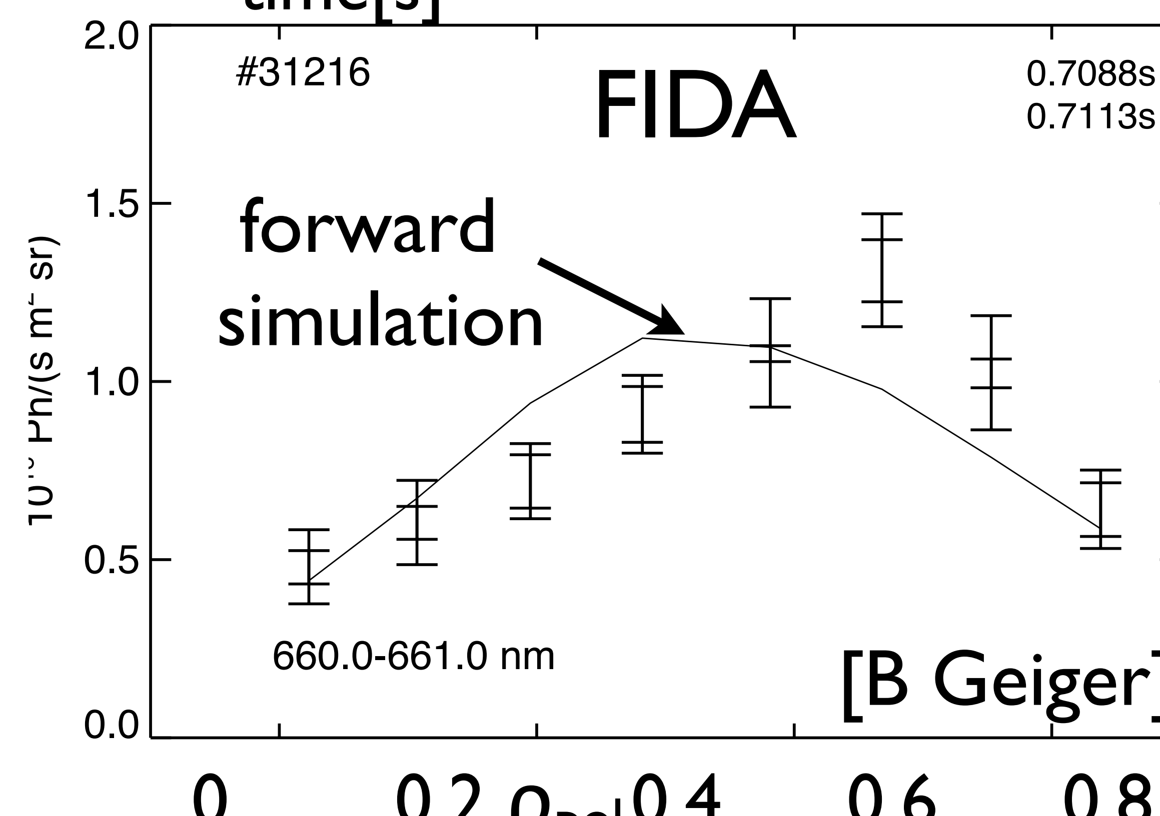

why co-NBI drive EGAMs at AUG and not at DIII-D?

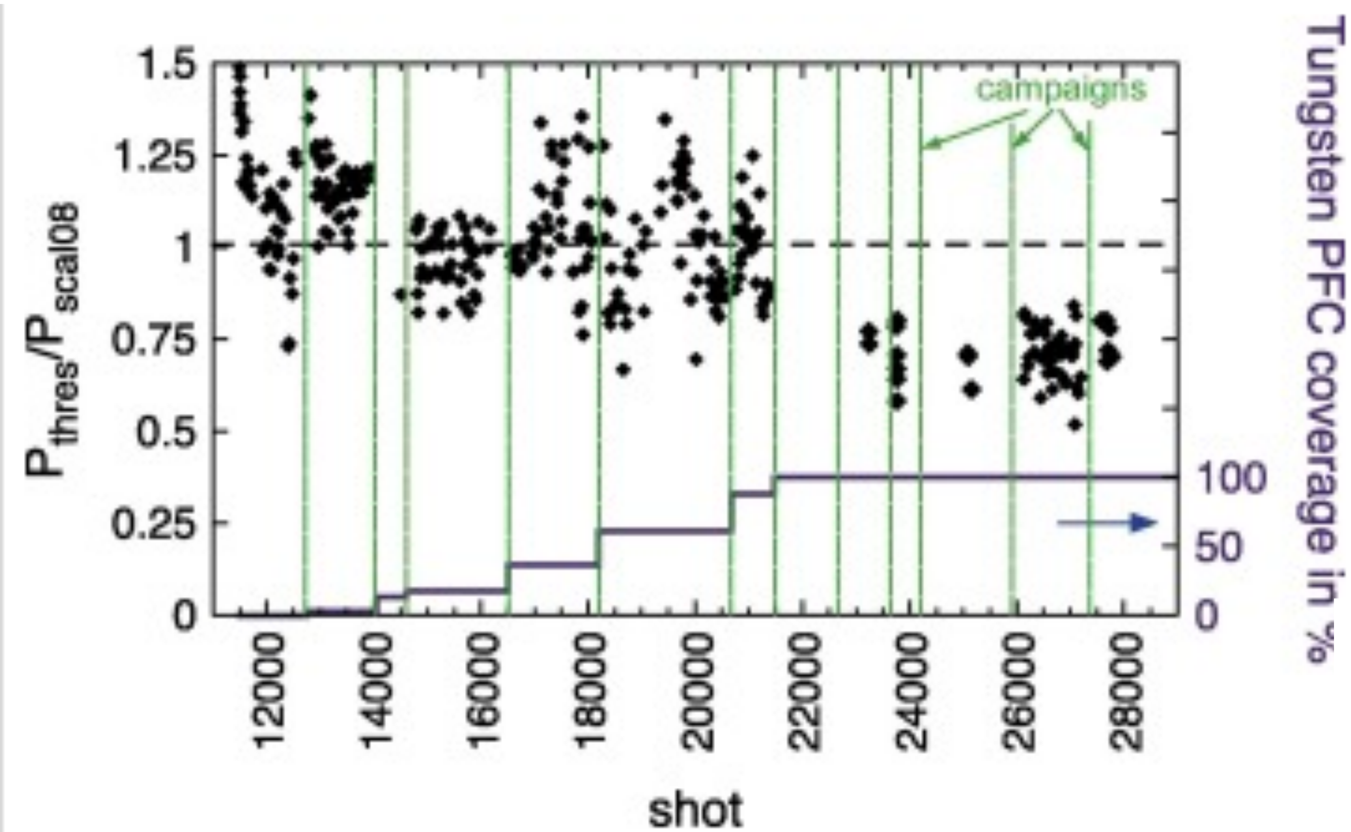

first EGAMs at AUG: #20492: July 2005

radially localised between 0.1-0.5ρ_{pol}

co-NBI, off axis

frequency close to GAM continuum frequency!

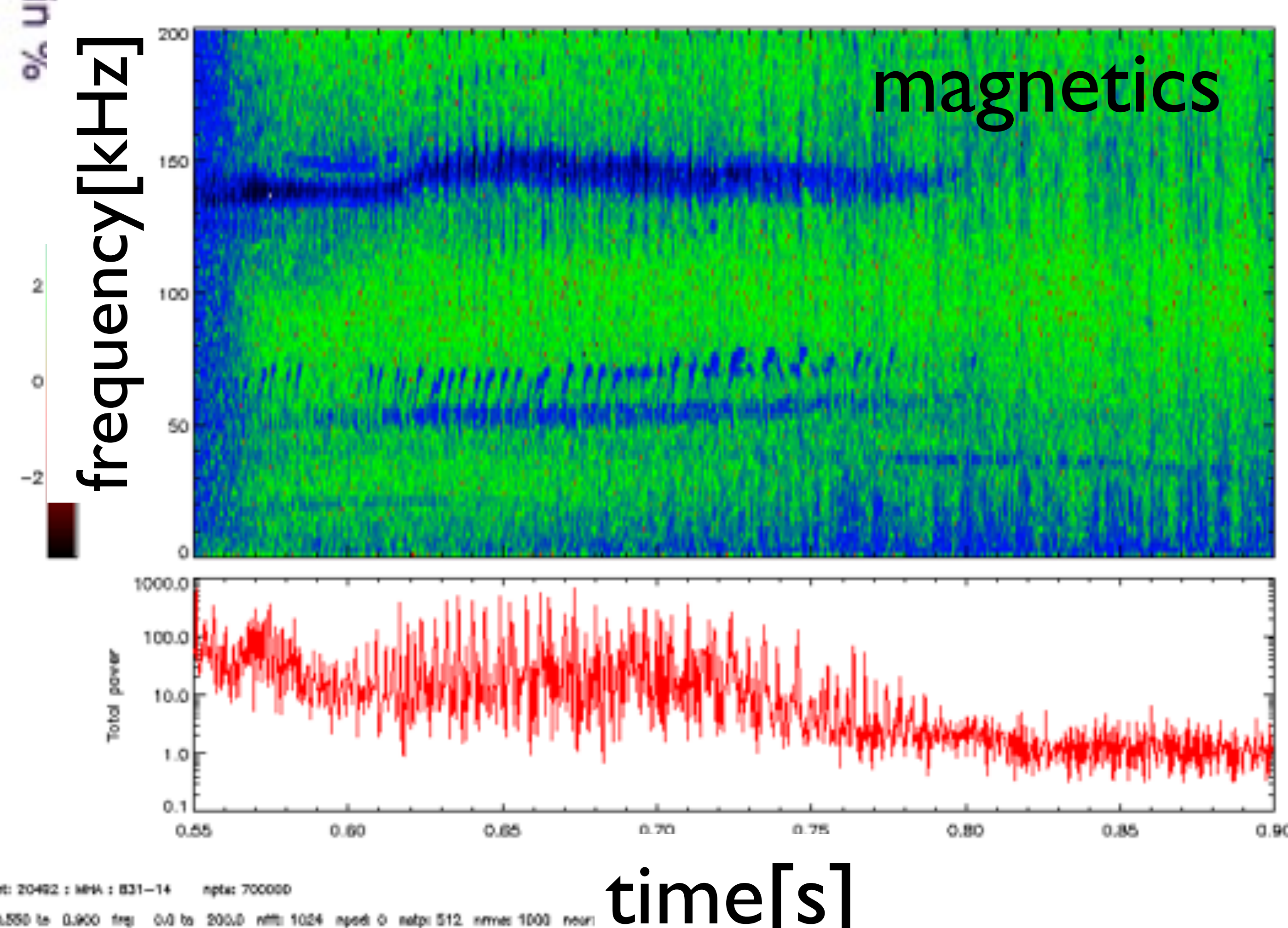

other devices:

Observation and explanation of the JET n=0 chirping mode (ICRF) [Boswell,Berk, Oct 2006]

Intense Geodesic Acoustic-like Modes Driven by Suprathermal Ions in a Tokamak Plasma (DIII-D, counter NBI)
R. Nazikian et al PRL 2008

central Te for several EGAM discharges

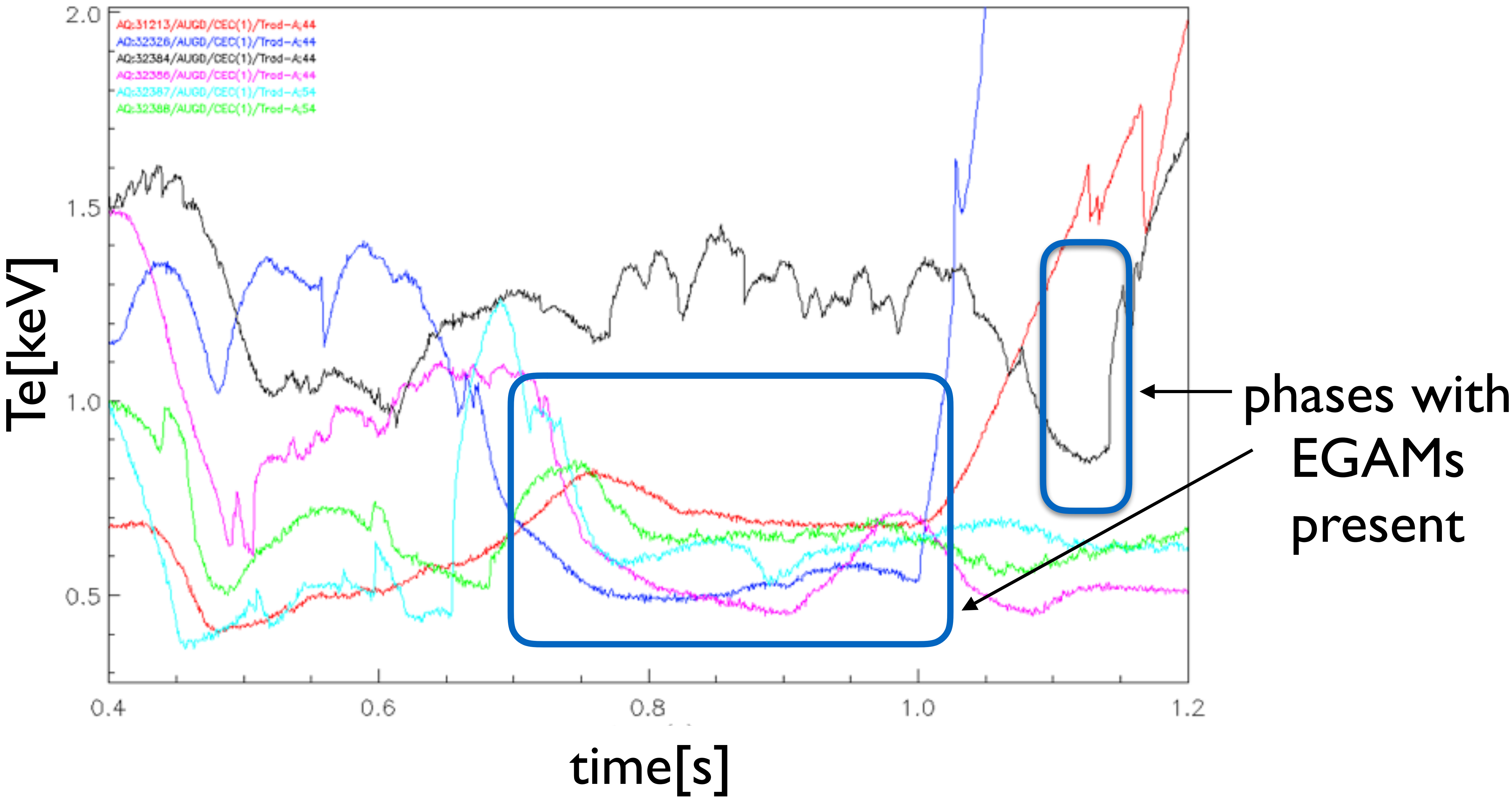

#32326(NB only, EGAMs, AEs) vs #32328 (NB+ECRH, no EGAMs, AEs) : profiles

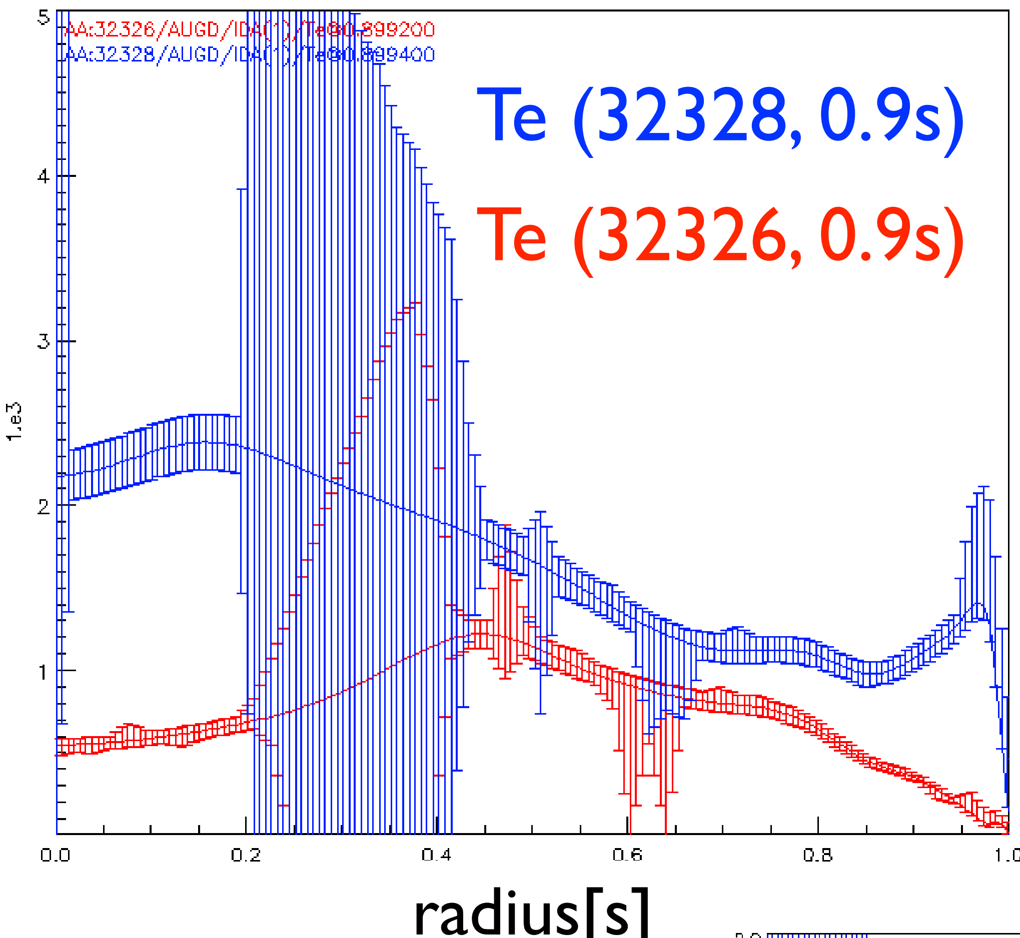

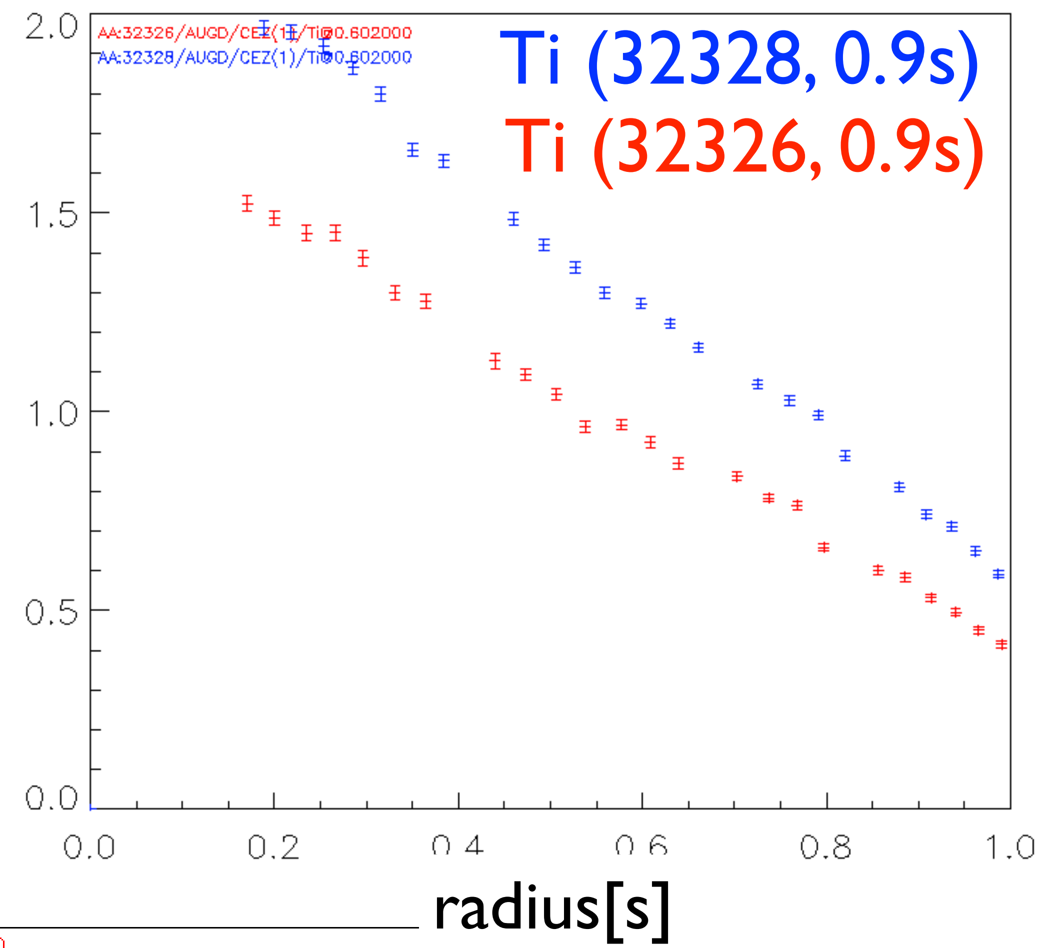

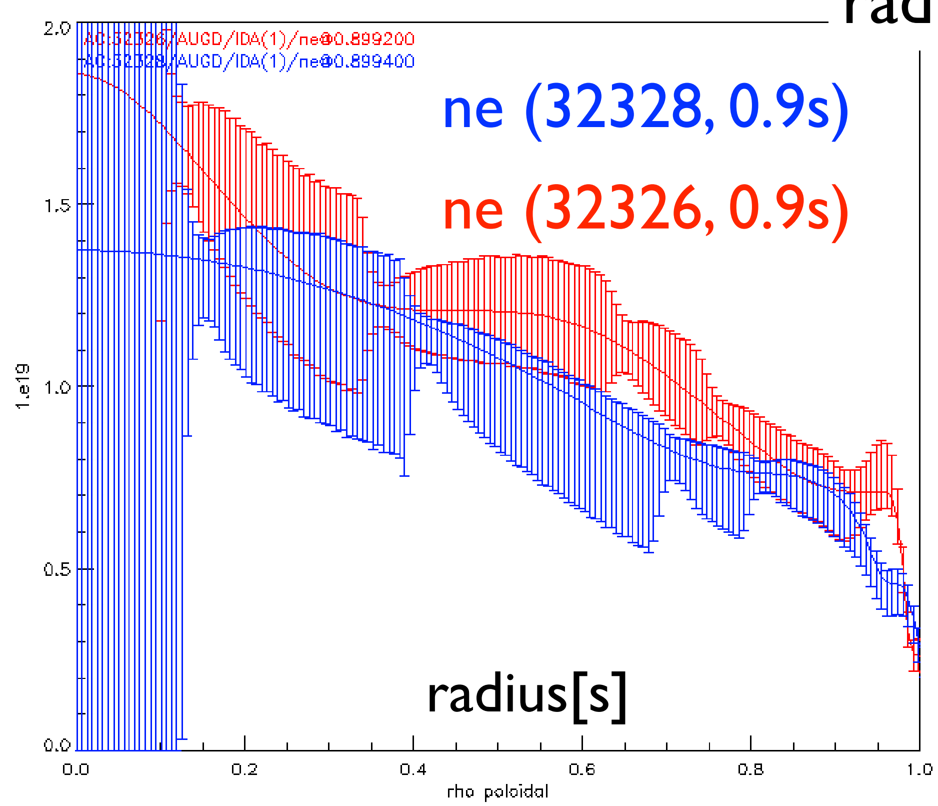

low Te, Ti despite 2.5MW neutral beam injection are key ingredients

onset conditions for EGAMs and BAEs [Lauber IAEA TM 2013]

q≥2, Te, Ti<1.8keV

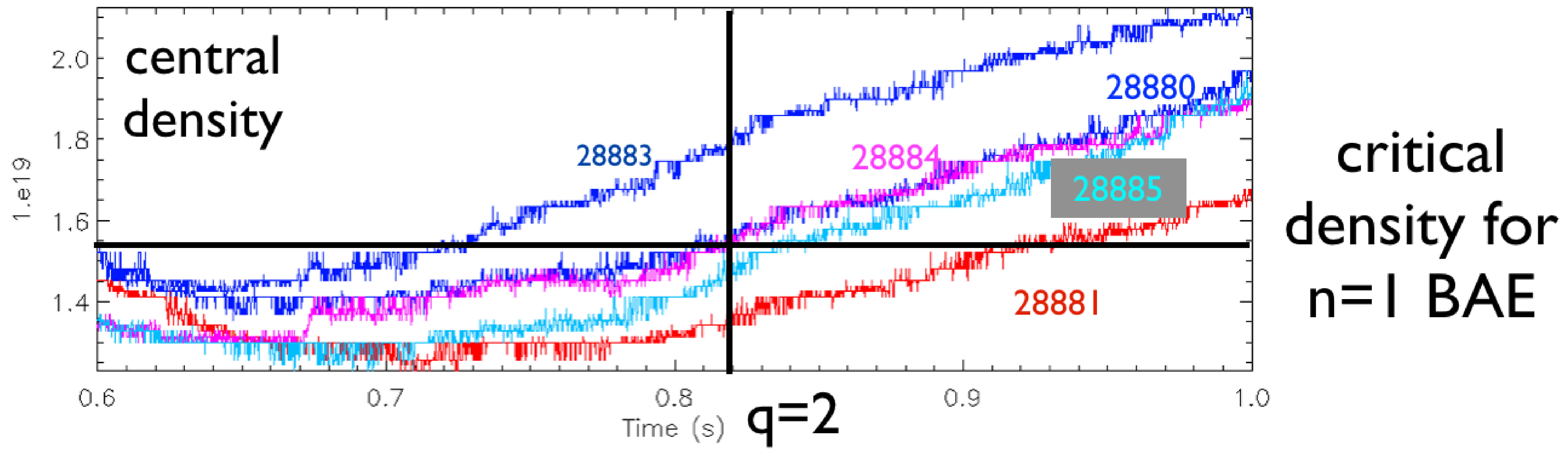

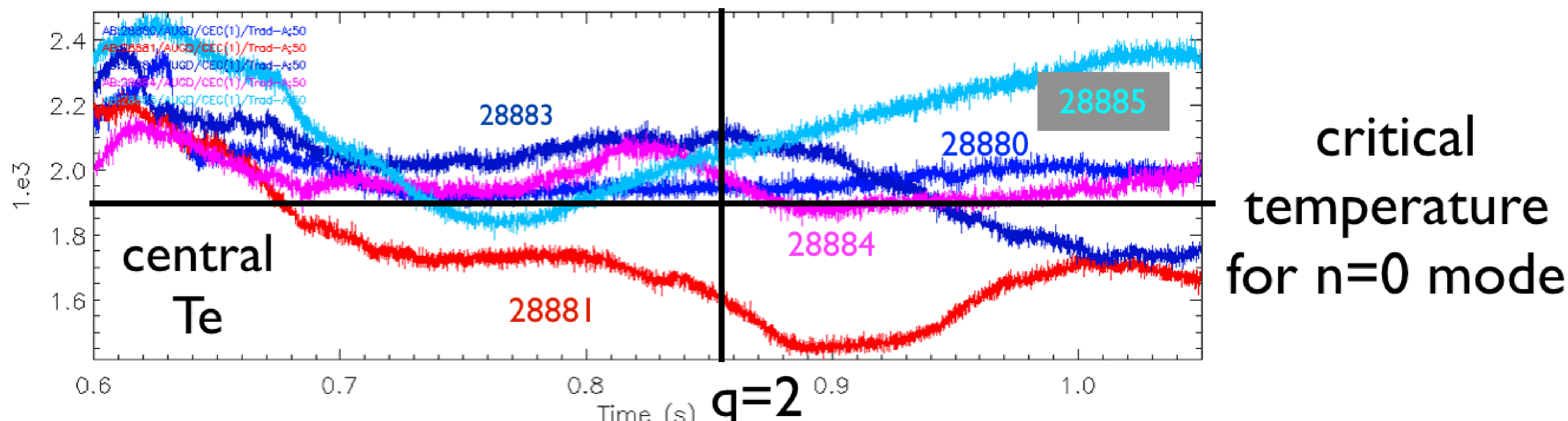

- $\omega(T_1) = \sqrt{(T_1/T_0)}\ \omega(T_0)$ → frequency of BAE/GAM varies from shot to shot by about 10% (5kHz)

onset conditions for EGAMs: confirmed by new experiments

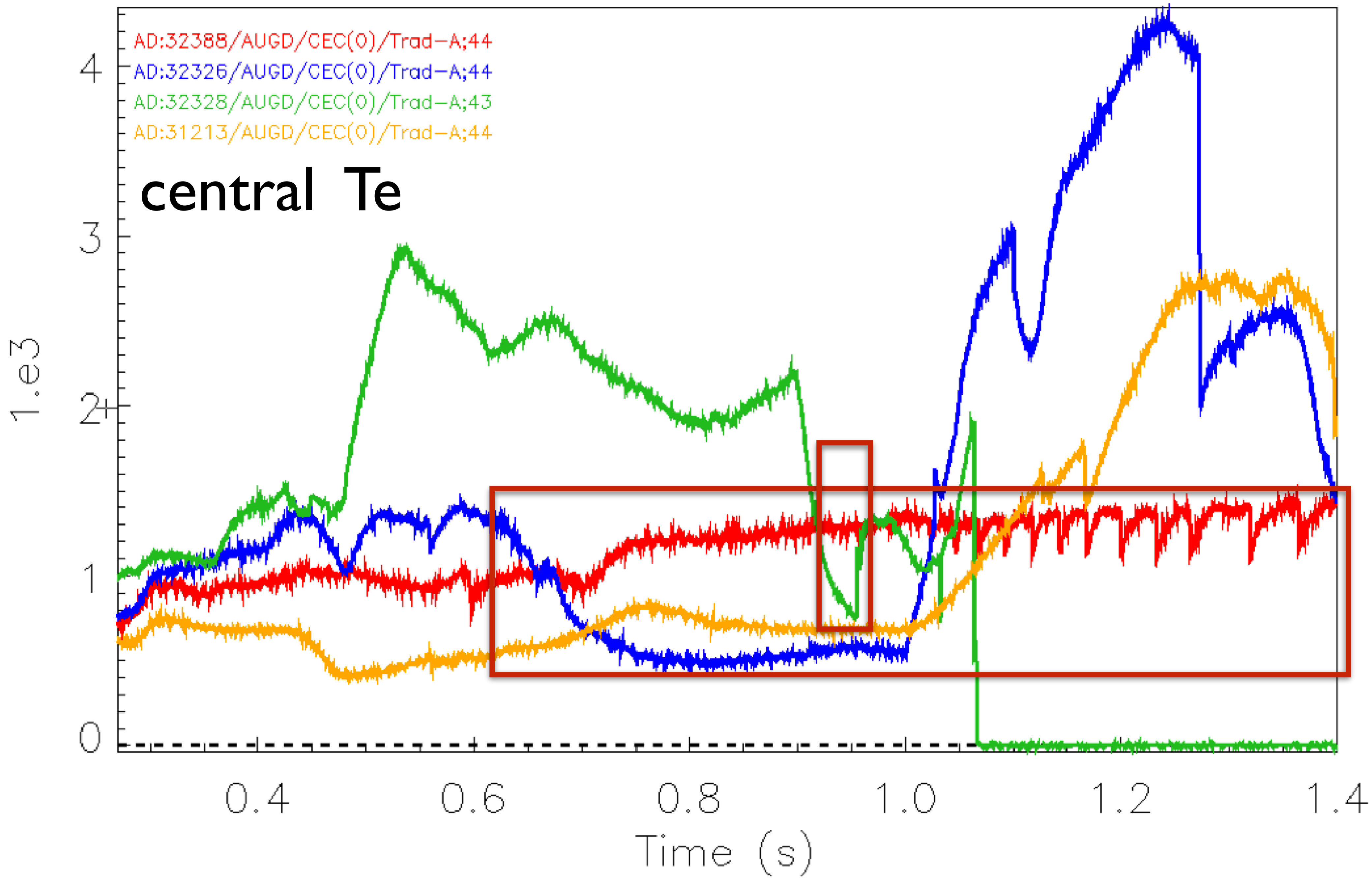

longer, more stable phases with EGAMs in new experiments

fast ion distribution [Transp, B. Geiger]

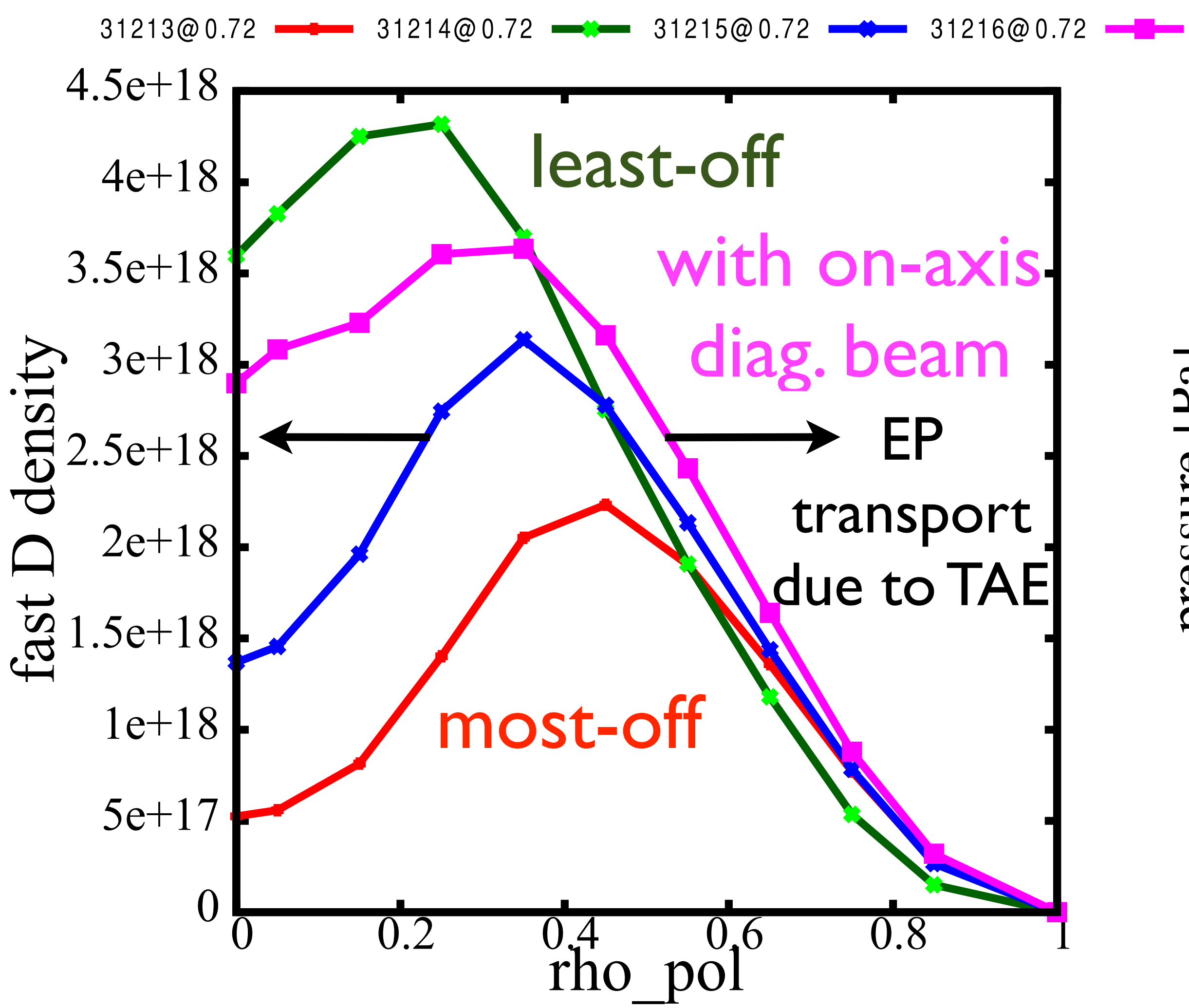

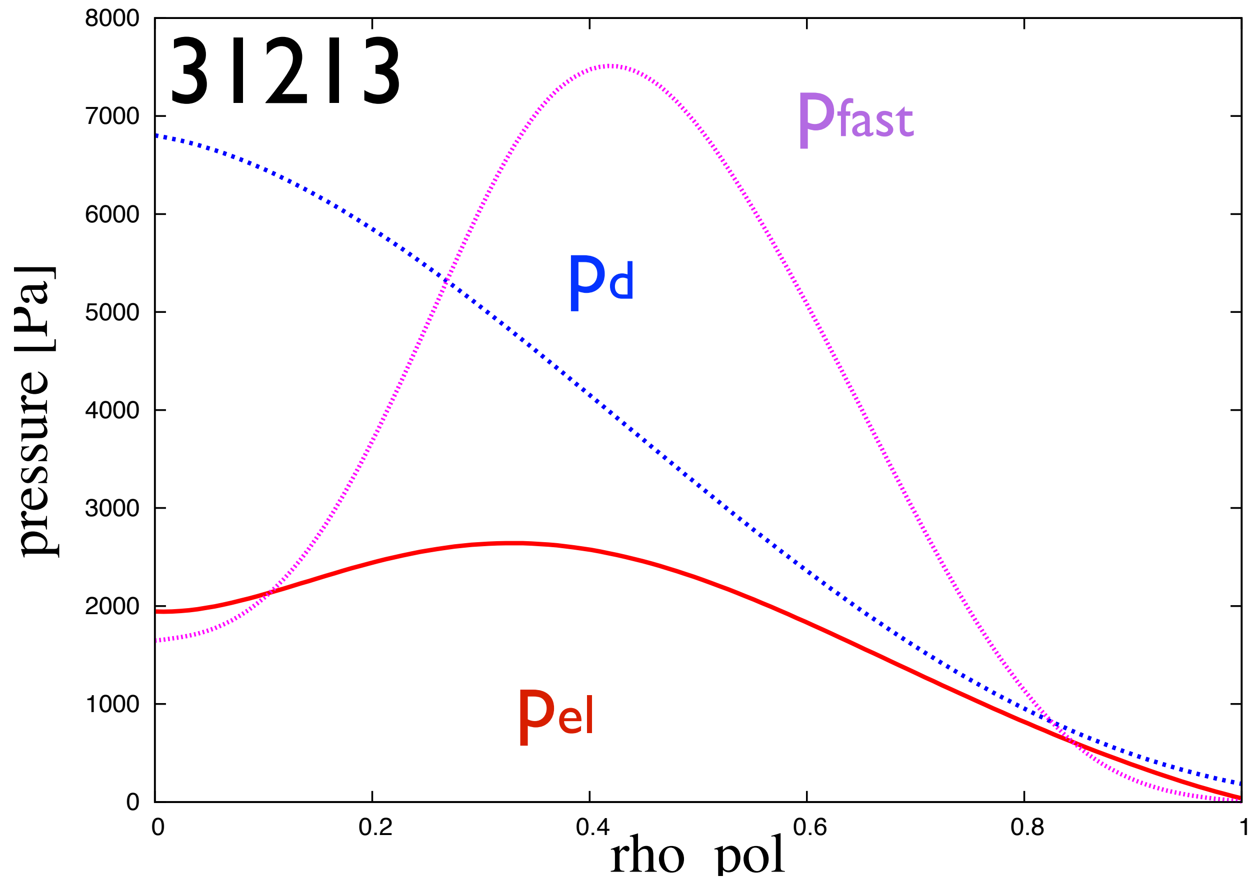

$p_{EP} \gtrsim p_e + p_d$

$\beta_{EP}/\beta_{th} > 1$; $T_f \sim 90\, T_i$

DEMO-like conditions for these two parameters

the physics picture of this scenario:

- the accumulation of W in the core decreases the background Te, Ti and thus reduces the ion Landau damping of AEs and GAMs
- hollow Te profiles form
- large values of $R_0 \nabla \beta_\alpha / \beta_{back}$ can arise
- central ECRH can counteract this accumulation; the increased Landau damping (exponential dependence on Ti) brings the system below excitation threshold (#32328) → threshold typically Ti ≲ 1.8keV for q>2
- Emax/Ti,th ~90 is comparable to burning plasma parameters (ITER/DEMO: 3,5MeV/30keV)
- opens possibility to study experimentally the interaction between Alfvénic modes, EGAMs i.e. zonal structures and background turbulence: due to the EGAM excitation a direct channel from EPs to n=0 modes can be investigated

fundamental physics questions to be clarified:

strongly non-linear EP dynamics at AUG (in contrast to DIII-D) for sub-Alfvénic neutral beam injection raises the following questions:

- experimental conditions?
- why can system arrive at state well above marginal stability (critical gradient models would not allow for that state)
- study non-linear evolution of various ES and EM modes
- study interaction between modes
- study interaction with turbulence
- study scenarios that match projected DEMO parameters in β_{fast}/β_{th} and T_{fast}/T_{th}

obtain confidence in models and codes towards understanding the self-organisation of a burning plasma

scenario developed further (I)

- small density feed-forward: more stable transition through $q=2/q_{edge}=4$ region
- optimised beam blips for measuring Ti

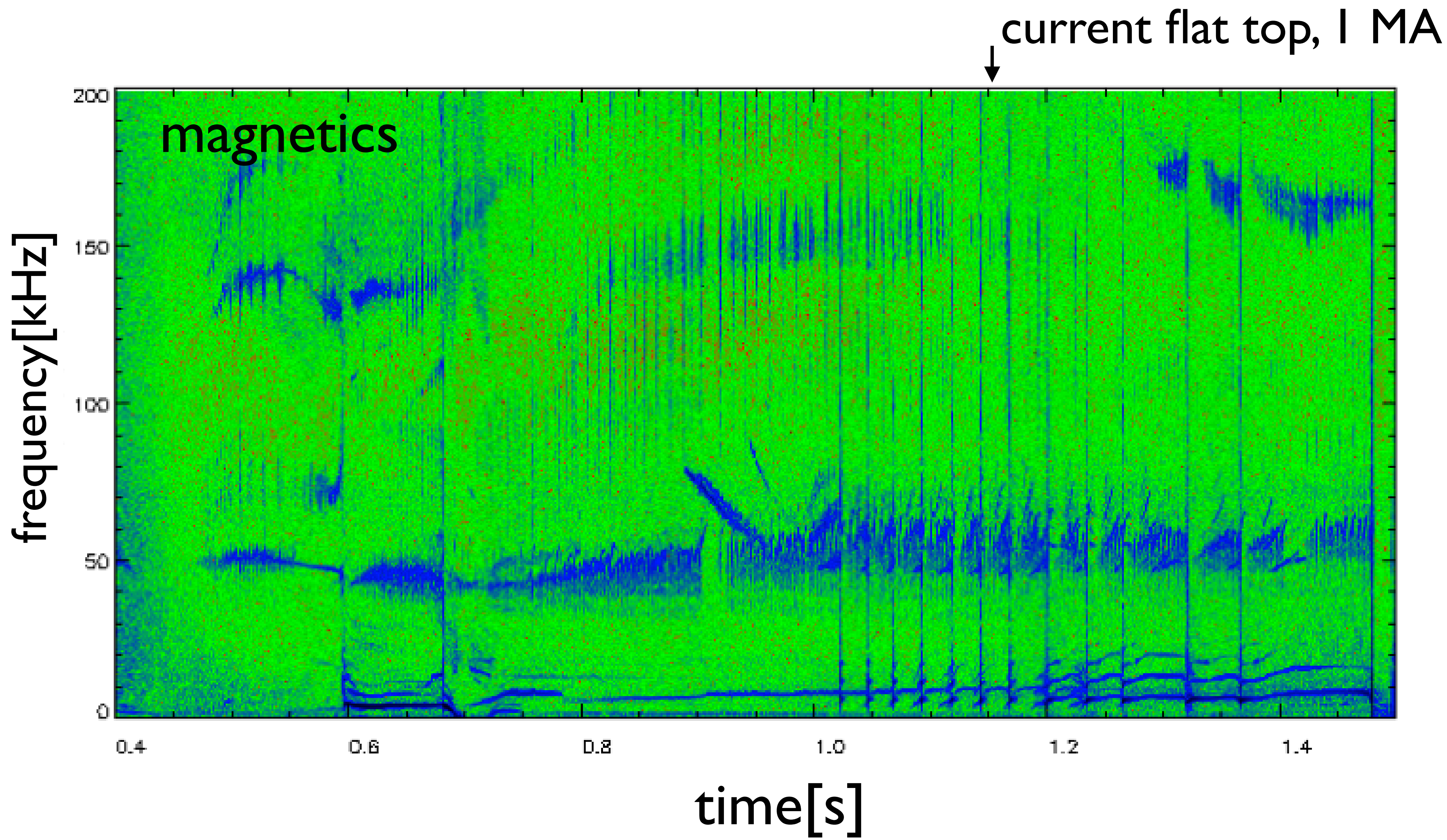

regular sawtooth like crashes at q=2 surface

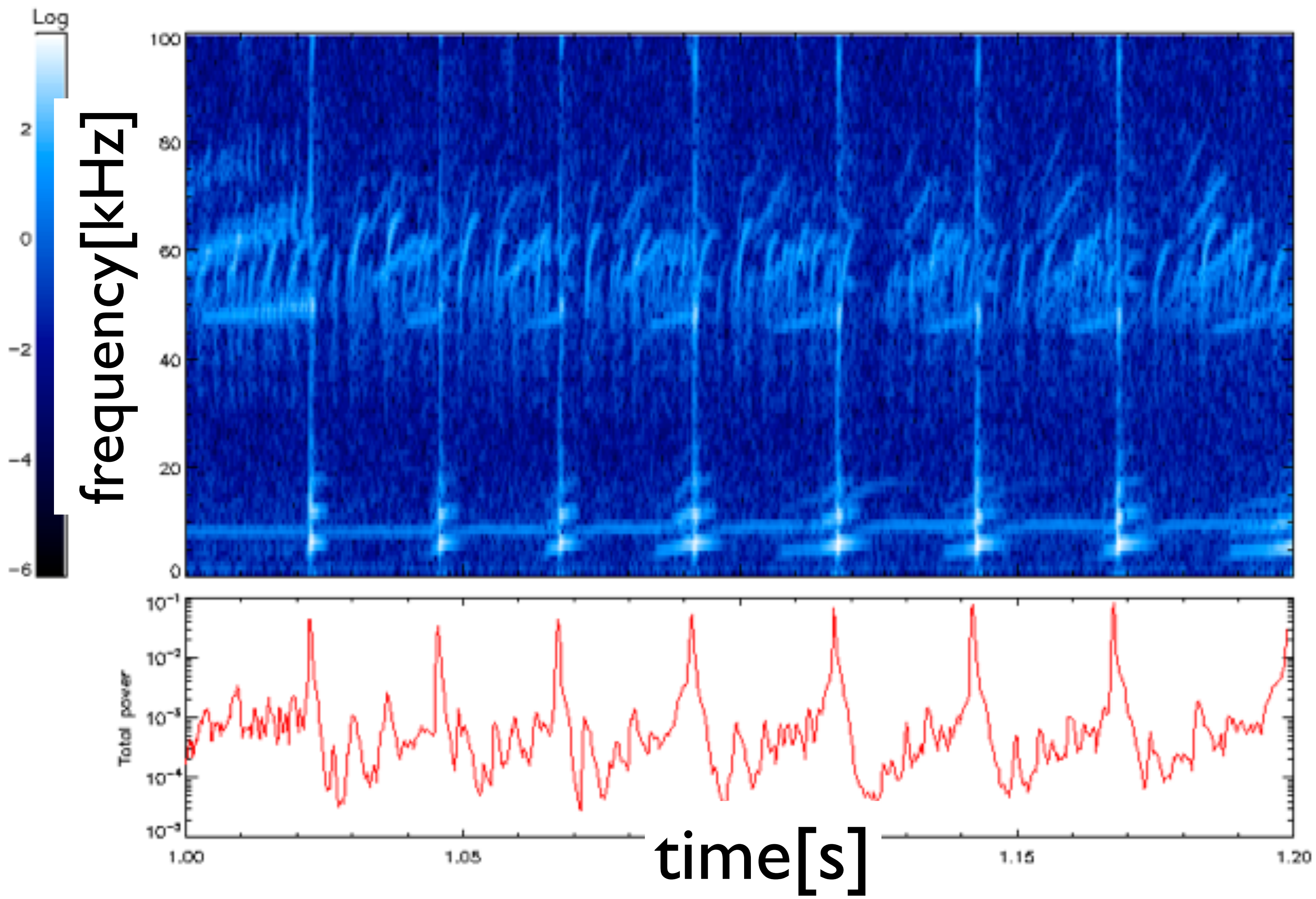

- q=2 sawtooth crashes like in 2001-05 JET/JT60U discharges (current holes) - is this how advanced scenarios JT-60SA will look like? [A Bierwage, 2016/17]
- EGAMs persistent during these crashes
- almost no q-dependence of f_{EGAM} is observed
- surprisingly no variation of EGAM onset frequency - constant Ti!

successful change of plasma position and shape after t>0.8s: mainly different NB deposition position

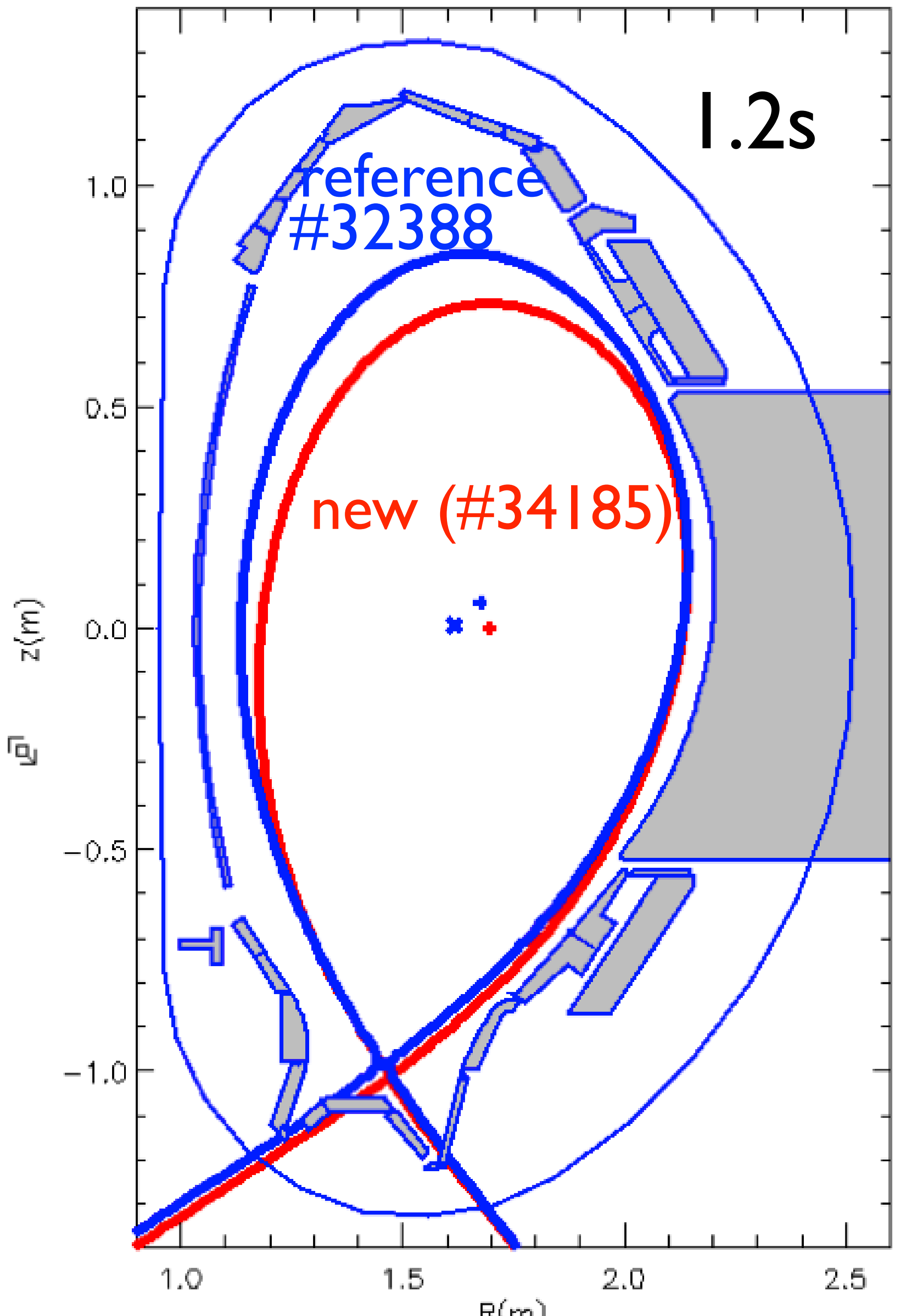

AUG Flux: ρ_{pol}	AUG Flux: Ψ_{pol}
AUGD/EQI(1)	AUGD/EQI(1)
AUGD/EQI(1)	Shot: 34185
Shot: 32388	Time: 1.200
Time: 1.200	
From GQI	From GQI
I_p : 1.02MA	I_p : 1.01MA
β_p : 0.21	β_p : 0.23
l_i : 0.91	l_i : 0.84
ma: 1.677 : 0.05	ma: 1.698 :−0.002
cc: 1.619 : 0.007	cc: 1.640 :−0.063
$\delta_{\_}$: −0.022	$\delta_{\_}$: −0.082
δ_v : 0.361	δ_v : 0.389
κ : 1.742	κ : 1.728
a_{hor} : 0.497m	a_{hor} : 0.478m
q_{95}: −3.88	q_{95}: −3.52
R_{aus} : 2.144m	R_{aus} : 2.142m
vol : 13.45m^3	vol : 12.44m^3
Δ_e : 0.058m	Δ_e : 0.058m
z_{gi} : −1.116m	z_{gi} : −1.150m
z_{ga} : −1.346m	z_{ga} : −0.801m

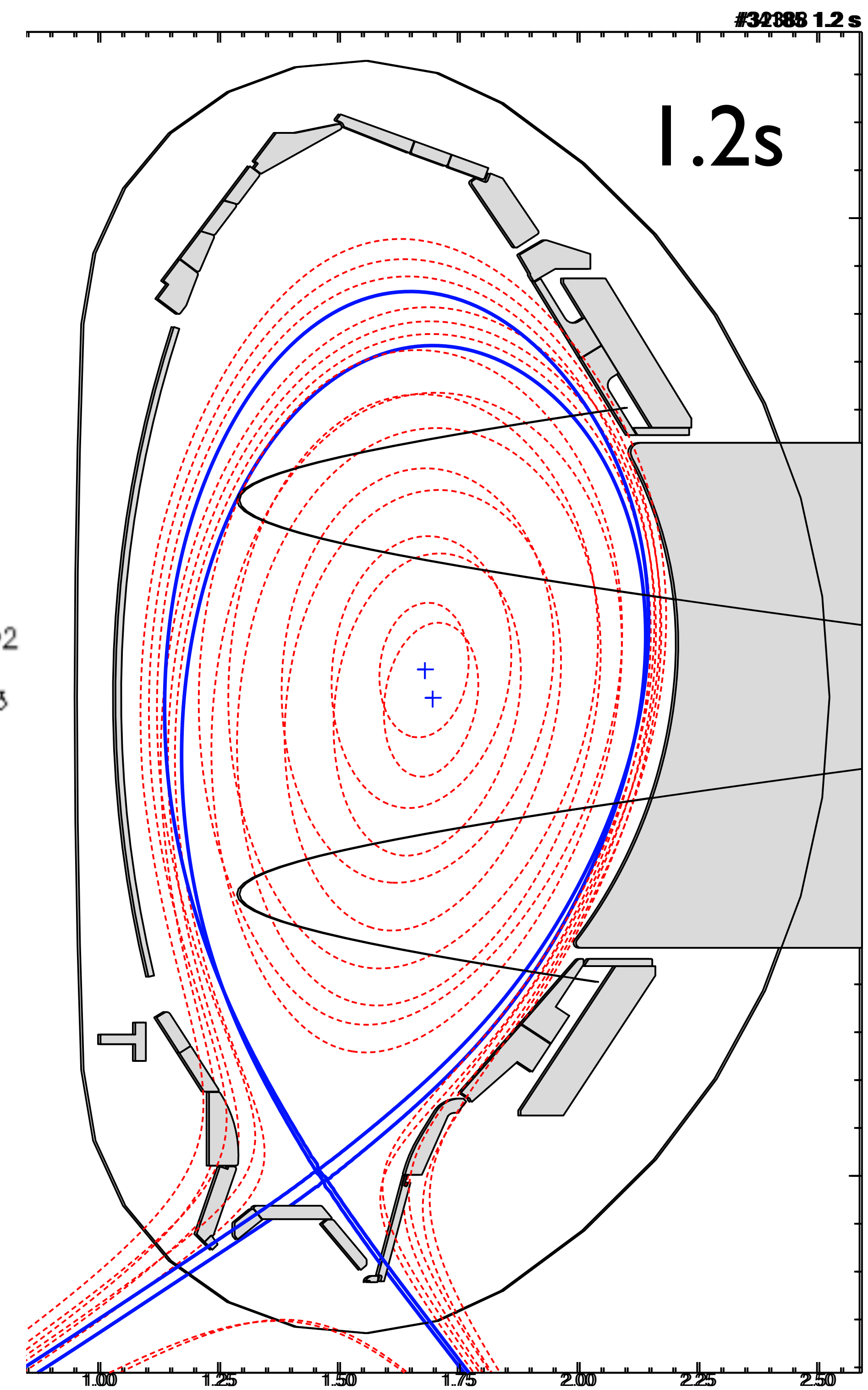

results in different inductance, q-profile, elongation scenario developed further (II)

reference (#32388)

new shape (#34185)

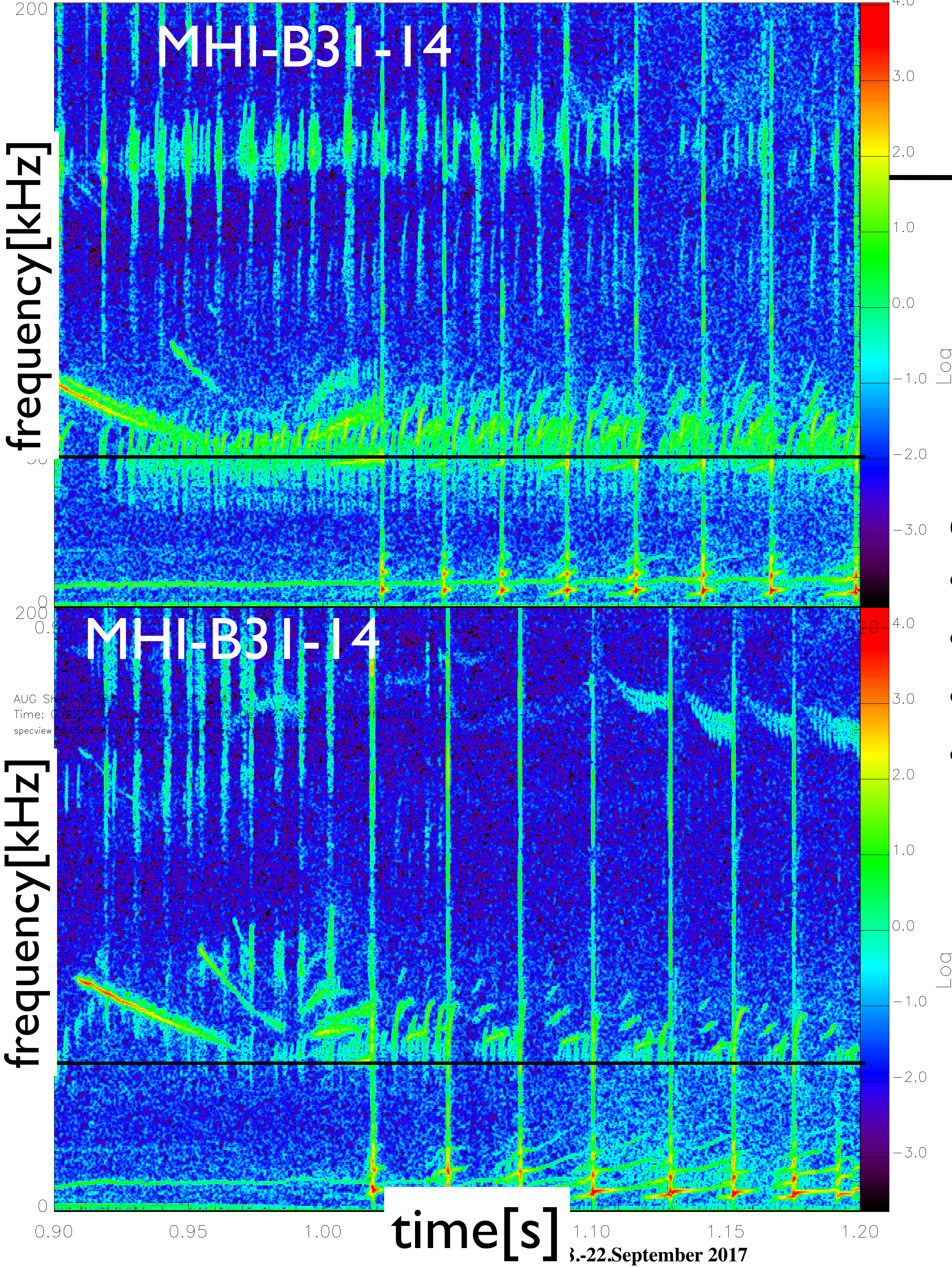

different dynamics for:

- TAEs
- EGAMs
- TAE/EGAM coupling
- q=2 crashes

scenario developed further (III)

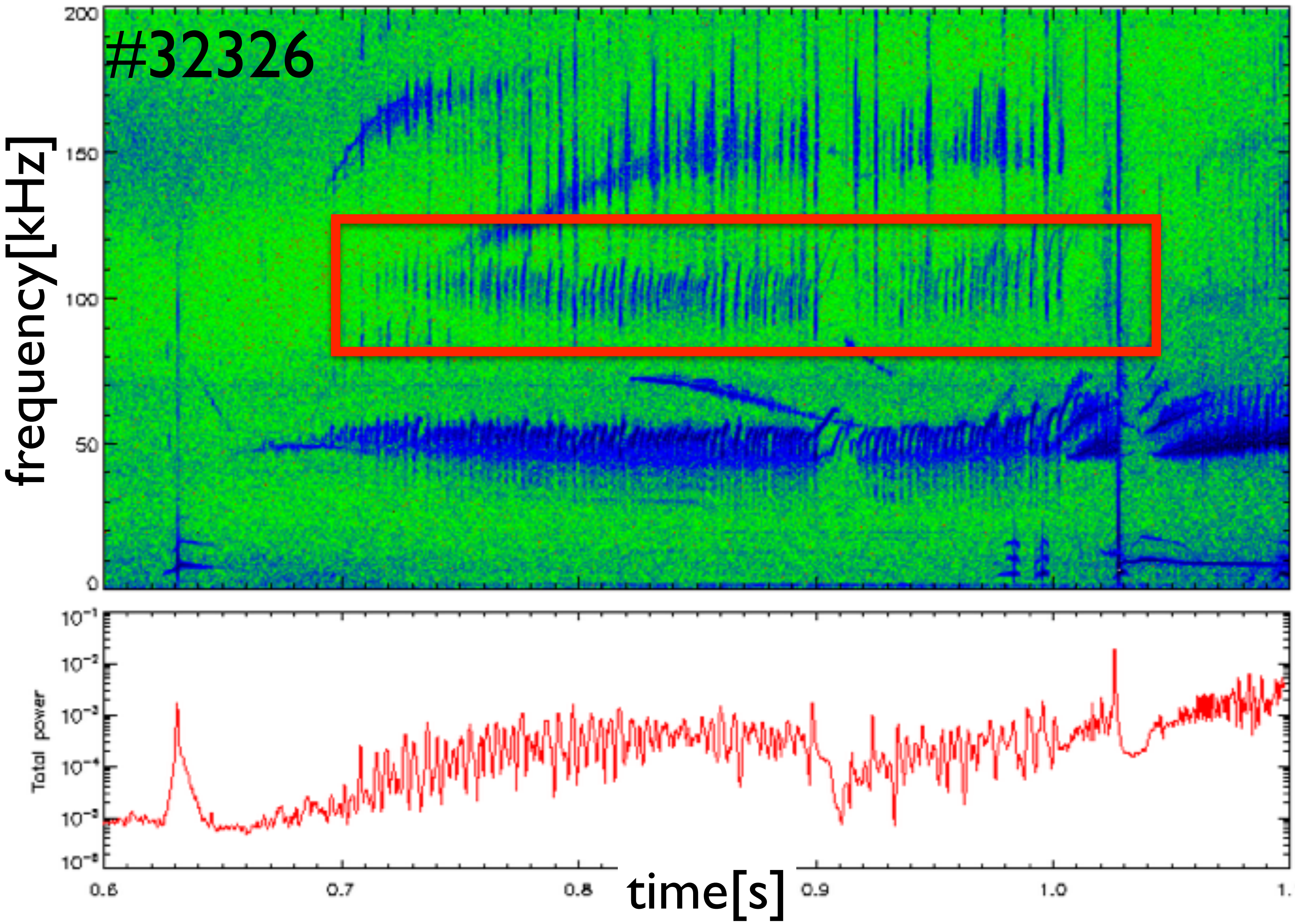

2nd order EGAM excitation! signature of density perturbation?

DIII-D,Fu [2011]: 2nd order outboard midplane density perturbation is comparable to first-order perturbation

at
AUG:
first order
EGAM
harmonics
dominates,
2nd order
perturbation
more visible
on high field
side

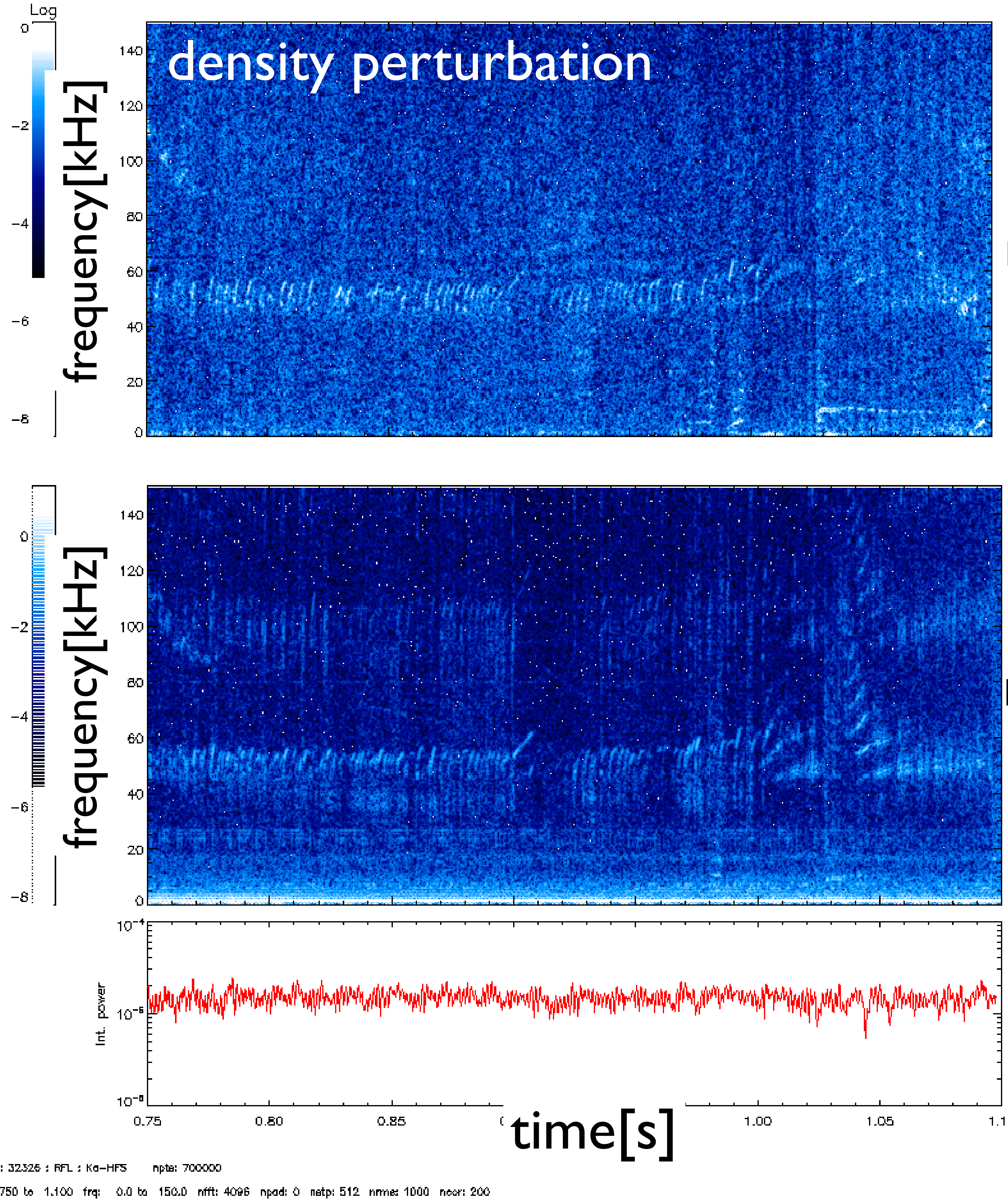

reflectometry:
low field side

reflectometry
high field side

- Chirping **EGAMs at ~50 kHz** with **(-2,0)** (propagating in electron diamagnetic direction)
- Chriping/bursting **TAEs at ~150 kHz** with **(-3,+1)**

AUG #32388

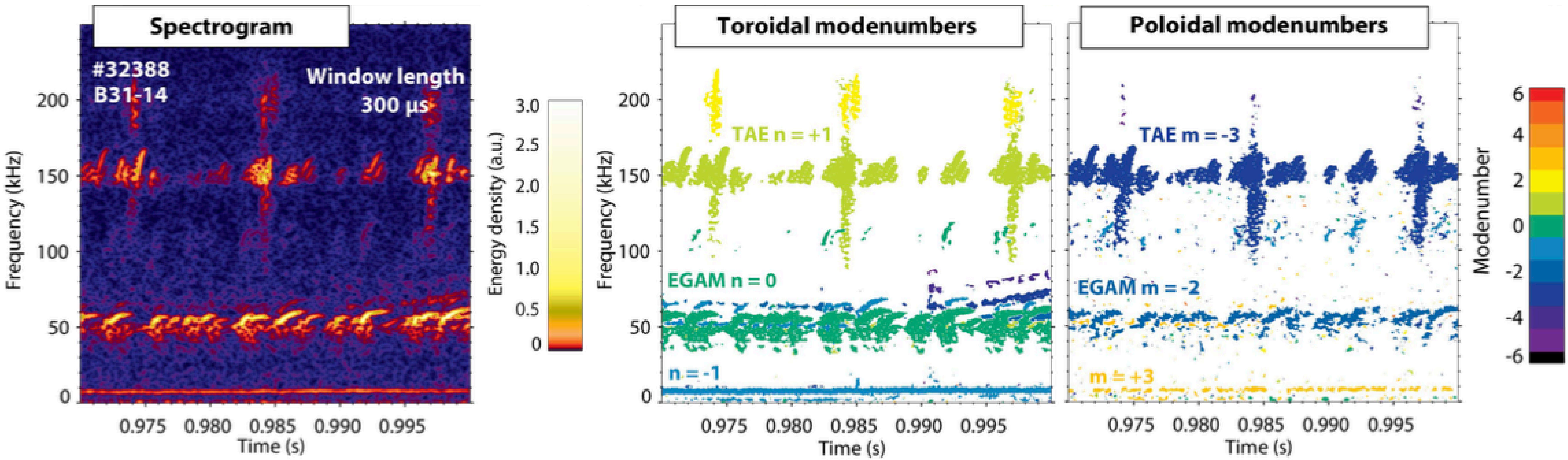

signals with rapid chirping (amplitudes, frequency) may cause 'spurious' bicoherence

Phase randomized bicoherence probability density function calculation

signals with rapid chirping (amplitudes, frequency) may cause 'spurious' bicoherence
phase randomized bicoherence probability density function calculation

- High bicoherence around at (55, 55) kHz indicates **strongly nonlinear EGAMs.** (see spectrogram at ~110 kHz)
- **Without filtering interaction with TAEs is not clear**

- Filtering shows high, significant bicoherence around (155, 55) kHz
- Indicates the **nonlinear interaction between EGAMs and TAEs**

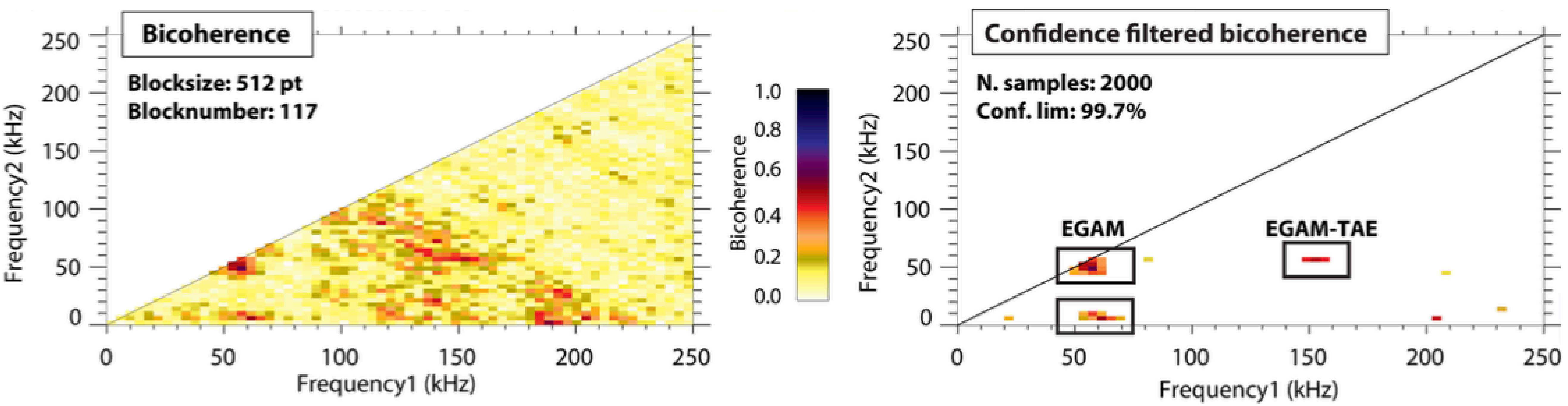

modeling efforts

- linear drive
- radial propagation
- non-linear interaction: wave-wave
- non-linear interaction: wave-particle

LIGKA: recent updates

- linear local and global GK solver: QN, GKM and GKE, non perturbative mode structures

- continuous spectrum: null-space of 2nd order operator

- in addition to fully numerical solver, new analytical finite orbit width version: Taylor expansion to 2nd order for EPs and thermal ions:
  k_r as parameter or 4th order terms; recovers [Zonca 1998] in appropriate limit

- antenna, nyquist contour and vector iteration solver

- LIGKA_lib as library for wrapper or other codes (HAGIS)

LIGKA model equations

$$\overbrace{-\frac{\partial}{\partial t}\left[\nabla\cdot\frac{\nabla_\perp\delta\phi}{v_A^2}\right]}^{\text{Inertia (2nd order)}}+\overbrace{\boldsymbol{B}\cdot\nabla\frac{\nabla\times(\nabla\times\delta A_\parallel\boldsymbol{b})}{B}}^{\text{Field line bending}}+\overbrace{(\boldsymbol{b}\times\nabla\delta A_\parallel)\cdot\nabla\frac{\mu_0 j_\parallel}{B}}^{\text{Current gradient ('kink')}}$$

$$=\underbrace{-\sum_a \mu_0\int \mathrm{d}^2v\, e_a\{\boldsymbol{v}_\mathrm{d}\cdot\nabla J_0\delta f\}_a}_{\text{Pressure--curvature coupling ('ballooning')}}+\underbrace{\sum_a\left[\boldsymbol{b}\times\nabla\left(\frac{\beta_{a\perp}}{2\Omega_a}\right)\right]\cdot\nabla\nabla_\perp^2\delta\phi}_{\text{Diamagnetic correction for inertia}}$$

$$\underbrace{+\sum_a\frac{3\beta_{a\perp}}{8\Omega_a^2}\nabla_\perp^4\frac{\partial\delta\phi}{\partial t}}_{\text{4th--order inertia ('kinetic Alfvén wave')}}+\underbrace{\boldsymbol{B}\cdot\nabla\frac{1}{B}\sum_a\frac{\beta_a}{4}\nabla_\perp^2\delta A_\parallel}_{\text{High--beta field line bending correction (negligible)}};$$

$$0=\underbrace{\sum_a e_a\int \mathrm{d}^2v\{J_0\delta f\}_a}_{\text{Charge density compression}}+\underbrace{m_\mathrm{i}\nabla_\perp\cdot\frac{n_\mathrm{i}\nabla_\perp\delta\phi}{B^2}+\frac{3P_{\mathrm{i}\perp}}{4B^2\Omega_\mathrm{i}^2}\nabla_\perp^4\delta\Phi}_{\text{FLR polarization terms}},$$

$$\frac{\partial\delta h}{\partial t}+(v_\parallel\boldsymbol{b}+\hat{\boldsymbol{v}}_\mathrm{d})\cdot\nabla\delta h=\left[\frac{\boldsymbol{b}\times\nabla f_\mathrm{eq}}{eB}\cdot\nabla-\frac{\partial f_\mathrm{eq}}{\partial E}\frac{\partial}{\partial t}\right]$$

$$\times J_0\left[\delta\phi-\left(1-\frac{\hat{\boldsymbol{v}}_\mathrm{d}\cdot\nabla}{\mathrm{i}\omega}\right)\delta\psi\right].$$

IPP

based on #31213@0.84s a reference case was created

ASDEX Upgrade

http://www2.ipp.mpg.de/~pwl/NLED_AUG/data.html

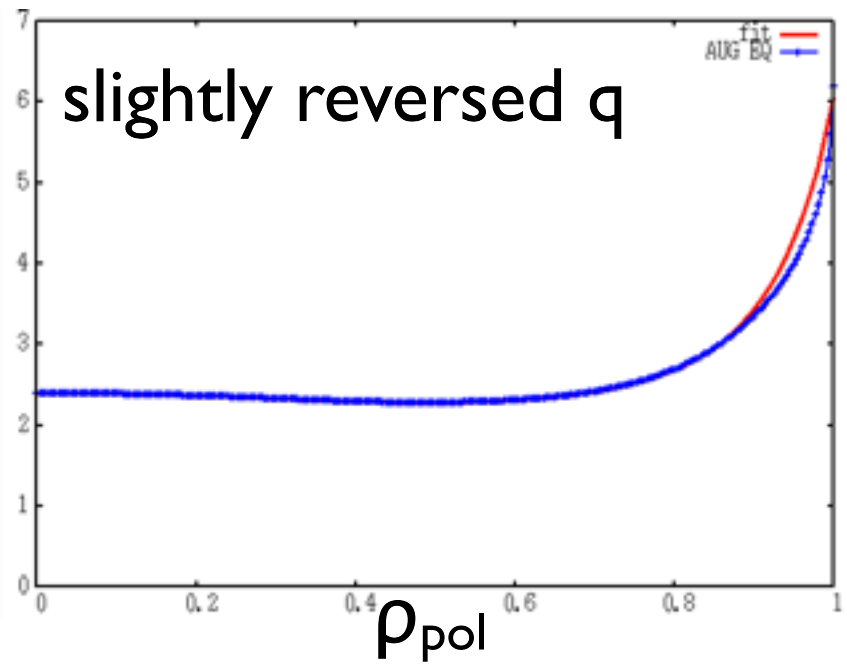

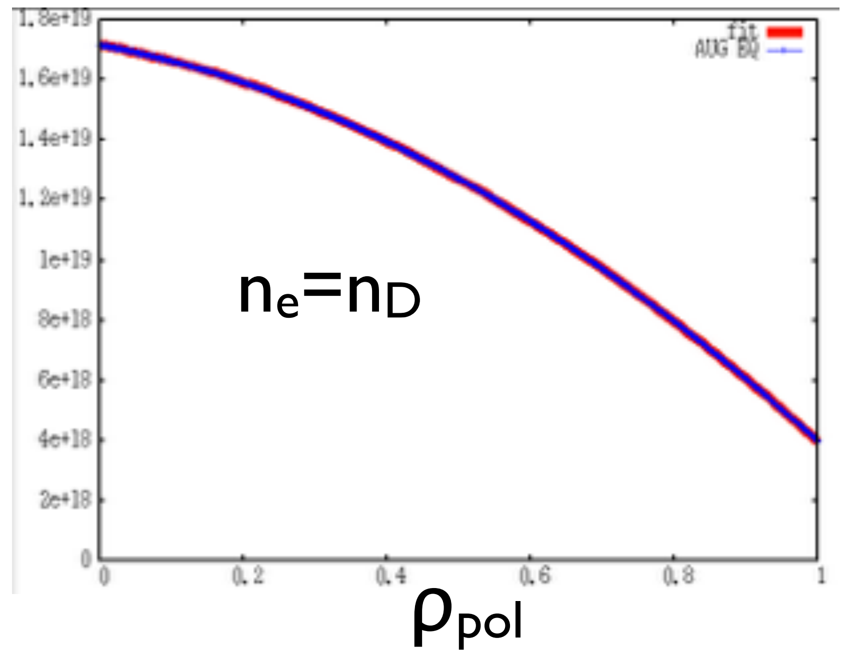

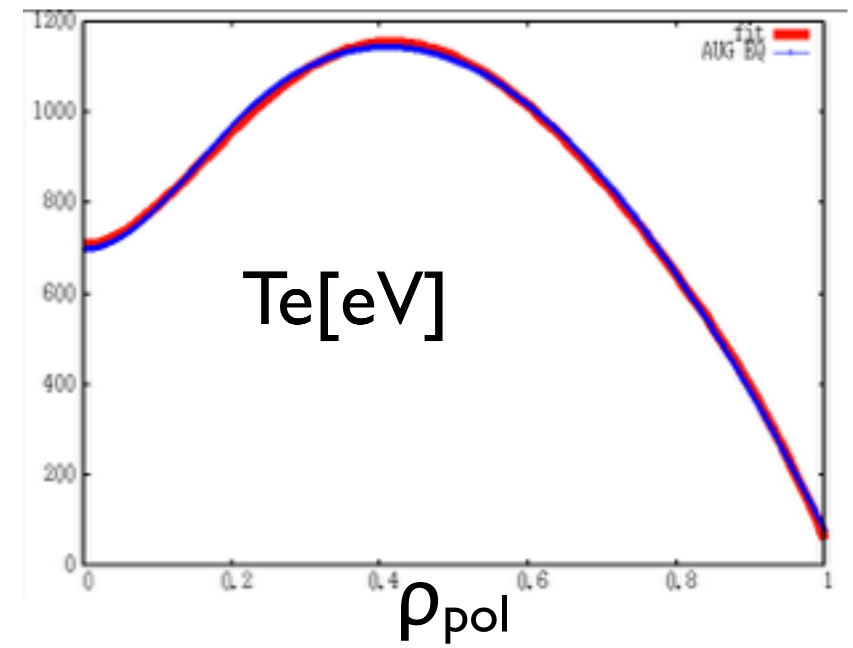

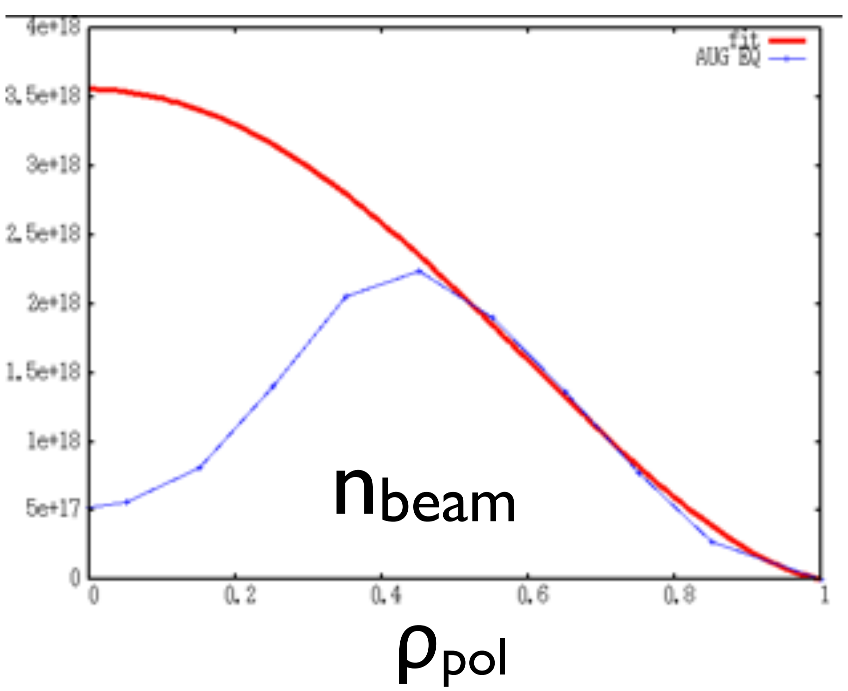

benchmark
steps:

step1: flat Te, Ti,ne
step 2: ne, flat Te, Ti
step 3: ne, Te=Ti
step 4: ne, Te≠Ti

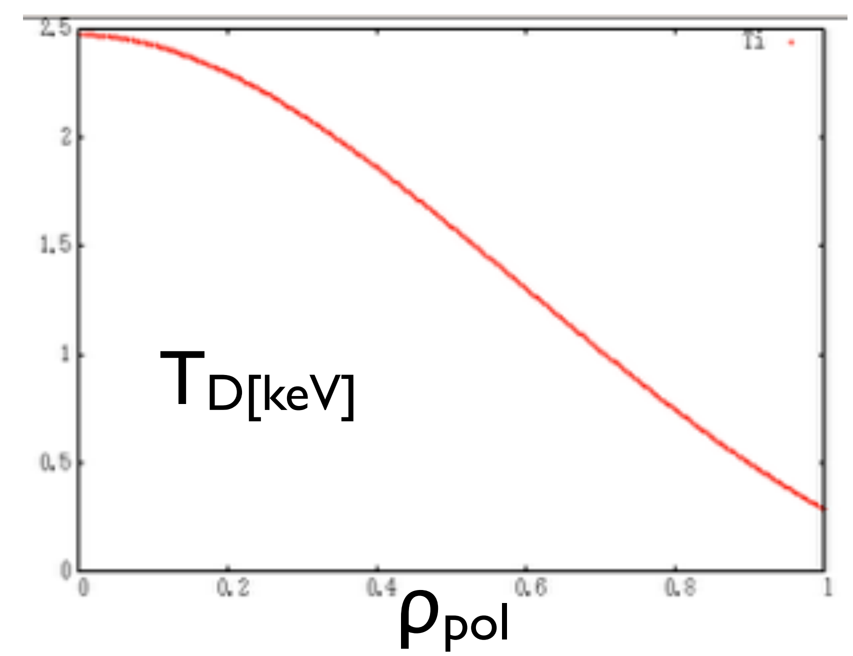

importance of radial propagation

- analytical models point out importance of radial GAM/EGAM propagation [Zonca 2008, Qiu, 2009,Smolyakov 2009, Sasaki, Miki&Idomura 2015, Palermo 2017, etc..]

- nonlinear simulations GYSELA, GTS [Zarzoso, Schneller] and nl-analytical models [Sasaki] emphasise the role of radial GAM/EGAM propagation for turbulence spreading

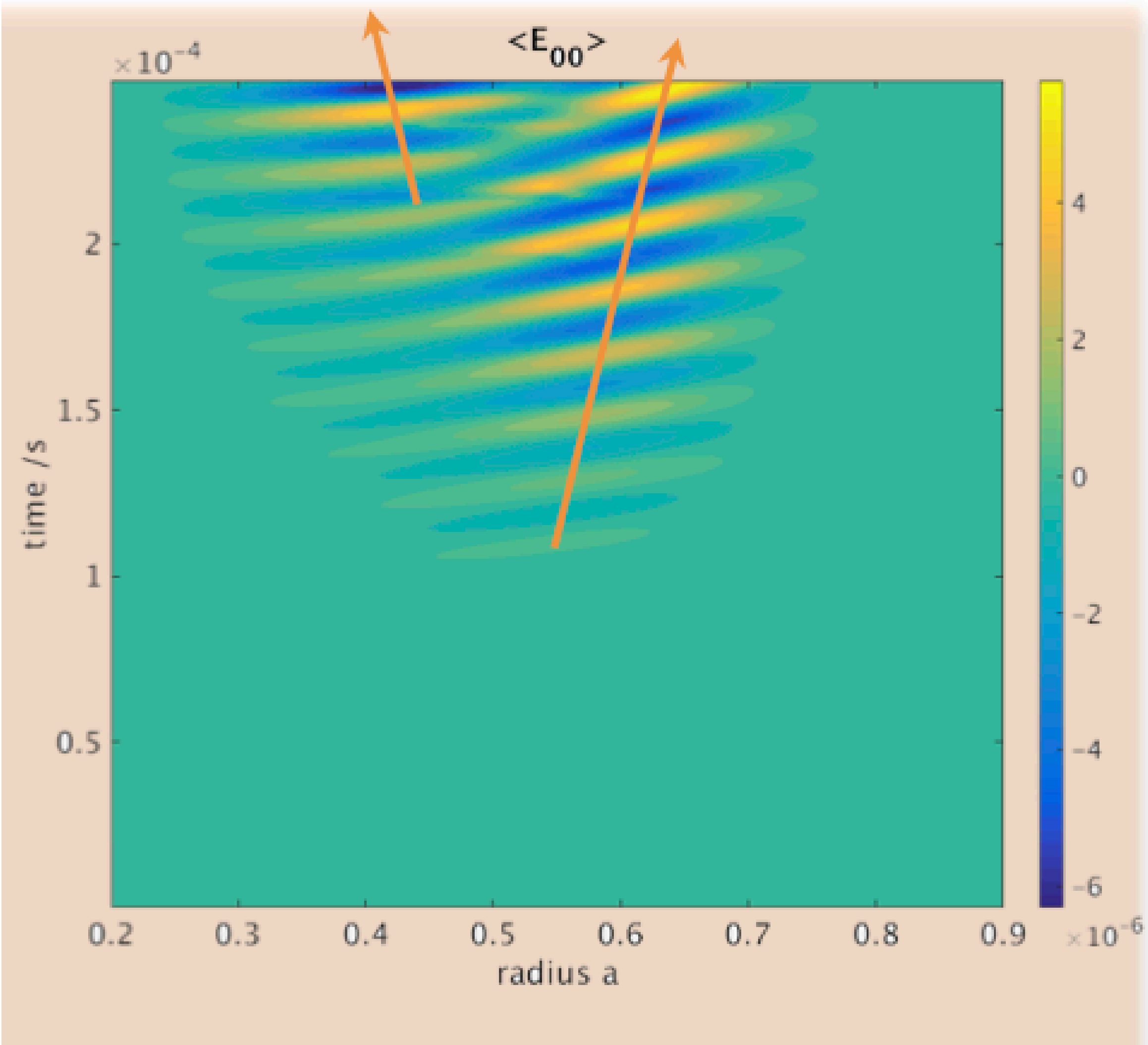

[Schneller, 2017 talk Friday]

experimentally: no (or small) radial propagation but rather radial shrinking of the modes was found

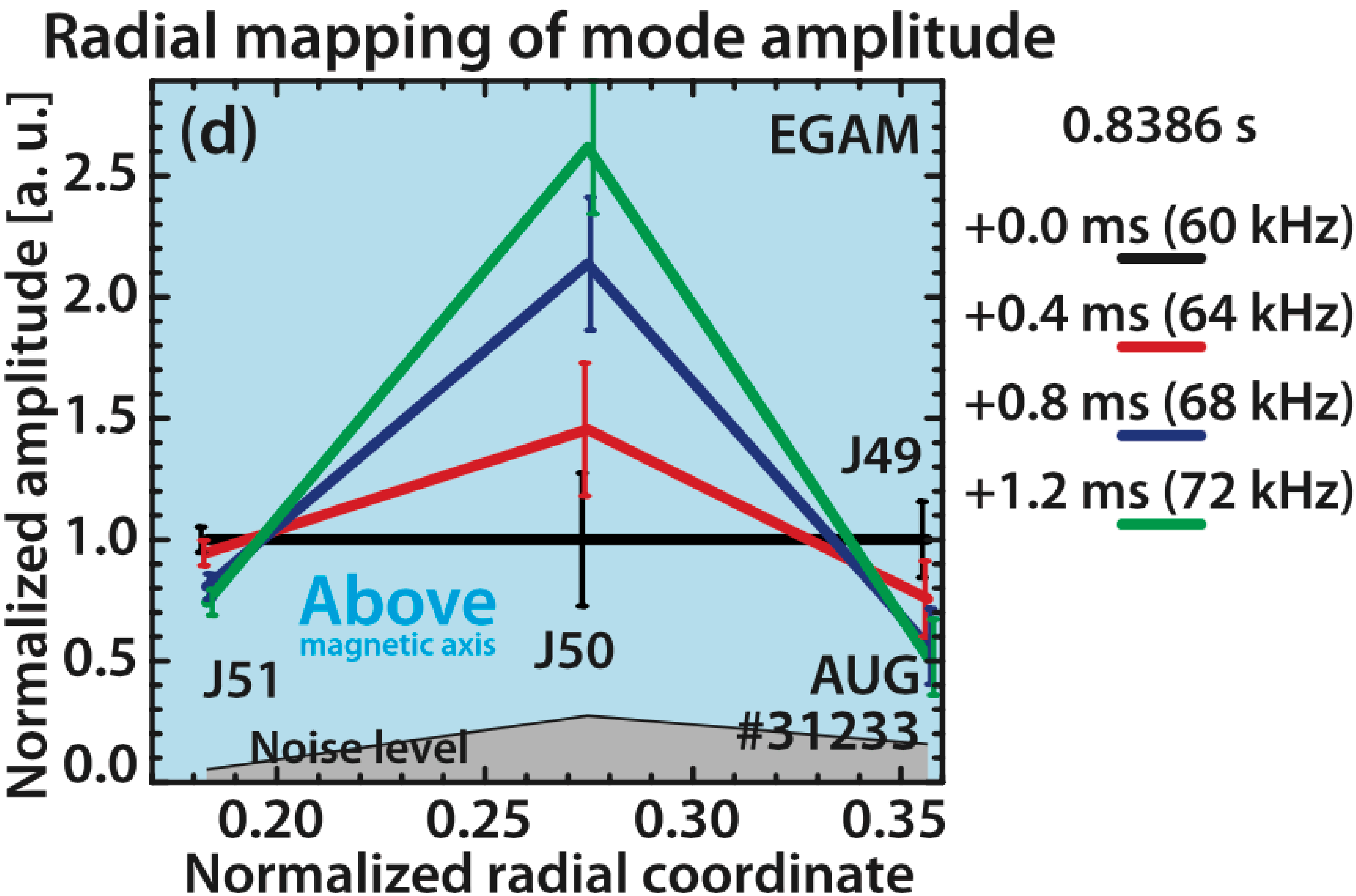

[Horvath, NF 2016]

finite orbit width (FOW) dispersion relation for LIGKA

$$\omega^2\left(1-\frac{\omega_{*p}}{\omega}\right) - k_\parallel^2\omega_A^2R_0^2 = 2\frac{v_{thi}^2}{R_0^2}\left(-\Big[H(x_{m-1})+H(x_{m+1})\Big] + \tau\left[\frac{N^m(x_{m-1})N^{m-1}(x_{m-1})}{D^{m-1}(x_{m-1})}+\frac{N^m(x_{m+1})N^{m+1}(x_{m+1})}{D^{m+1}(x_{m+1})}\right]\right)$$

no FOW,
circulating particle
approximation

[Zonca 1996,2009 Lauber 2009]

$$\Big(\omega^2 - H_{0,0} + \frac{N_{-1,0}{N^G}_{0,-1}}{D_{-1,-1}} + \frac{N_{1,0}{N^G}_{0,1}}{D_{1,1}}\Big)$$

$$+\ \varrho^2\Big(H^{FLR}_{0,0} - \frac{D^{FLR}_{-1,-1}N_{-1,0}{N^G}_{0,-1}}{{D^2}_{-1,-1}} - \frac{D^{FLR}_{1,1}N_{1,0}{N^G}_{0,1}}{D^2_{1,1}}$$
$$+\ \frac{N_{-1,0}N^{G,FLR}_{0,-1}+N^{FLR}_{-1,0}{N^G}_{0,-1}}{D_{-1.-1}} + \frac{N^{FLR}_{1,0}{N^G}_{0,1}+N_{1,0}N^{G,FLR}_{0,1}}{D_{1.1}}\Big)$$

$$+\ \rho^2\Big(J_{0,0} + \frac{N_{-1,0}{Q^G}_{0,-1}+{N^G}_{0,-1}Q_{-1,0}}{D_{-1,-1}} + \frac{{N^G}_{0,1}Q_{1,0}+N_{1,0}{Q^G}_{0,1}}{D_{1,1}}$$
$$+\ \frac{P_{-2,0}{P^G}_{0,-2}}{D_{-2,-2}} + \frac{P_{0,0}{P^G}_{0,0}}{D_{0,0}} + \frac{P_{2,0}{P^G}_{0,2}}{D_{2,2}}$$
$$+\ \frac{E_{-2,-1}E_{-1,-2}N_{-1,0}{N^G}_{0,-1}}{D_{-2,-2}{D^2}_{-1,-1}} + \frac{E_{-1,0}E_{0,-1}N_{-1,0}{N^G}_{0,-1}}{{D^2}_{-1,-1}D_{0,0}}$$
$$+\ \frac{E_{-1,0}E_{0,1}N_{1,0}{N^G}_{0,-1}}{D_{-1,-1}D_{0,0}D_{1,1}} + \frac{E_{0,-1}E_{1,0}N_{-1,0}{N^G}_{0,1}}{D_{-1,-1}D_{0,0}D_{1,1}}$$
$$+\ \frac{E_{0,1}E_{1,0}N_{1,0}{N^G}_{0,1}}{D_{0,0}D^2_{1,1}} + \frac{E_{1,2}E_{2,1}N_{1,0}{N^G}_{0,1}}{D^2_{1,1}D_{2,2}}$$
$$-\ \frac{E_{-2,-1}N_{-1,0}{P^G}_{0,-2}}{D_{-2,-2}D_{-1,-1}} - \frac{E_{0,-1}N_{-1,0}{P^G}_{0,0}}{D_{-1,-1}D_{0,0}} - \frac{E_{0,1}N_{1,0}{P^G}_{0,0}}{D_{0,0}D_{1,1}}$$
$$-\ \frac{E_{2,1}N_{1,0}{P^G}_{0,2}}{D_{1,1}D_{2,2}} - \frac{E_{-1,-2}{N^G}_{0,-1}P_{-2,0}}{D_{-2,-2}D_{-1,-1}} - \frac{E_{-1,0}{N^G}_{0,-1}P_{0,0}}{D_{-1,-1}D_{0,0}}$$
$$-\ \frac{E_{1,0}{N^G}_{0,1}P_{0,0}}{D_{0,0}D_{1,1}} - \frac{E_{1,2}{N^G}_{0,1}P_{2,0}}{D_{1,1}D_{2,2}} - \frac{F_{-1,-1}N_{-1,0}{N^G}_{0,-1}}{{D^2}_{-1,-1}}$$
$$-\ \frac{F_{-1,1}N_{1,0}{N^G}_{0,-1}}{D_{-1,-1}D_{1,1}} - \frac{F_{1,-1}N_{-1,0}{N^G}_{0,1}}{D_{-1,-1}D_{1,1}} - \frac{F_{1,1}N_{1,0}{N^G}_{0,1}}{D^2_{1,1}}\Big)$$

2nd order FLR+FOW

[Zonca 1998 , Lauber to be published]

- generalised expression (wrt. ω*) for FOW effects, implemented in LIGKA
- equivalent to EGAM FOW equations: Qiu [2009], Miki & Idomura [2015]
- fast analytical model for FOW effects: solve equations both locally (scan k_r) and globally
- opens possibility for systematic EPM threshold checks
- extension to non-Maxwellian distribution functions on the way

benchmarking FOW/FLR version with [Zonca e tal 1998,2008]

ASDEX Upgrade

$$\Lambda_0^2 \simeq 1 - \frac{q^2}{\Omega^2}\left(\frac{7}{4}+\frac{T_e}{T_i}\right) - \frac{q^2}{\Omega^4}\left(\frac{23}{8}+\frac{2T_e}{T_i}+\frac{T_e^2}{2T_i^2}\right) + i\pi^{1/2}q^2\Omega^3 e^{-\Omega^2}\left[1+(1+2T_e/T_i)/\Omega^2\right].$$

[ZLR,ZOW]

$$\Lambda_0^2 \rightarrow \Lambda_0^2 - (k_\zeta^2\rho_i^2/2)\left(3/4+(q^2/\Omega)S_0(\Omega)\right)$$

[FLR,FOW]

$(q^2(7/4+T_e/T_i) \gg 1)$

$$\frac{3}{4}+\frac{q^2}{\Omega}S_0(\Omega) \simeq \frac{3}{4} - \frac{q^2}{\Omega^2}\left(\frac{13}{4}+3\frac{T_e}{T_i}+\frac{T_e^2}{T_i^2}\right) + \frac{q^4}{\Omega^4}\left(\frac{747}{32}+\frac{481}{32}\frac{T_e}{T_i}+\frac{35}{8}\frac{T_e^2}{T_i^2}+\frac{1}{2}\frac{T_e^3}{T_i^3}\right) - i\pi^{1/2}q^4 e^{-\Omega^2/4}\left[\Omega^5/256+(1+T_e/T_i)\Omega^3/32\right]$$

KGAM benchmark: analytical theory vs LIGKA

q=3.25

τ=0.05

$$\frac{3}{4}+\frac{q^2}{\Omega}S_0(\Omega)\simeq\frac{3}{4}-\frac{q^2}{\Omega^2}\left(\frac{13}{4}+3\frac{T_e}{T_i}+\frac{T_e^2}{T_i^2}\right)$$
$$+\frac{q^4}{\Omega^4}\left(\frac{747}{32}+\frac{481}{32}\frac{T_e}{T_i}+\frac{35}{8}\frac{T_e^2}{T_i^2}+\frac{1}{2}\frac{T_e^3}{T_i^3}\right)$$
$$-i\pi^{1/2}q^4e^{-\Omega^2/4}\left[\Omega^5/256+(1+T_e/T_i)\Omega^3/32\right]$$

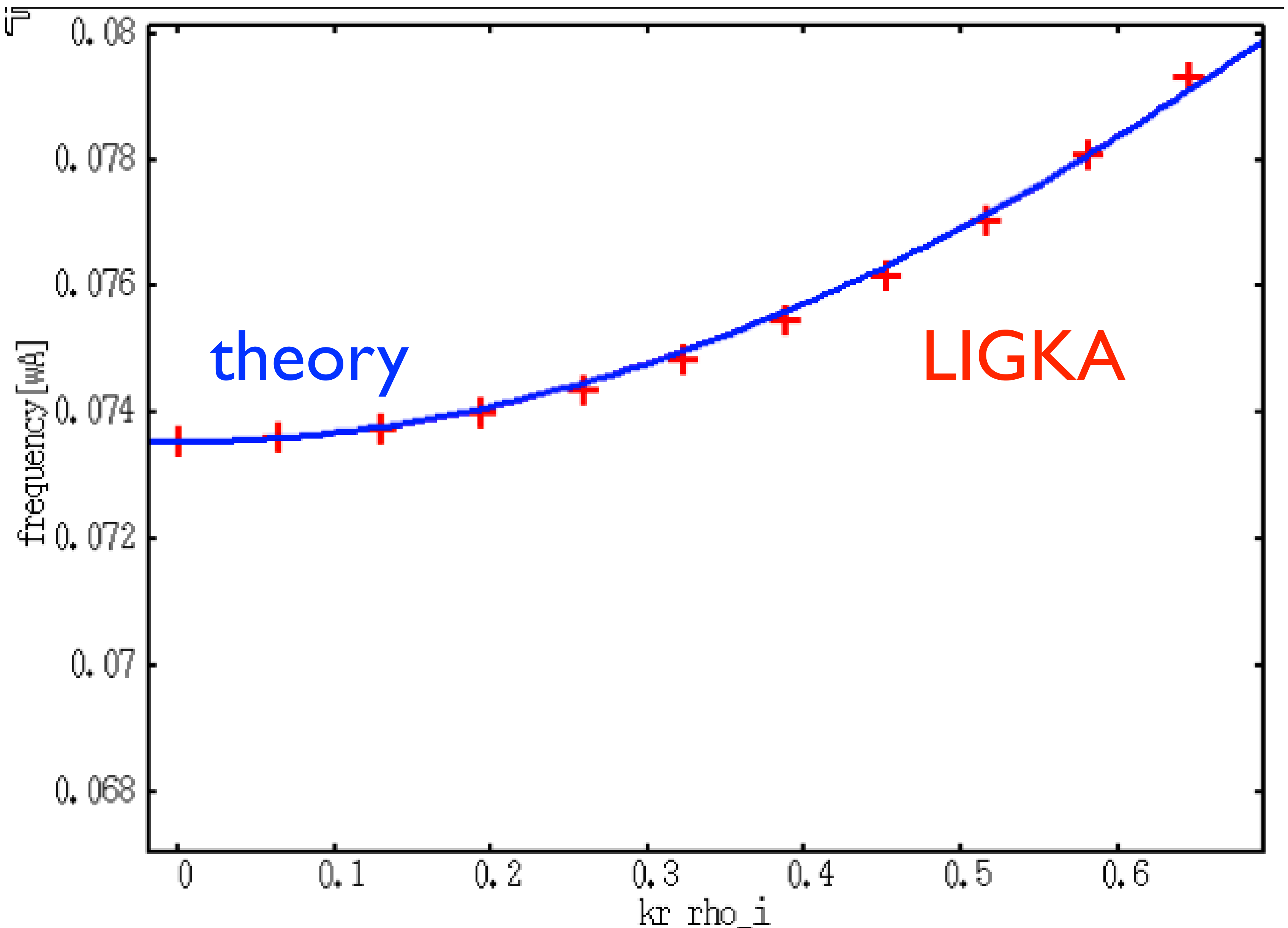

KGAM benchmark: analytical theory vs LIGKA

ASDEX Upgrade

q=3.25
τ=0.05

$$\frac{3}{4}+\frac{q^2}{\Omega}S_0(\Omega)\simeq\frac{3}{4}-\frac{q^2}{\Omega^2}\left(\frac{13}{4}+3\frac{T_e}{T_i}+\frac{T_e^2}{T_i^2}\right)$$
$$+\frac{q^4}{\Omega^4}\left(\frac{747}{32}+\frac{481}{32}\frac{T_e}{T_i}+\frac{35}{8}\frac{T_e^2}{T_i^2}+\frac{1}{2}\frac{T_e^3}{T_i^3}\right)$$
$$-i\pi^{1/2}q^4e^{-\Omega^2/4}\left[\Omega^5/256+(1+T_e/T_i)\Omega^3/32\right]$$

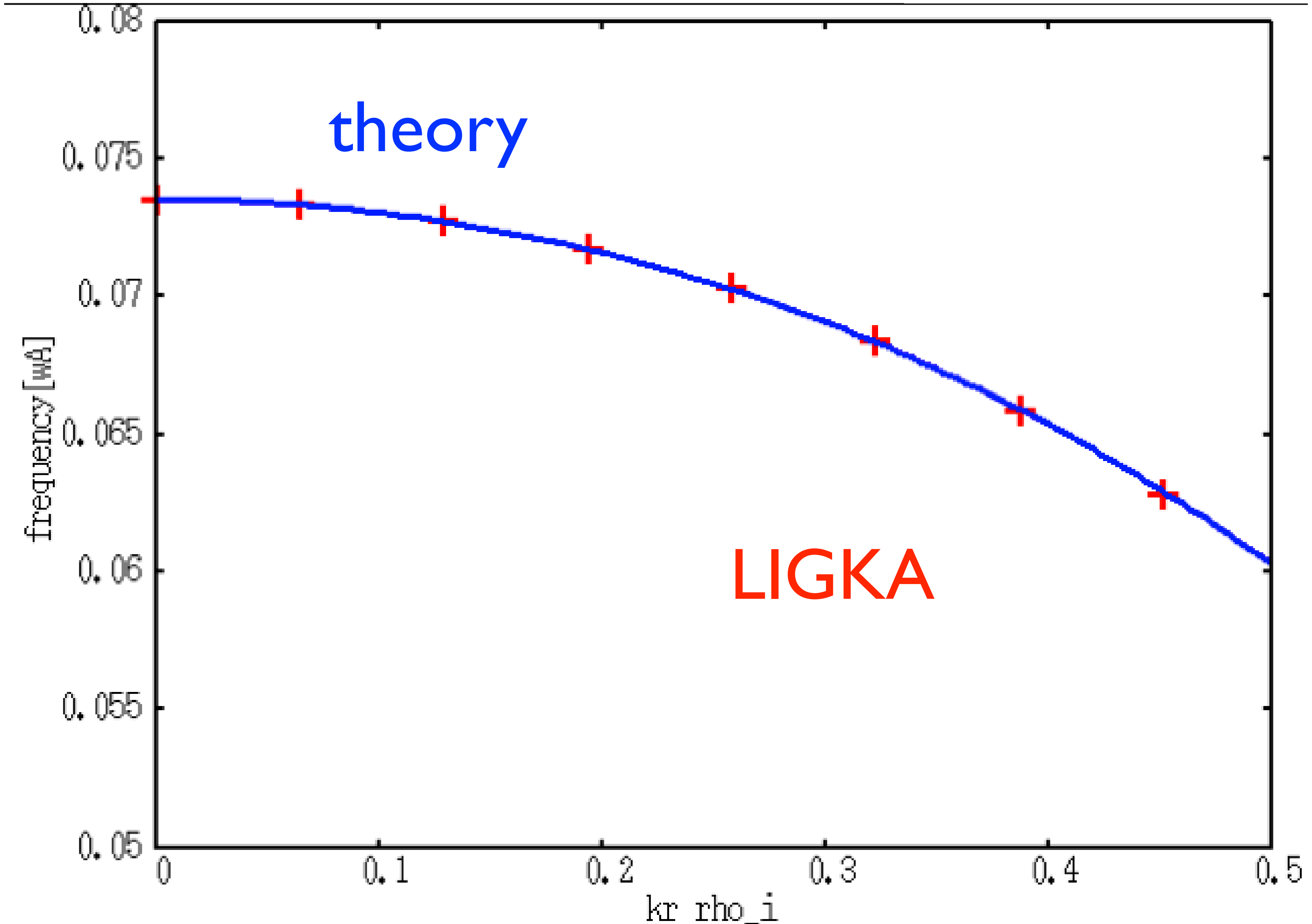

KGAM benchmark: analytical theory vs LIGKA

ASDEX Upgrade

q=3.25

τ=0.05

$$\frac{3}{4}+\frac{q^2}{\Omega}S_0(\Omega)\simeq\frac{3}{4}-\frac{q^2}{\Omega^2}\left(\frac{13}{4}+3\frac{T_e}{T_i}+\frac{T_e^2}{T_i^2}\right)+\frac{q^4}{\Omega^4}\left(\frac{747}{32}+\frac{481}{32}\frac{T_e}{T_i}+\frac{35}{8}\frac{T_e^2}{T_i^2}+\frac{1}{2}\frac{T_e^3}{T_i^3}\right)-i\pi^{1/2}q^4e^{-\Omega^2/4}\left[\Omega^5/256+(1+T_e/T_i)\Omega^3/32\right]$$

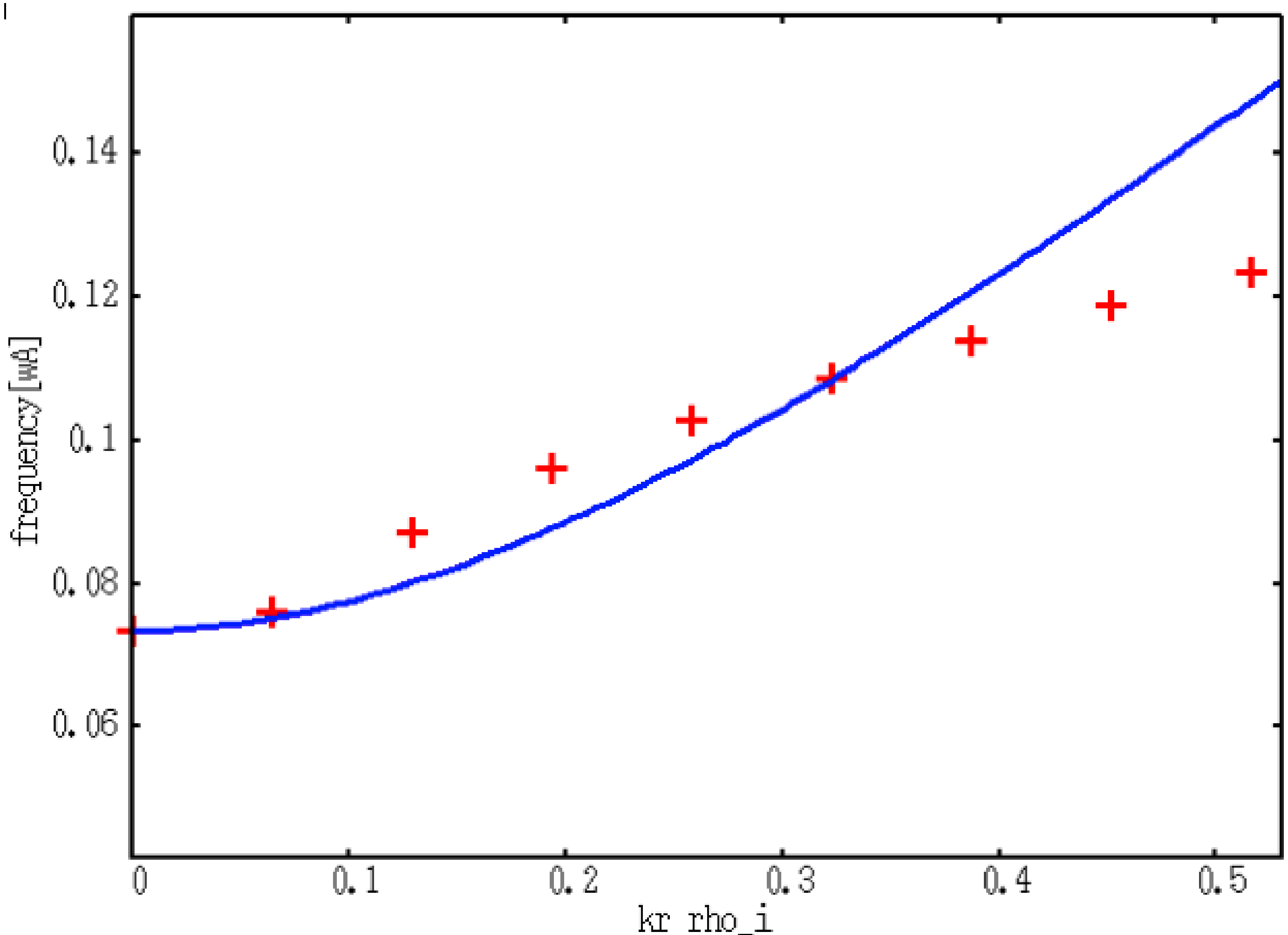

deviations for simple formula if equation is solved non-perturbatively

applied to AUG case

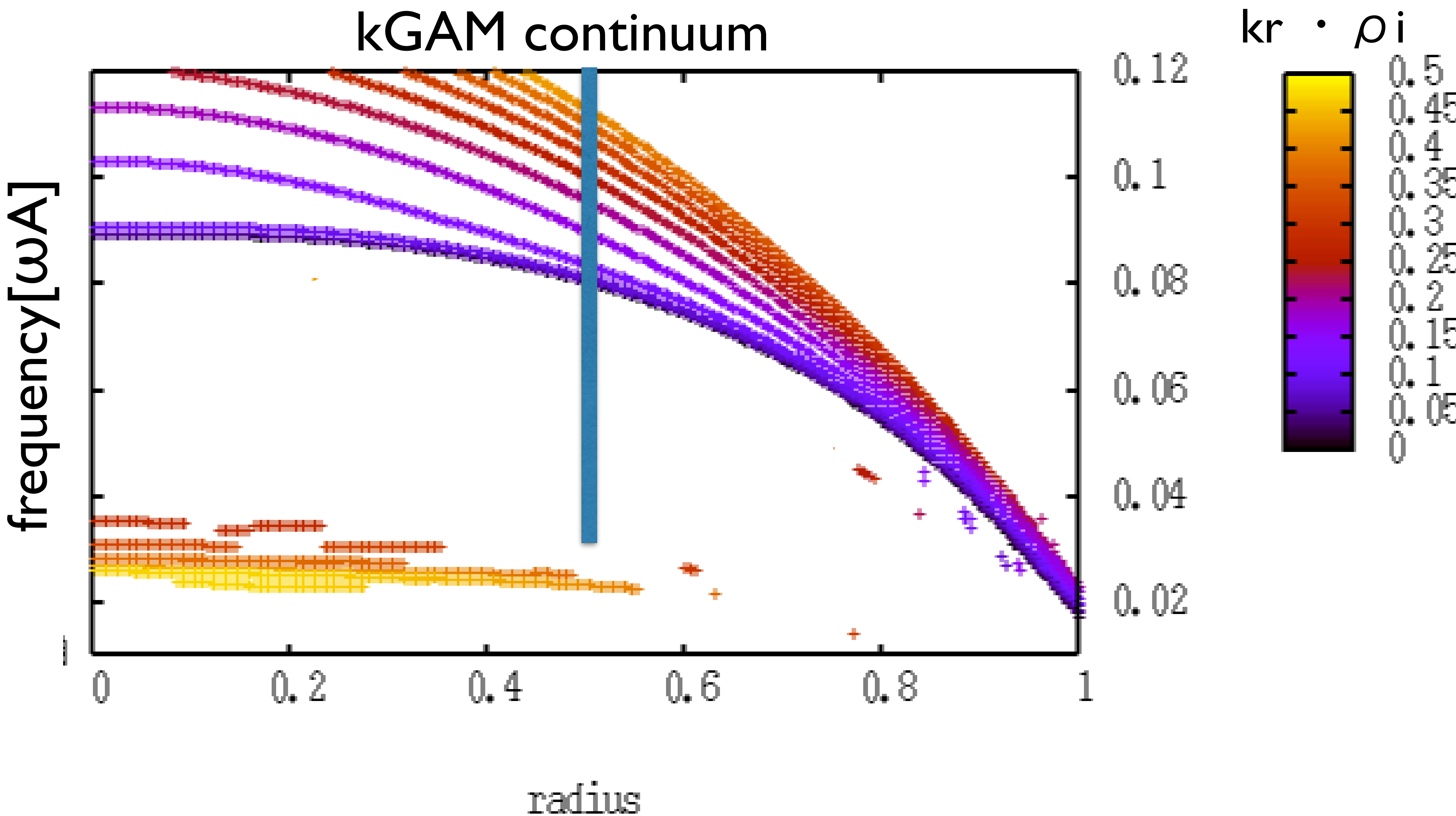

at qmin: ω(kr)

vg= ∂ω/∂kr can be determined from this:

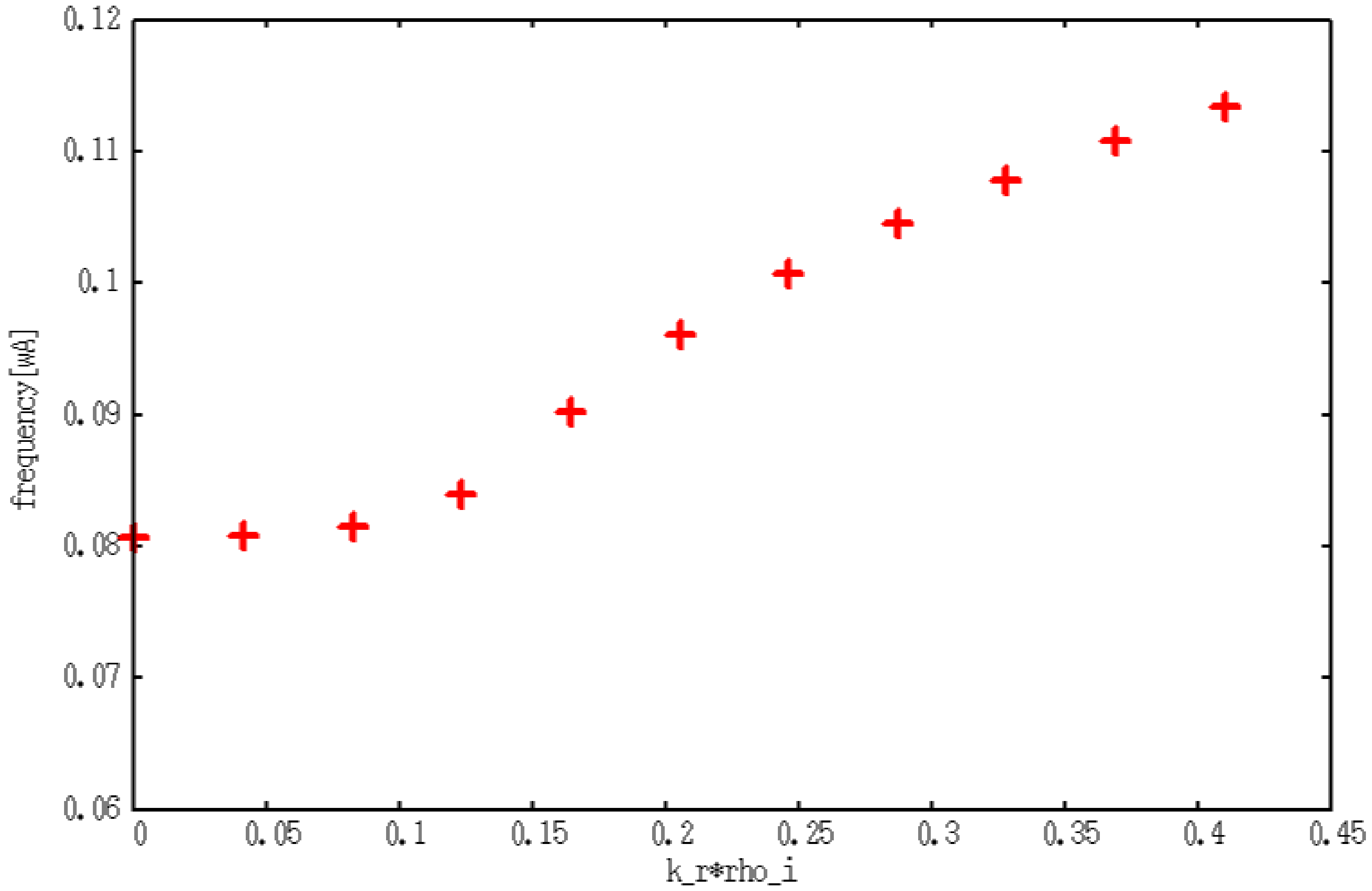

outward propagation q=2.1

at qmin: ω(kr)

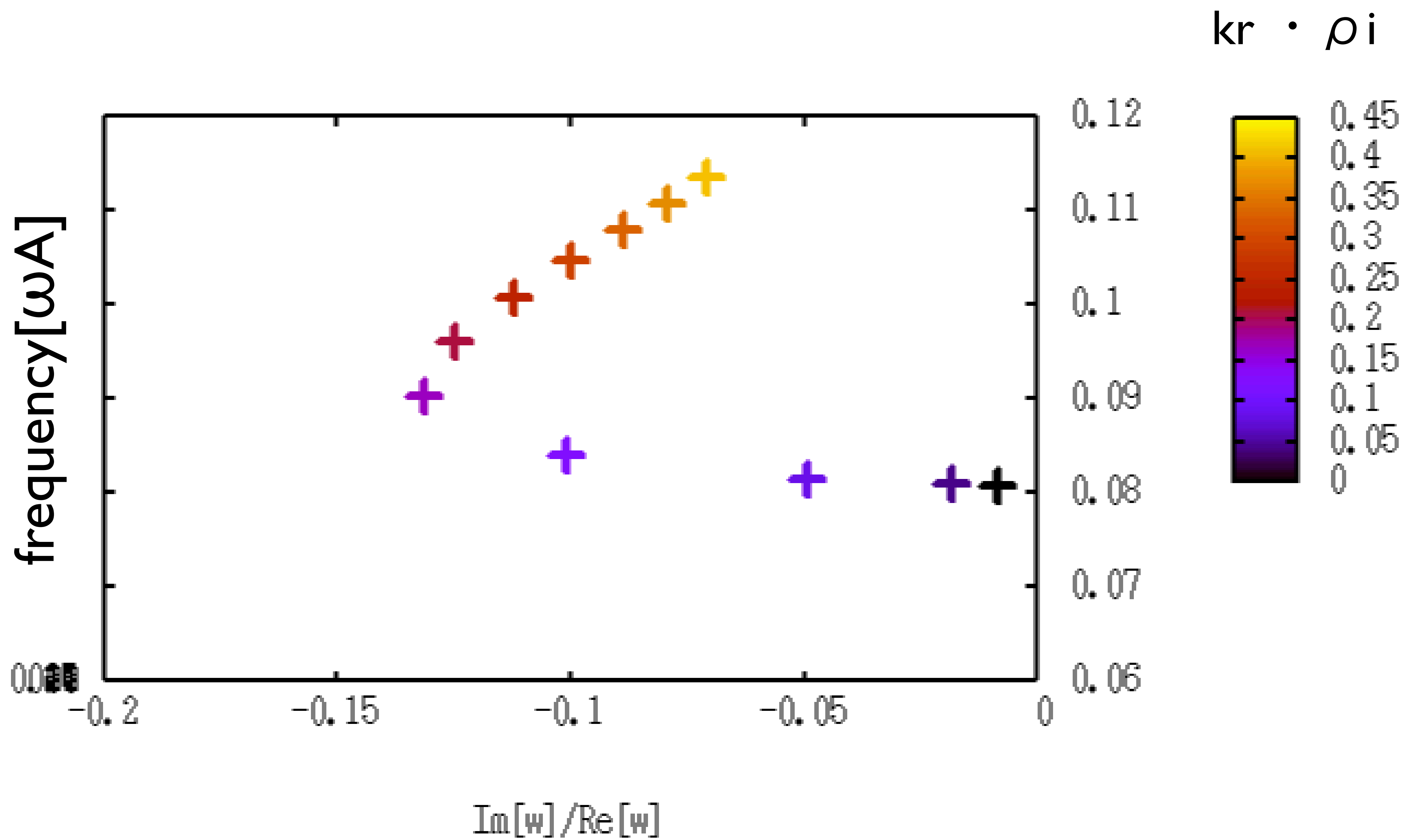

for short wavelength: frequency upshift causes reduced damping

for large Te/Ti: also inward propagation possible:

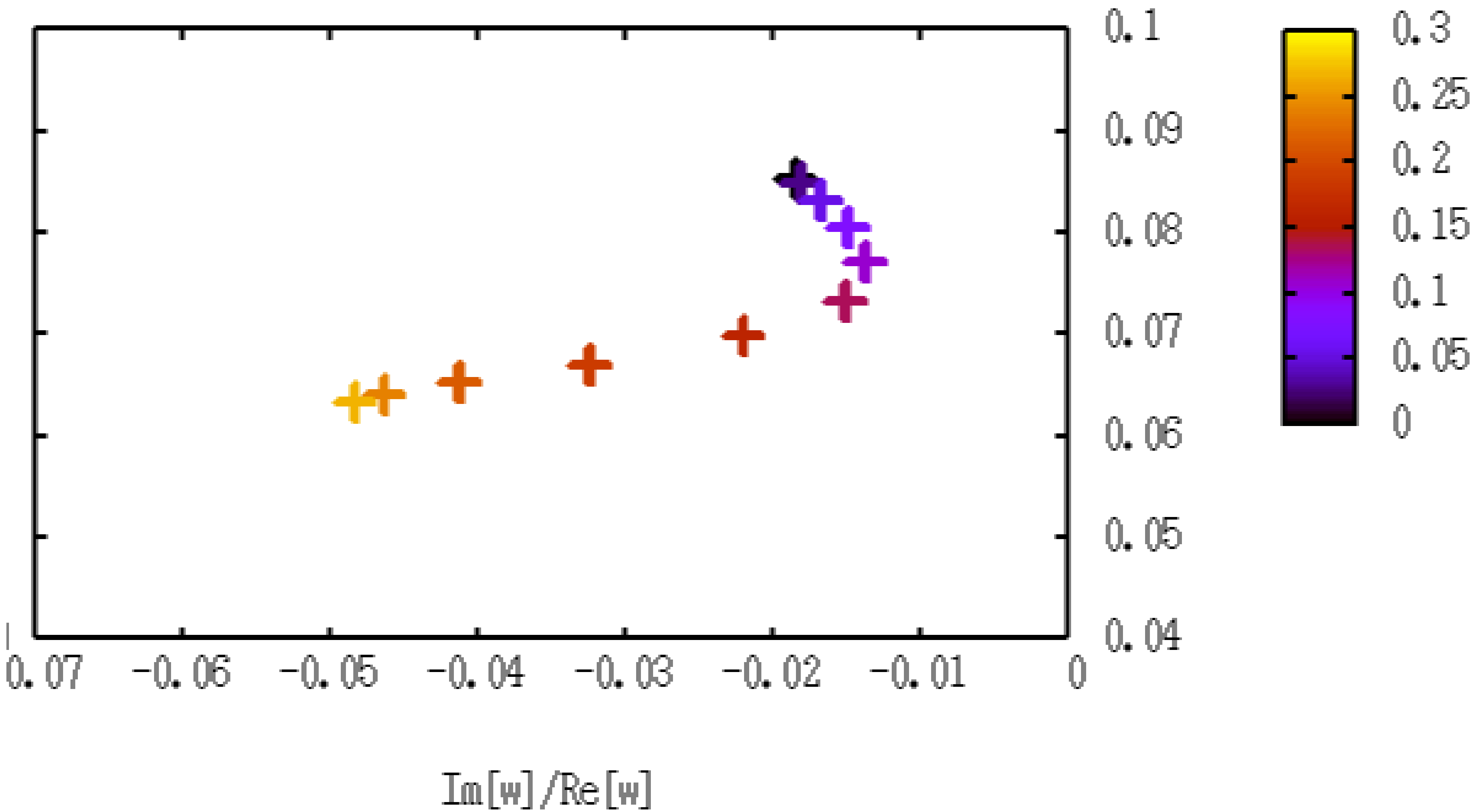

next step: apply quantitatively to EGAM physics
(kr is set by EP drift orbit width)

stable, global kGAM solutions emphasize importance of GAM continuum[LIGKA], exp. f_{EGAM} close to f_{GAM}

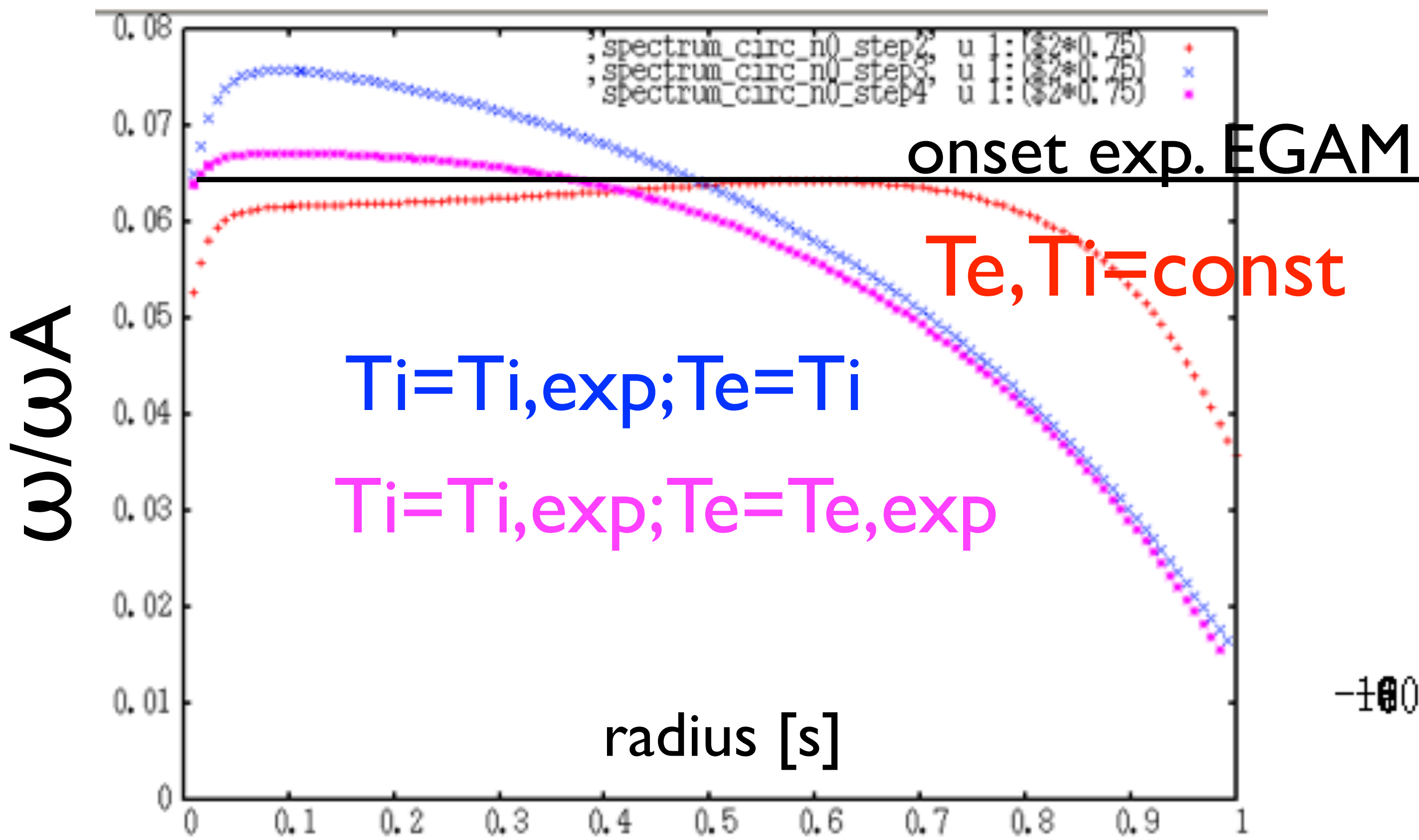

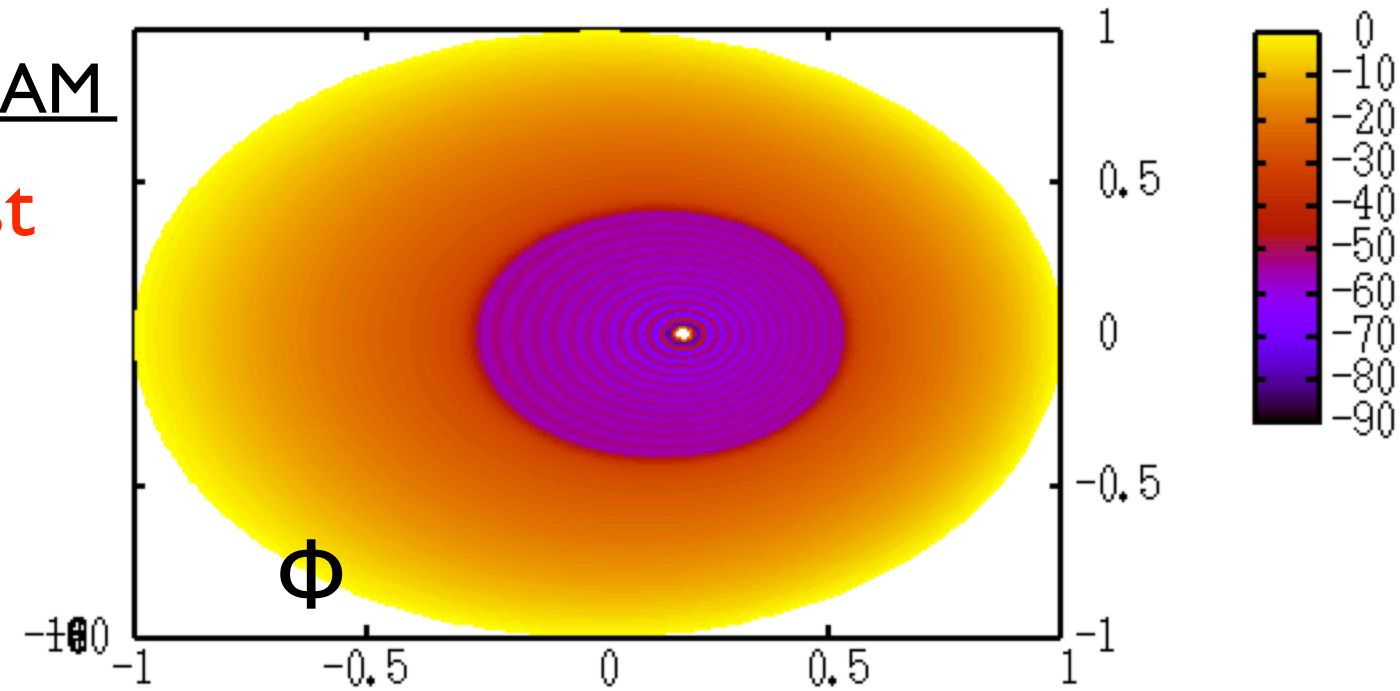

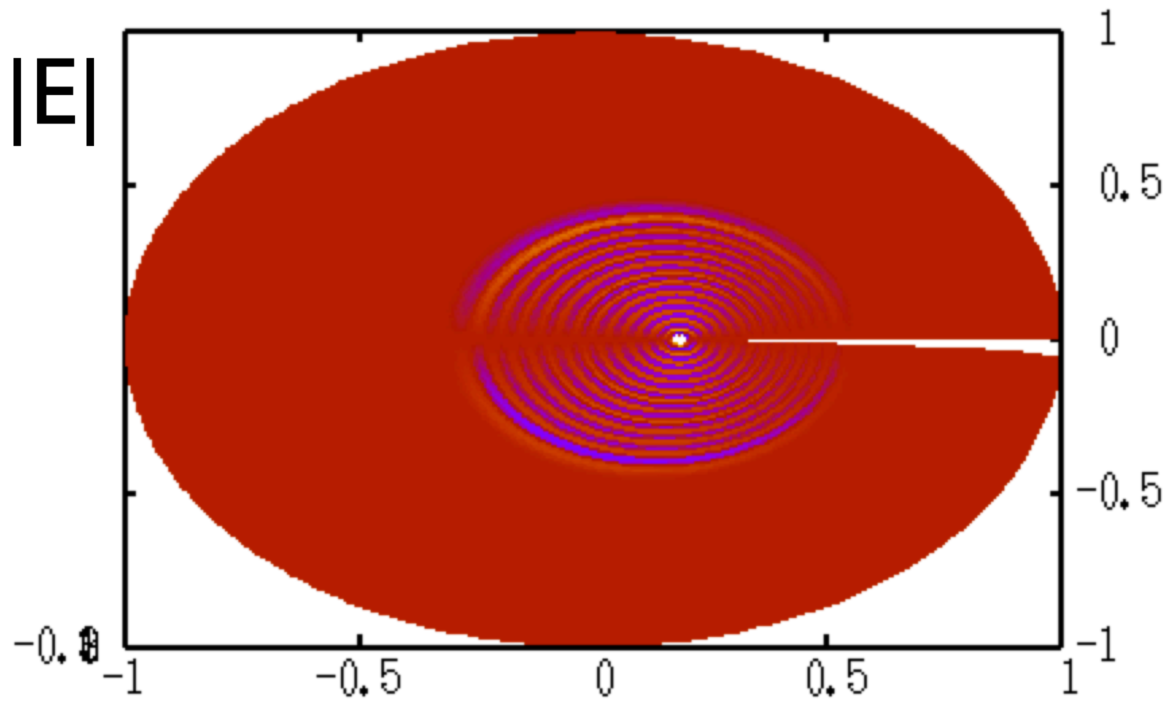

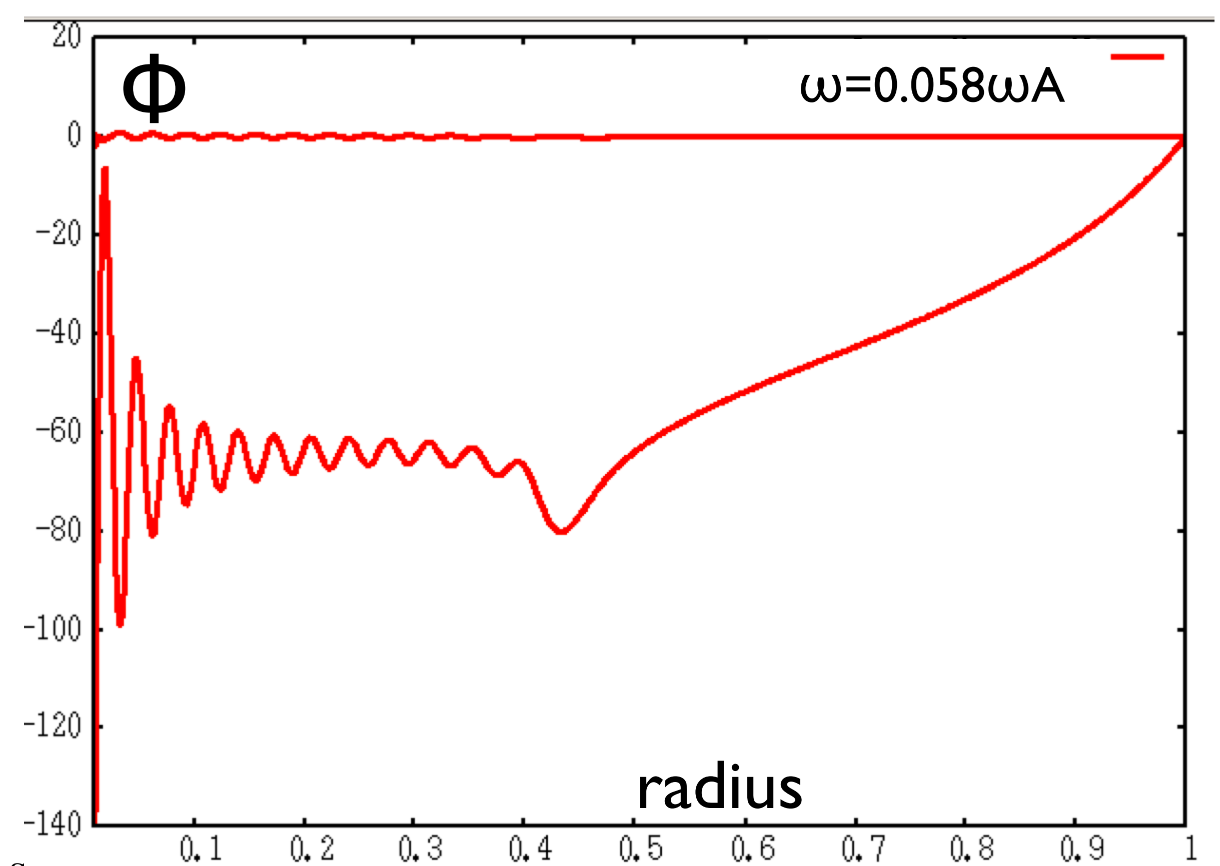

Effects of velocity anisotropy on the excitation of EGAMs;

Work in progress; To be submitted to Nuclear Fusion: Conf. series ,

I Chavdarovski, M Schneller, Z Qiu, A Biancalani;

- The local dispersion relation of energetic -particle-induced Geodesic acoustic mode (EGAMs) is derived for both circulating and trapped particle beam with single pitch angle slowing down and Maxwellian distribution.
- Solutions of the local dispersion relation for each case give the spectrum, the growth rate and the threshold of excitation as function of the slowing down critical energy (for the trapped) and the pitch angle (for circulating).
- Sample result: dispersion relation for trapped EP with slowing down distribution, as function of the bounce frequency and Λ. The logarithmic term gives the drive.

$$0 = -1+\frac{\omega_G^2}{\omega^2}+\frac{\pi}{8}N_b\frac{1}{\epsilon\Lambda_0 B_0}\left[\frac{3-2\Lambda_0 B_0(1-\epsilon)}{2(1-\Lambda_0 B_0(1-\epsilon)^{3/2})}\log\left(1-\frac{\omega_b^2}{\omega^2}\right)+\frac{1}{1-\Lambda_0 B_0(1-\epsilon)^{1/2}}\cdot\frac{\omega_b^2/\omega^2}{1-\omega_b^2/\omega^2}\right]$$

to be implemented together with anisotropic shifted Maxwellian into LIGKA

linear EGAM physics: codes agree rather well

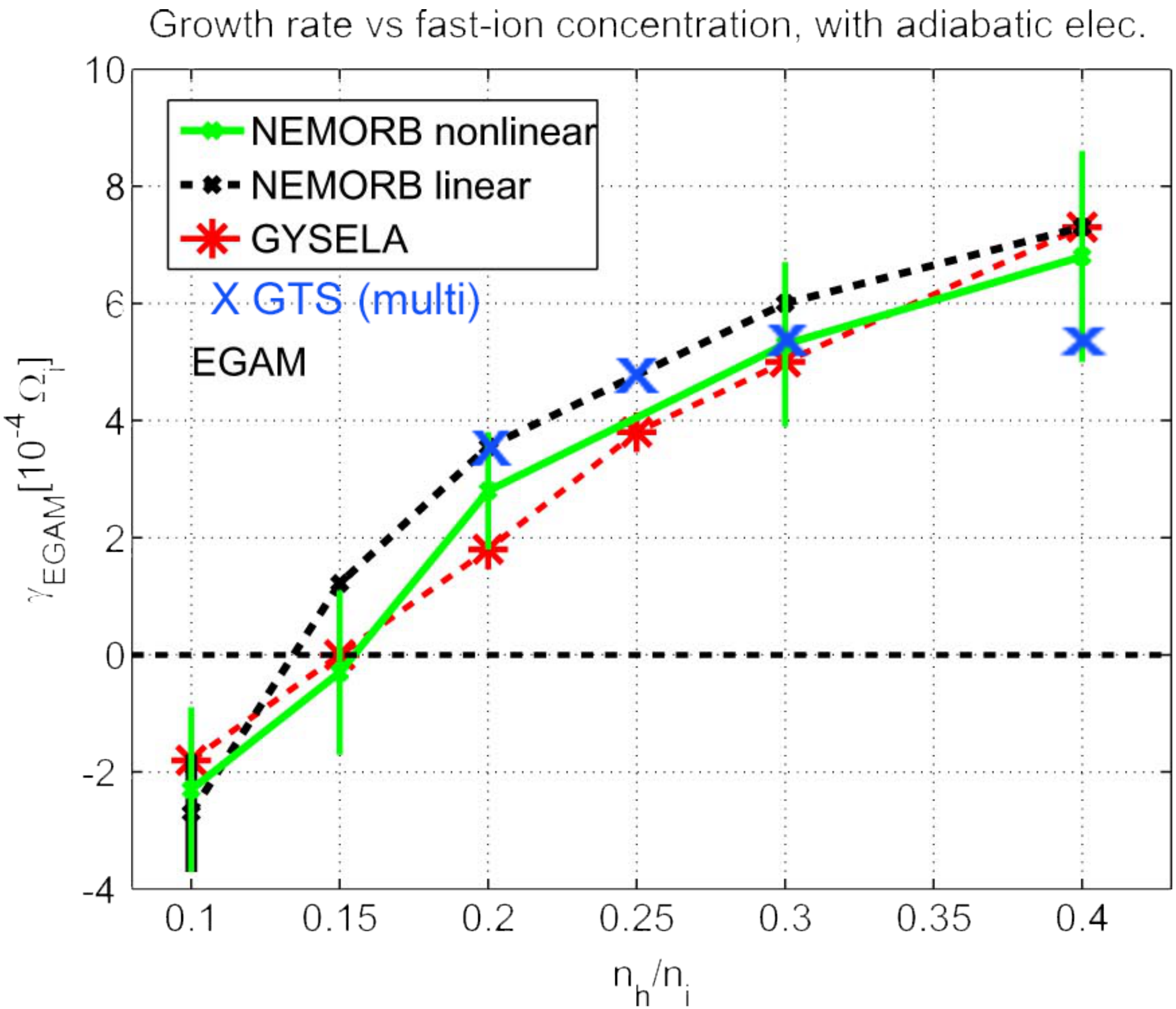

Saturation of EGAMs due to wave-particle nonlinearity

Work by A Biancalani, I Chavdarovski and Z Qiu. Currently on IPP pinboard.

- Only wave-particle nonlinearities are considered.
- The EGAM saturates mostly due to flattening of the EP profile in velocity space.
- Quadratic scaling of the saturated electric field with the linear growth rate is found, similarly to the beam-plasma instability: $\delta\bar{E}_r = \alpha_2 \gamma_L^2$

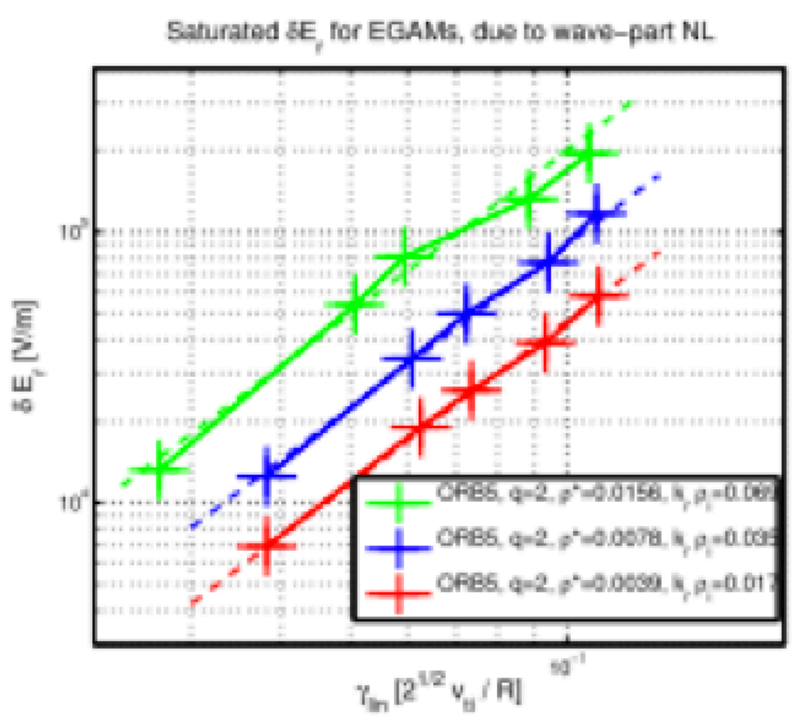

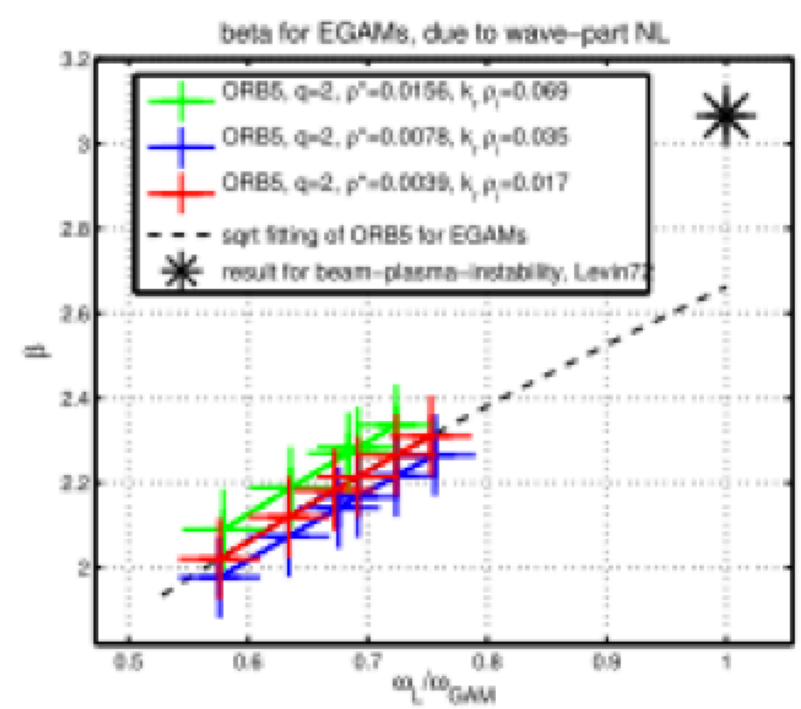

- The EP bounce frequency in the mode potential well is proportional to the linear growth rate : $\omega_b=2.7\,\gamma_L$. This factor is 3.2 for beam-plasma system.
- Near the saturation we observe a transition from adiabatic to non-adiabatic chirping, where the time derivative of the mode frequency is of the same order as the squared bounce frequency.
- Non-adiabatic chirping is due to non-perturbative response of the resonant particles, experiencing trapping and de-trapping in the mode.

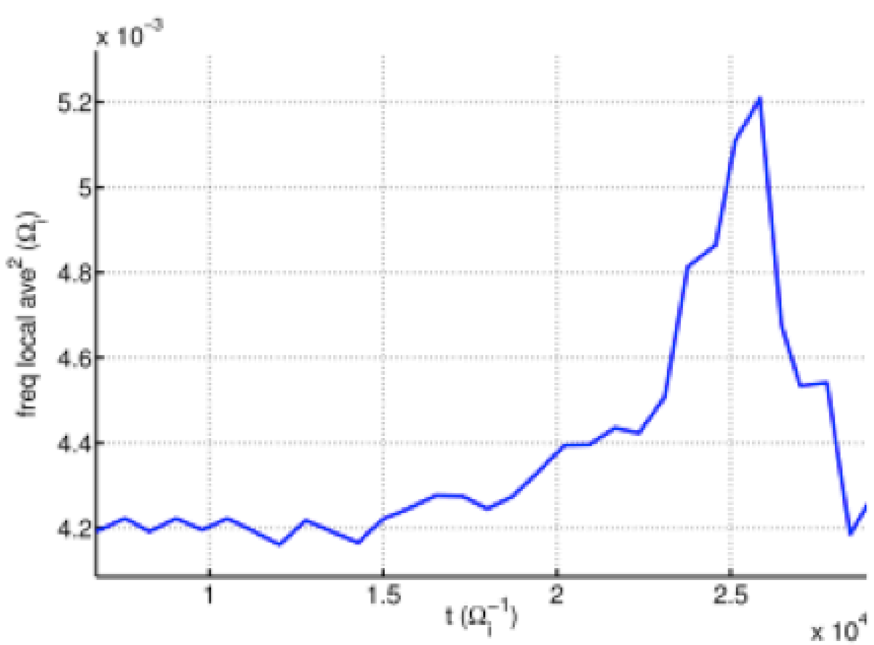

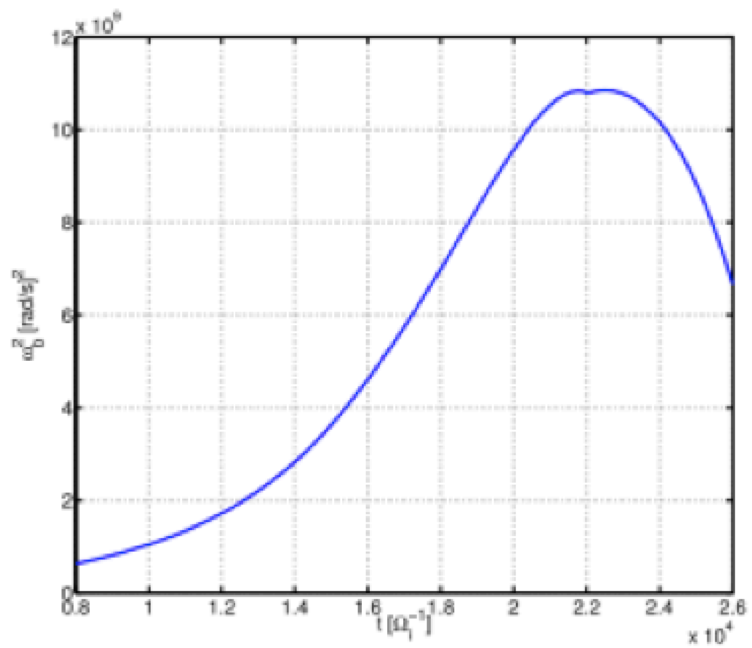

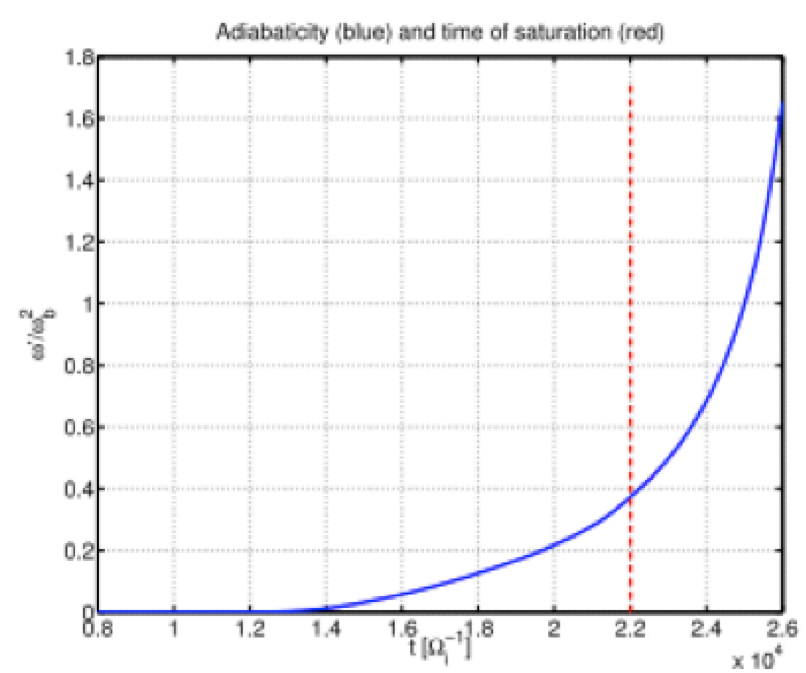

Non-linear generation of Zonal Flow and EGAMs second harmonic;

Published work Z Qiu , I Chavdarovski, A Biancalani and J Cao,

Physics of Plasmas 24, 072509 (2017);

- Both second harmonic and ZFZFs can be driven by EGAMs, with the finite orbit width (FOW) effects playing a dominant role in the nonlinear couplings, contrary to the thermal where toroidicity dominates
- The contribution of resonant EPs to the cross-section of the nonlinear couplings dominates that of the thermal plasma.
- The generated ZFZF has a radial scale length half of the pump EGAM and growth rate double the size.
- For GAMs perpendicular and parallel non-linearities cancel out , but present EP will dominate (Fu 2011). Second harmonic is generated with *l=1,2* resonances and radial scale half of the primary EGAM.

$$b_S \hat{\mathscr{E}}_{EGAM}(\omega_S)\hat{\Phi}_S = -\frac{ik_r T_i}{n_0 m\Omega}\left\langle \frac{\partial F_{0h}}{\partial E}\frac{3\omega\hat{\omega}_d^2}{(\omega^2-\omega_{tr}^2)(\omega_S^2-\omega_{tr}^2)}\right\rangle \times \frac{\hat{\Phi}_G\hat{\Phi}_G}{r}$$

$$\hat{\mathscr{E}}_{EGAM}(\omega_S) \equiv -1 + \frac{\omega_G^2}{\omega_S^2} + \frac{T_i}{n_0 m_i b_S}\left\langle \frac{\partial F_{0h}}{\partial E}\sum_{l=\pm1,\pm2}\frac{J_l^2(\hat{\Lambda}_S)\omega_S}{\omega_S - l\omega_{tr}}\right\rangle$$

conclusions

interesting and unique set of experimental AUG data:

- more stable EGAM scenarios developed
- non-linear coupling of EGAM and TAEs found
- second order EGAMs measured
- shrinking of mode structure found

modeling progress:

several linear and non-linear key physics items are being addressed

allows for physics understanding and development of fast reduced models while moving towards complete non-linear EM simulations

extra material

LIGKA and EUTERPE modeling started: TAE, n=1

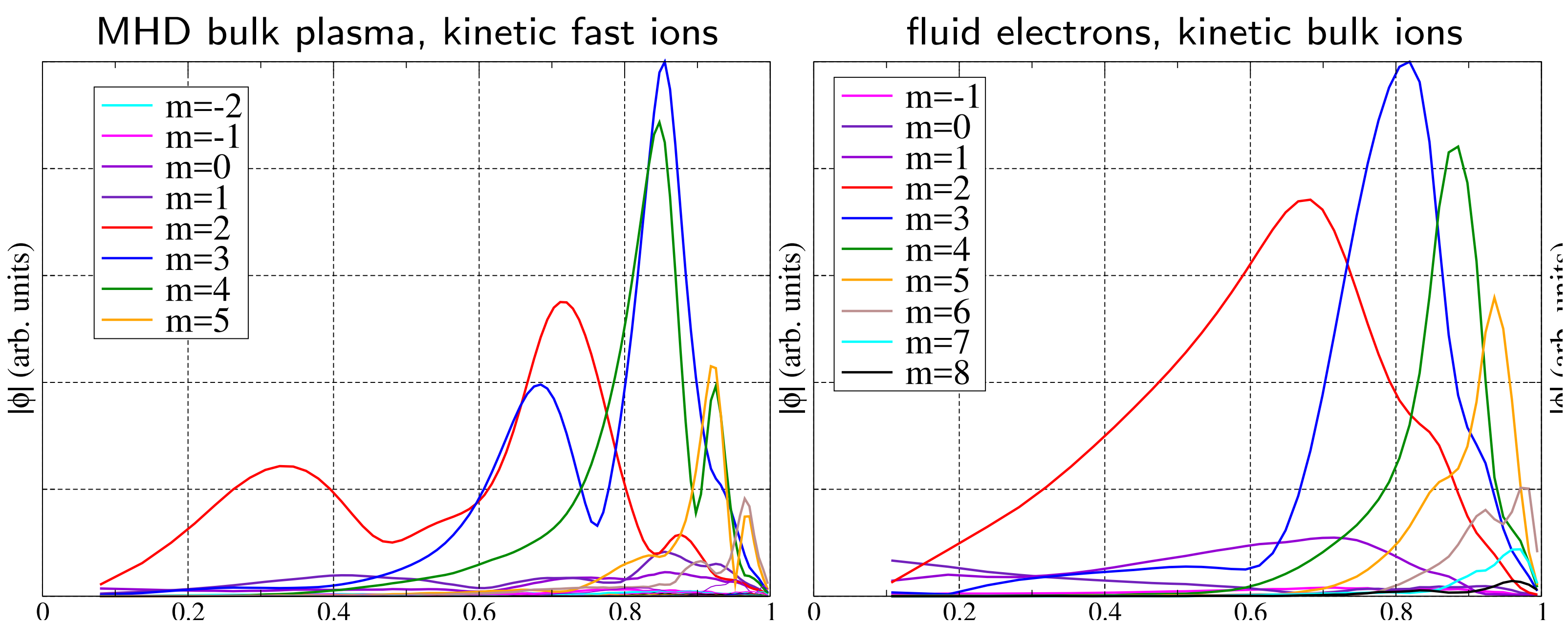

ρtor ρtor

Euterpe: [M. Cole] elliptic eq

ion diamagnetic propagation
exp: electron-diamagnetic propagation!

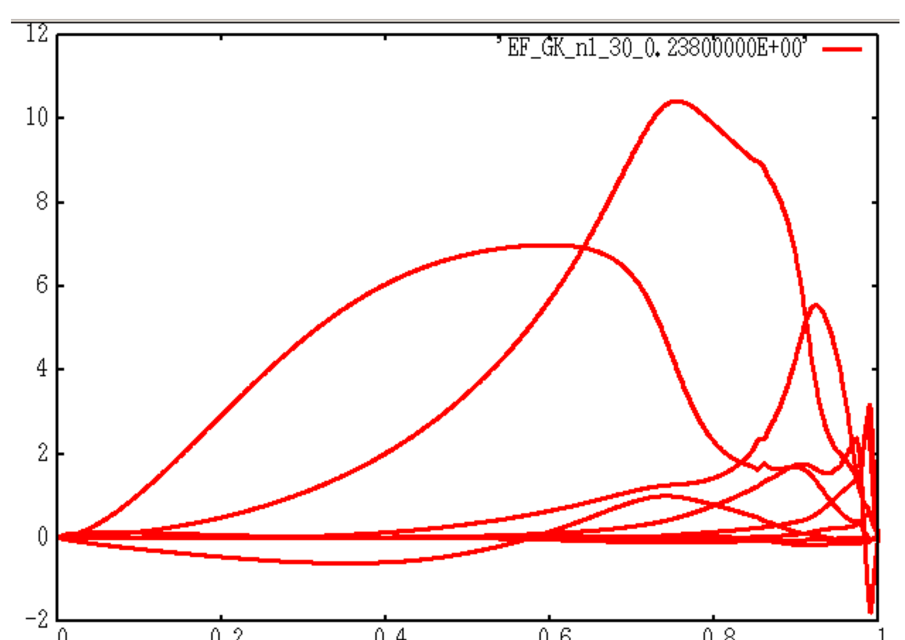

ρpol

LIGKA [Lauber]
AUG eq
ω=0.238 ωA,
γ/ω=1.5%

relevant control discharge:
almost no EGAM activity, but n=1 BAE/EPM

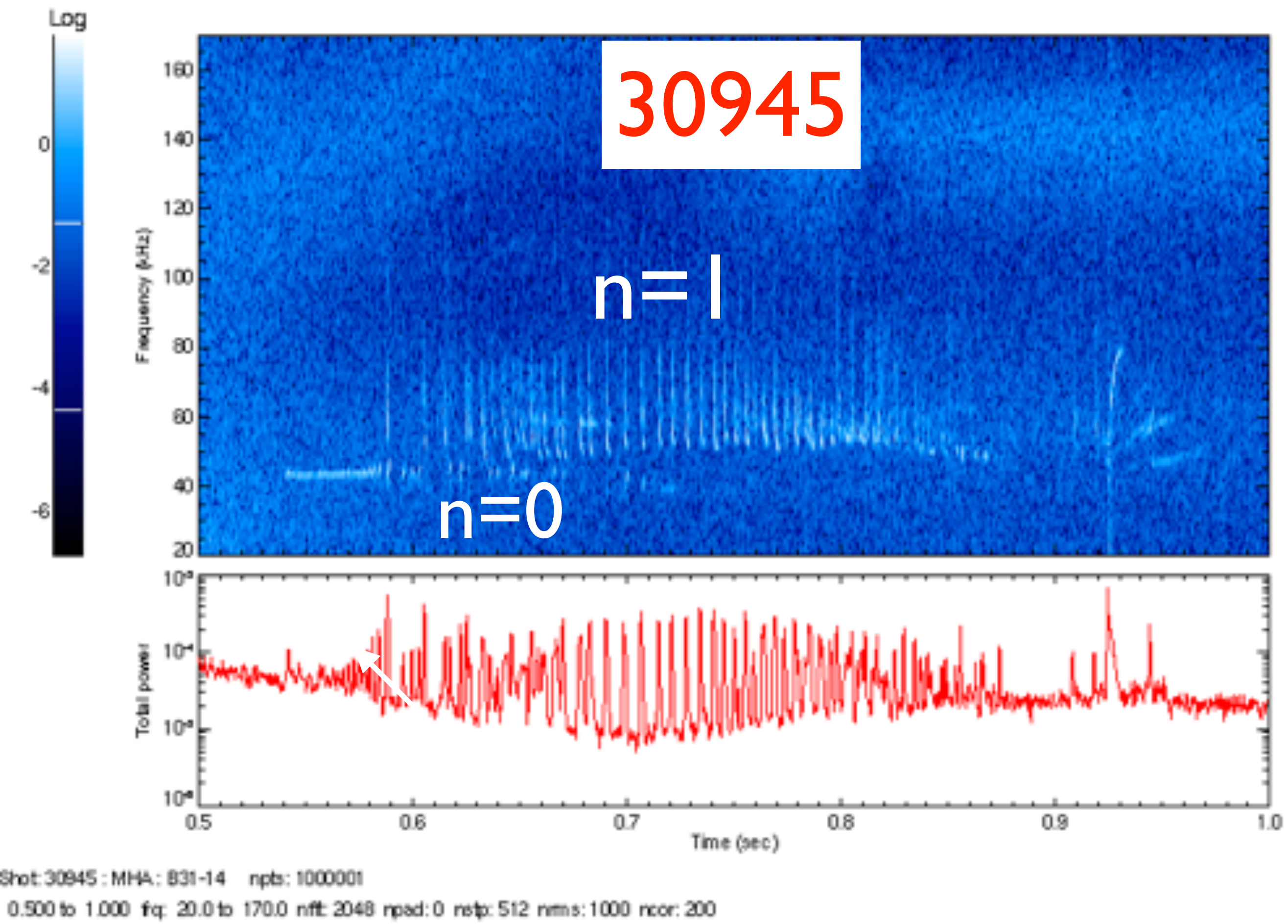

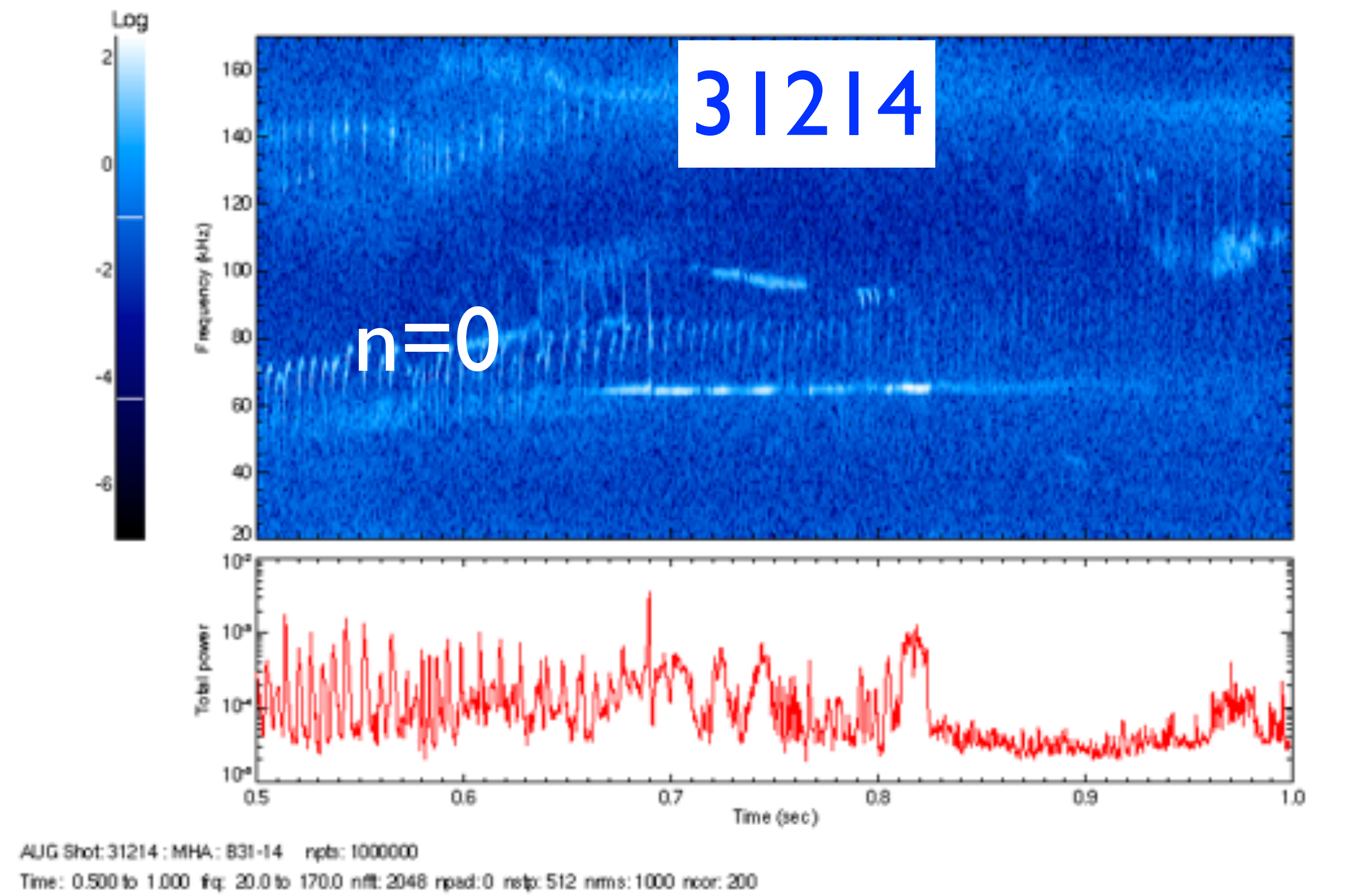

experimental difference: longer (30ms) on-axis pre-heating phase leads to very flat q-profile

note: BAE/EPM and GAM onset frequency almost constant
BAE/EPM onset above BAE continuum accumulation point
(toroidal rotation ~10kHz)

kinetic spectra

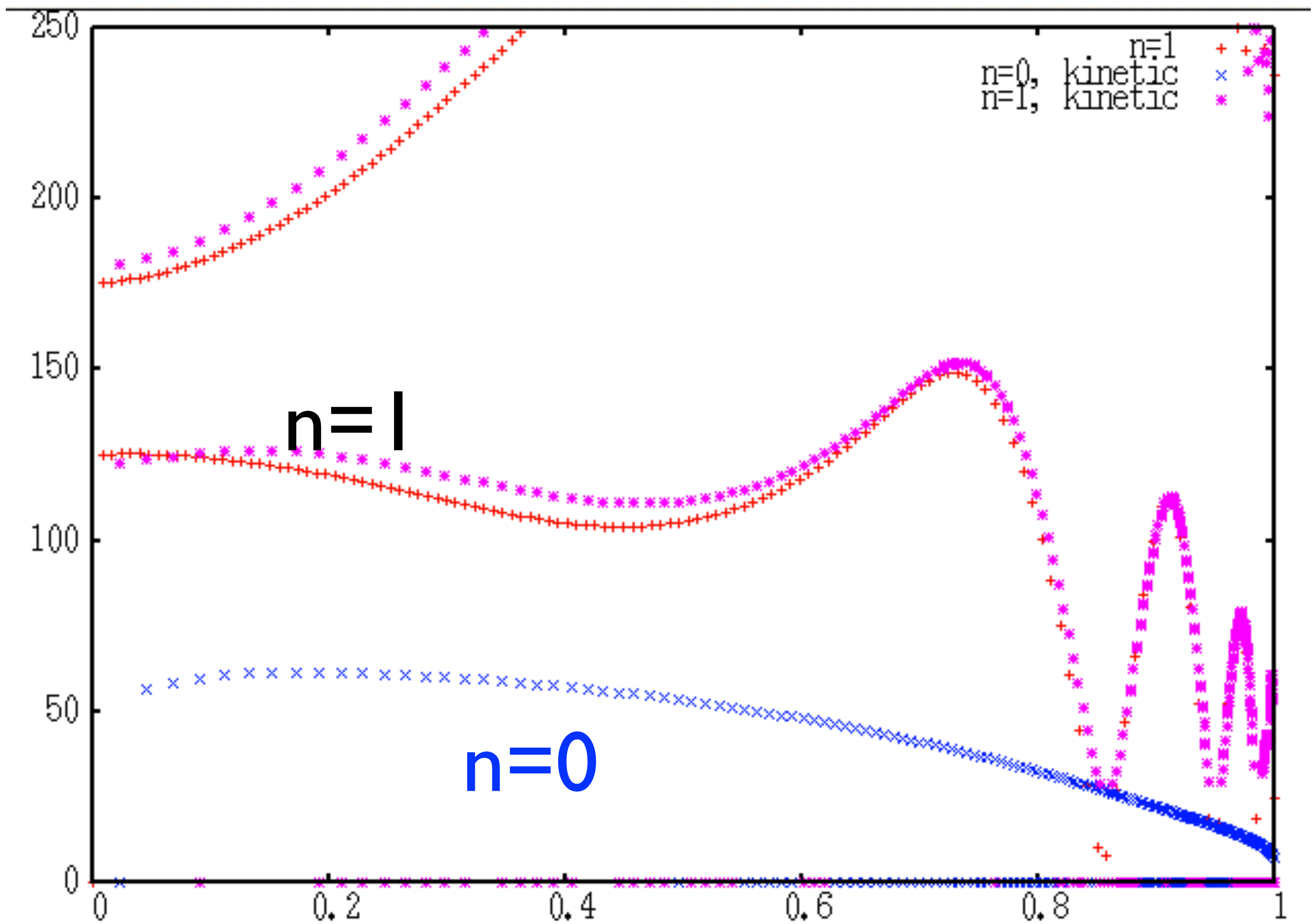

determine ∂ω/∂kr and match for discrete KBAE solutions

at BAE accumulation point (ρ=0.41): ~0 ✳
left from q=1 surface (ρ=0.355): <0 +
right from q=1 surface (ρ=0.459): >0 x

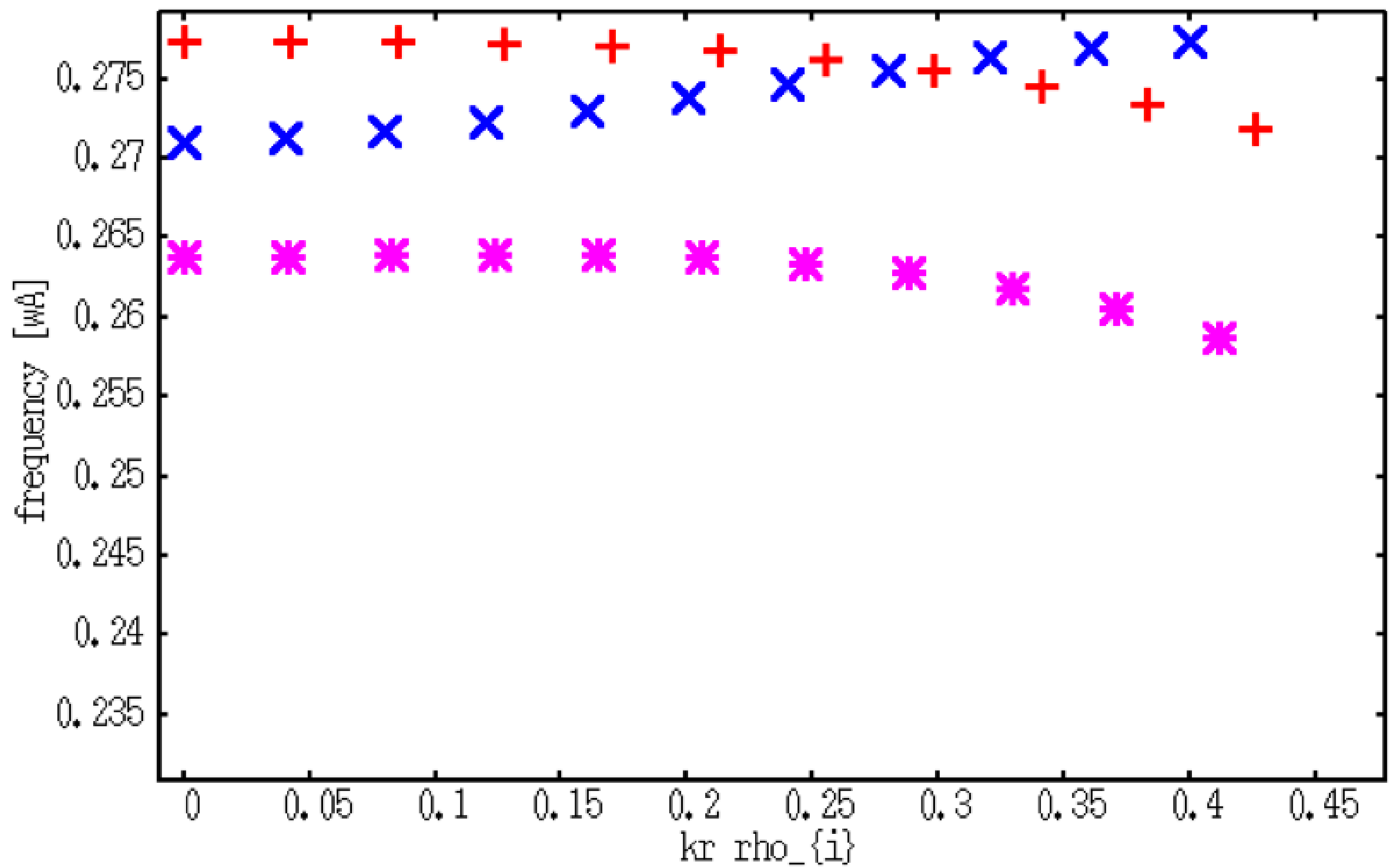

EP excitation and low-frequency modes to be studied

anisotropic NB distribution function:

[C. di Troia 2015]

ASDEX Upgrade

Equilibrium Distribution Function

- Constants of Motion at leading order if $B = \nabla\psi \times \nabla\phi + F\nabla\phi$
  - toroidal canonical momentum: $\mathcal{P}_\phi = \psi + (F/\omega_c)v_\parallel$
  - energy: $w = v^2/2 = v_\parallel^2/2 + \mu|B|$
  - $\lambda = \mu/w = (1 - v_\parallel^2/v^2)/|B|$, being $\mu = v_\perp^2/(2|B|)$
- Parameters
  - $\mathcal{N}$ is the overall regularization factor
  - T_w, α_w are the parameters of the $Gamma$ distribution in energy (at fixed λ)
  - $\mathcal{P}_{\phi 0}, \Delta_{P_\phi}$ are the parameters of the $Normal$ distribution in $\mathcal{P}_\phi$
  - $\lambda_0, \Delta_\lambda$ are the parameters of the $Normal$ distribution in λ (at fixed energy)
  - w_b, w_c are the parameters of the $SlowingDown$ distribution in energy

- $\mathcal{N} = 1.2 \times 10^{17}\ \mathrm{m}^{-3}$
- $T_w = 31.13$ keV,
- $\alpha_w = 1.0$,
- $\mathcal{P}_{\phi 0} = 0.035$ Wb,
- $\Delta_{P_\phi} = 0.02$ Wb
- $\lambda_0 = 0.08\ \mathrm{T}^{-1}$
- $\Delta_\lambda = 0.12\ \mathrm{T}^{-1}$
- $w_b = 93$ keV,
- $w_c = 15$ keV

$$f_{\mathrm{Ref1}}(\mathcal{P}_\phi, w, \lambda) = \mathcal{N}\frac{(1+\lambda/\lambda_0)(w/T_w)^{\alpha_w}}{\sqrt{2\pi}}\frac{\mathrm{H}(w_b - w)}{w^{3/2} + w_c^{3/2}} \times$$

$$\times \exp\left[-\frac{(\mathcal{P}_\phi - \mathcal{P}_{\phi 0})^2}{\Delta_{P_\phi}^2}\right] \exp\left[-\frac{w}{T_w}\left(\frac{\lambda - \lambda_0}{\Delta_\lambda}\right)^2\right]$$

first: shifted Maxwellian for EGAM benchmark

ideal n=1 SAW spectrum

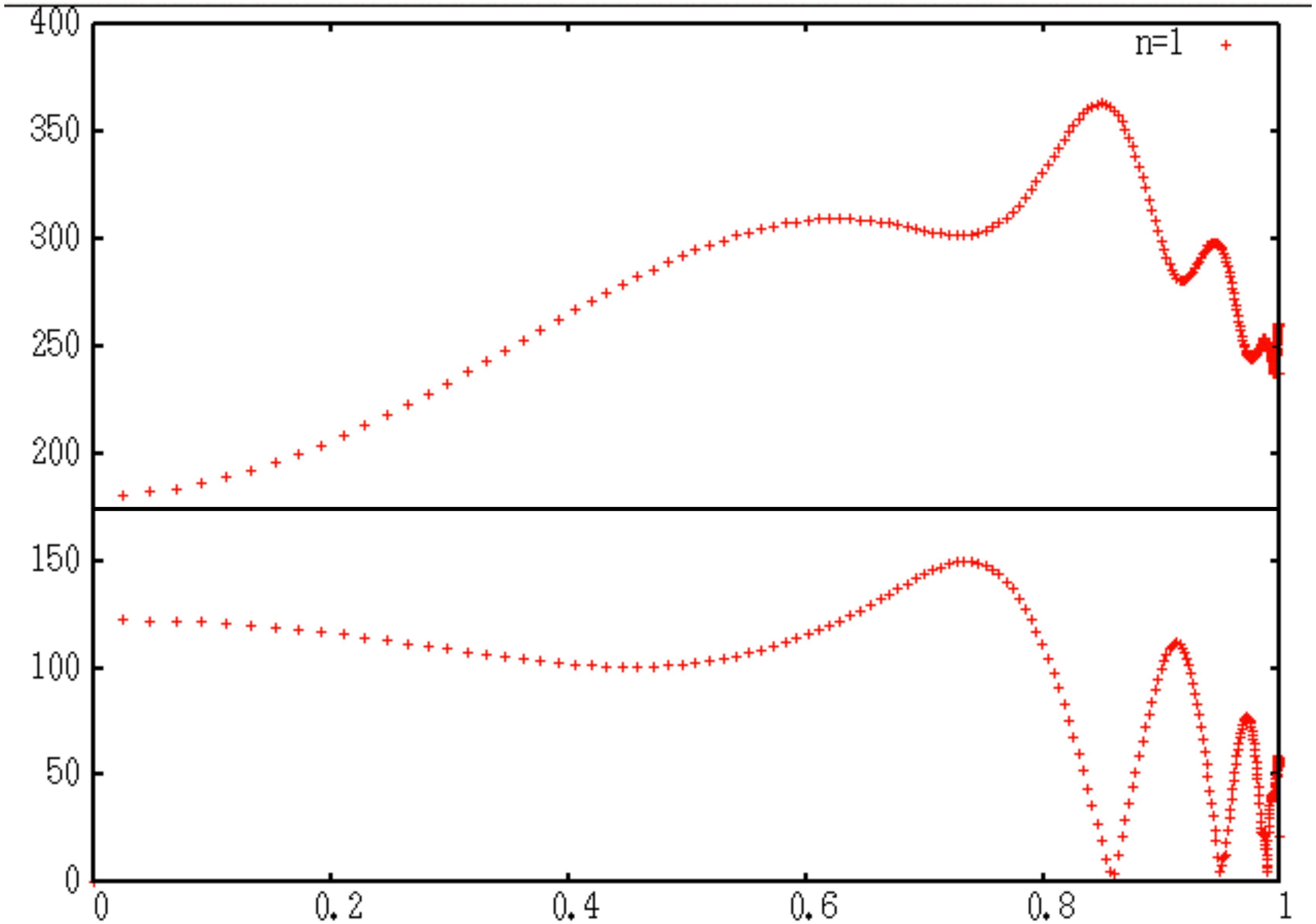

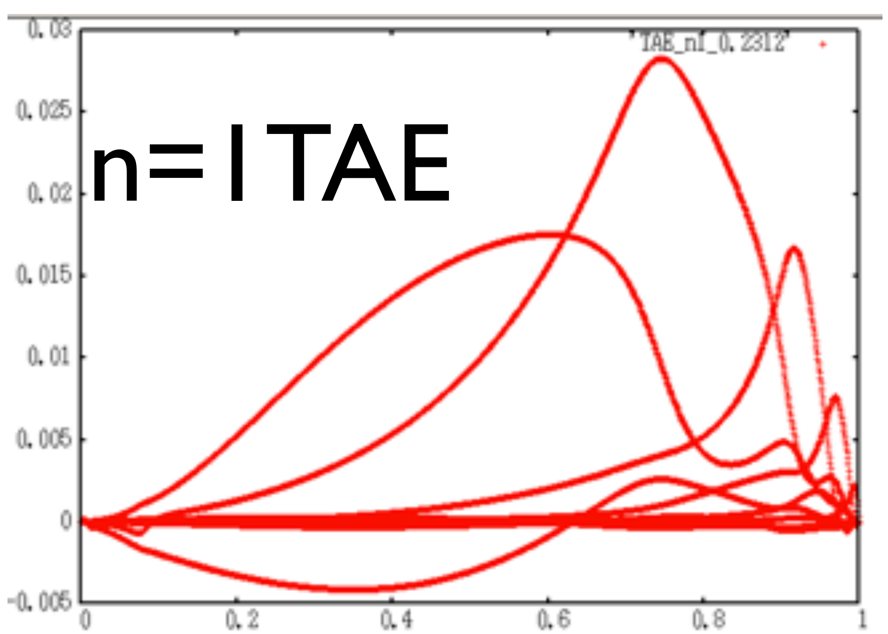

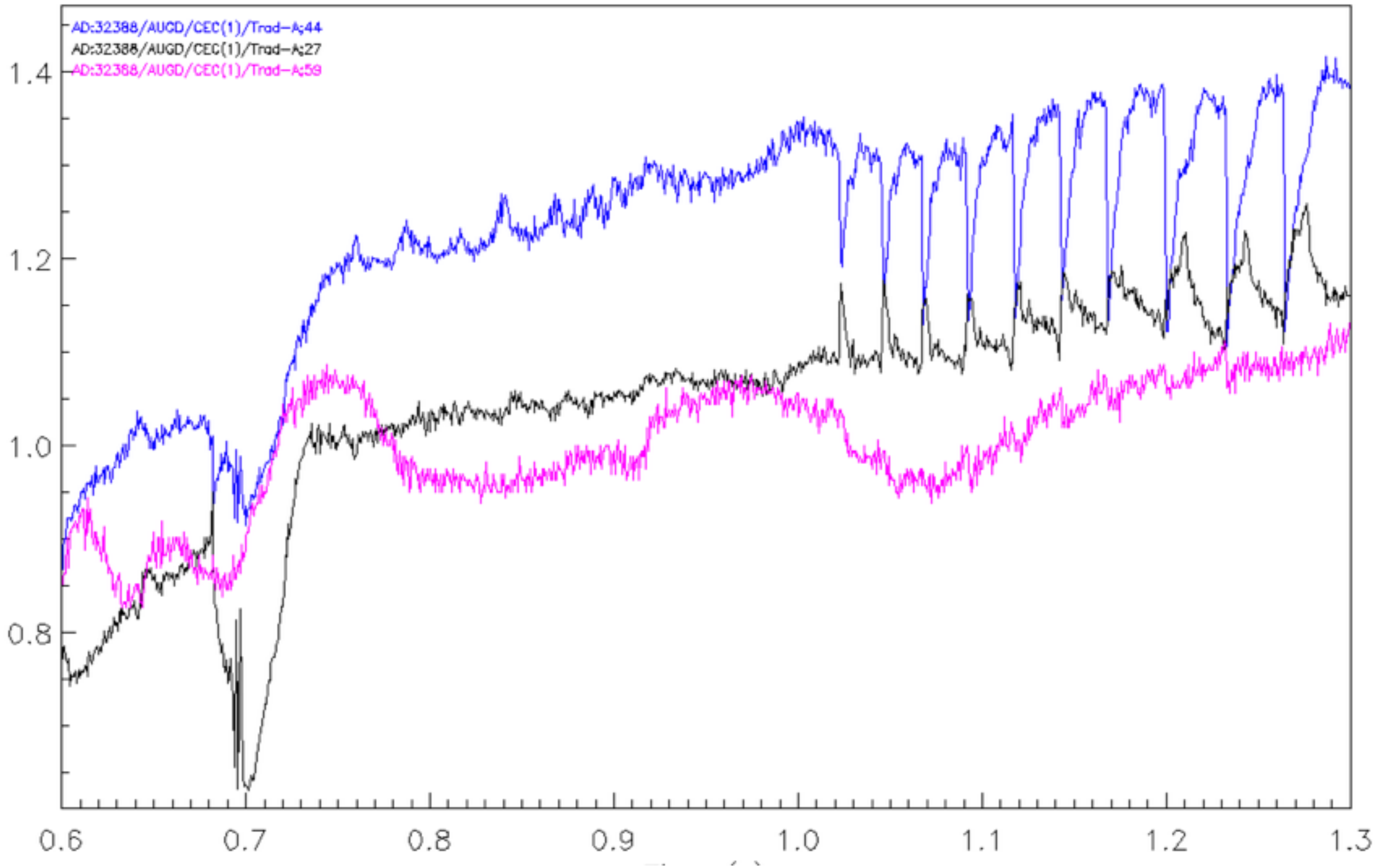
AD:32388/AUGD/CEC(1)/Trad-A;44
AD:32388/AUGD/CEC(1)/Trad-A;27
AD:32388/AUGD/CEC(1)/Trad-A;59
1.4
1.2
1.0
0.8
0.6
0.7
0.8
0.9
1.0
1.1
1.2
1.3

- **Bicoherence analysis** is a widely applied method for identifying quadratic nonlinear interactions of **stationary processes [1]**

$$b^2(f_1,f_2) = \frac{|\mathbf{A}[X(f_1)X(f_2)X^*(f_1+f_2)]|^2}{\mathbf{A}[|X(f_1)X(f_2)|^2]\mathbf{A}[|X^*(f_1+f_2)|^2]}, \text{ with } \mathbf{A}[Y] := \lim_{N\to\infty}\frac{1}{N}\sum_{i=1}^{N} Y_i,$$

- Signals exhibiting **rapidly changing amplitudes or frequencies** (typical in the case of strongly driven EPMs) may cause **high bicoherence even without phase coupling**

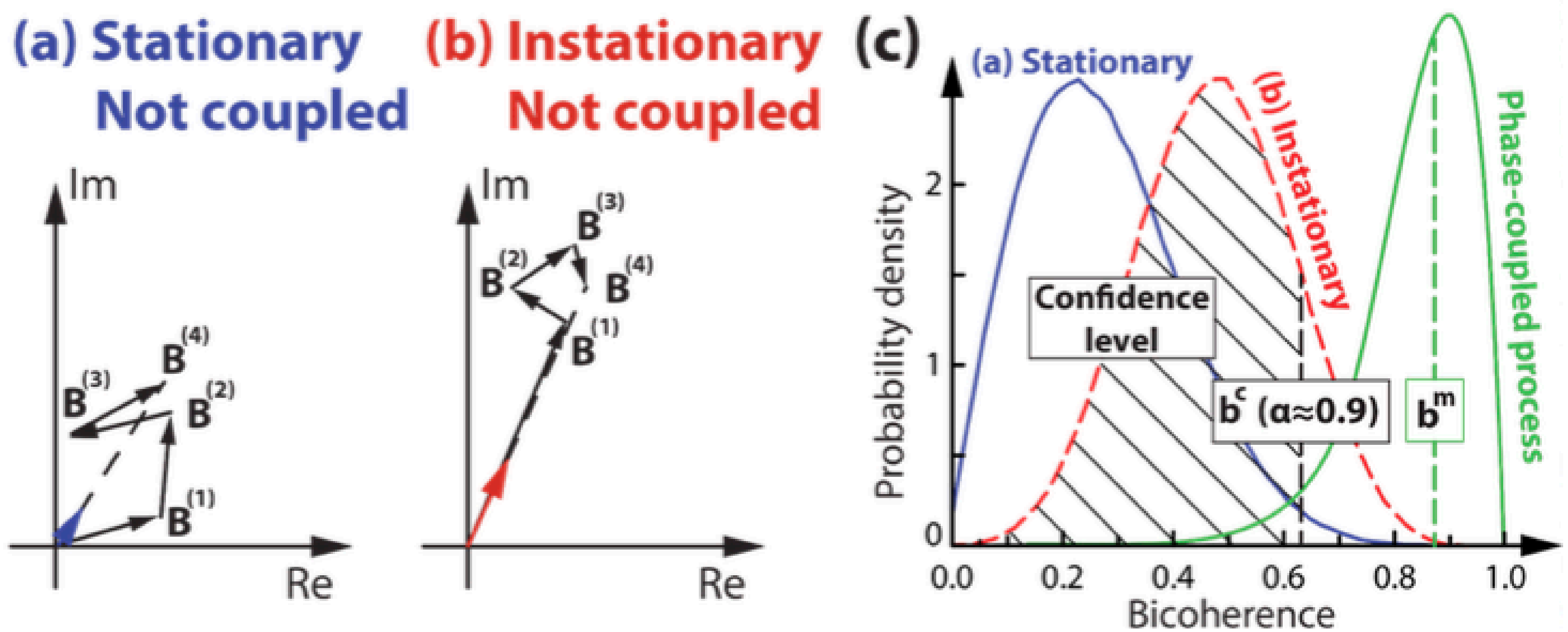

- **Phase randomized bicoherence probability density function** calculation for each (f_1,f_2) point, which will **describe** a random **process without** any **phase coupling.**

- We can set an **α confidence level**, which will define a **b_c critical bicoherence value** (at each (f_1,f_2) point)

$$\alpha = \int_0^{b^c} \rho(b)\mathrm{d}b$$

- **Bicoherence values higher than b_c** are from **non-phase coupled** process with **1-α probability**. **Confidence level** can be used as a **filtering parameter**, by only plotting bicoherence values higher than b_c, thus **eliminating probable false positives**

include small but finite kr (background only): finite Larmor radius and orbit width effects

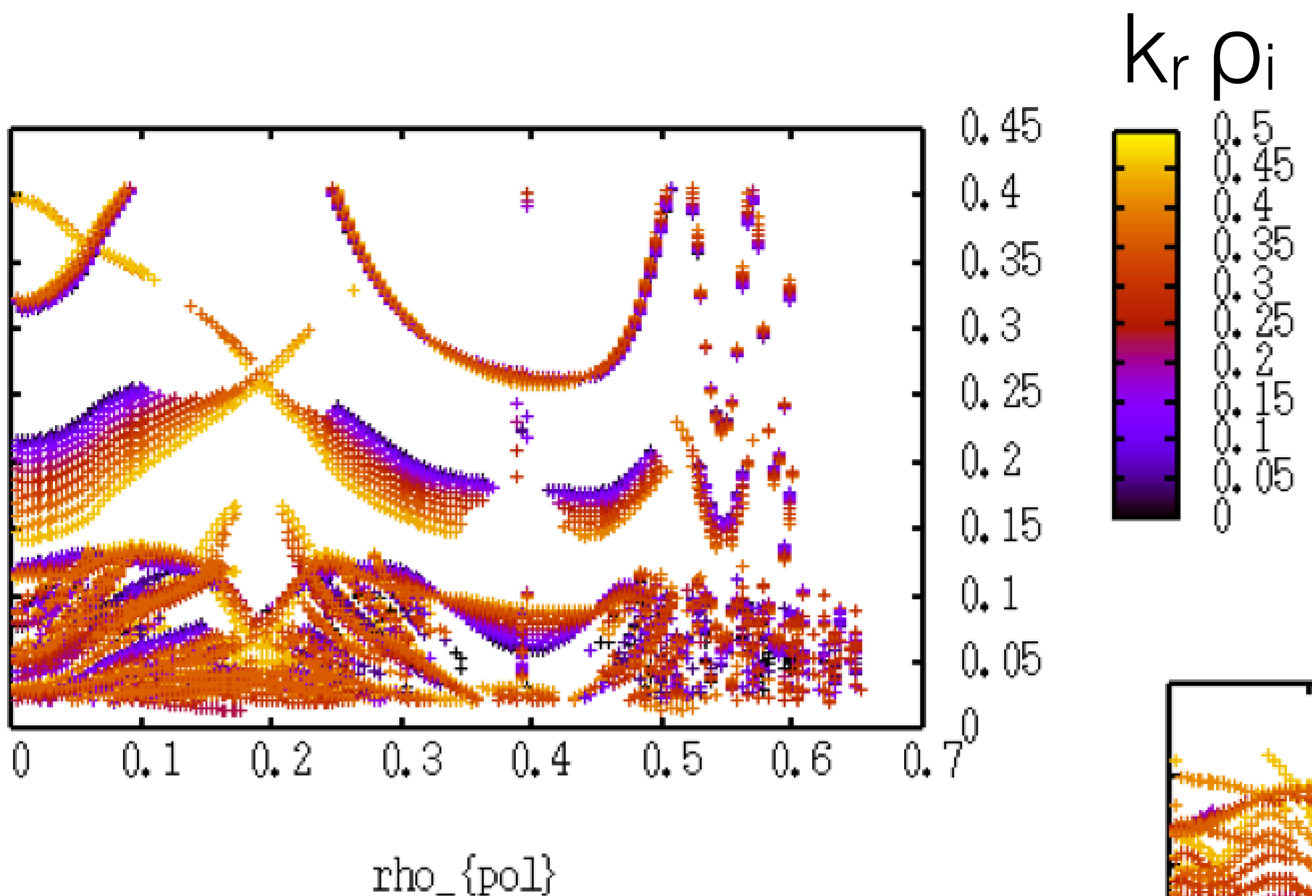

using analytical FLR+FOW model (see ITPA talk Seville, 2017,to be published)

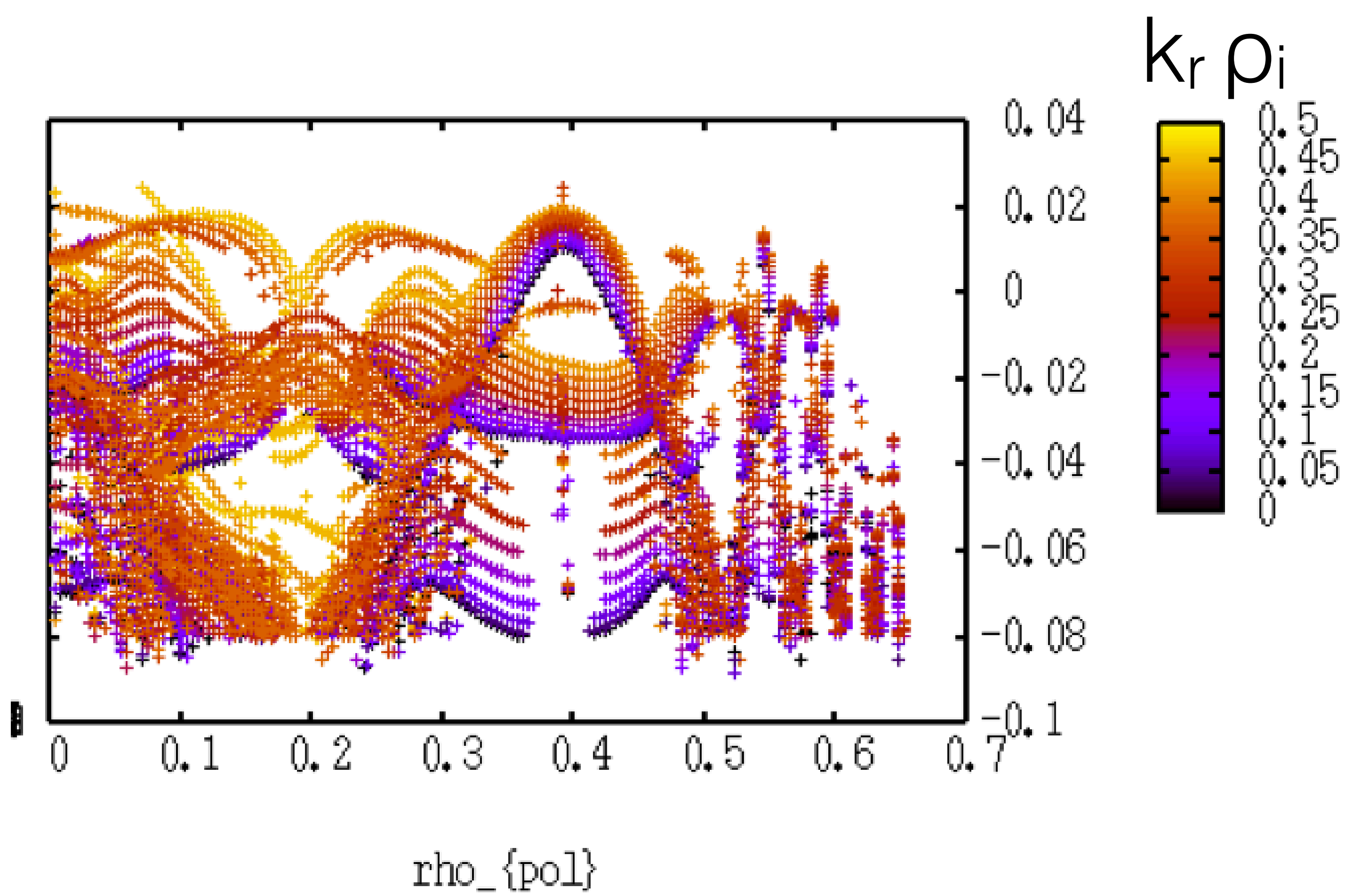

similar to radial GAM propagation studies

[Zonca 2008, Qiu, 2009,Smolyakov 2009, Sasaki, Miki&Idomura 2015, Palermo 2017, etc..]

discharges with the same total heating power

ASDEX Upgrade

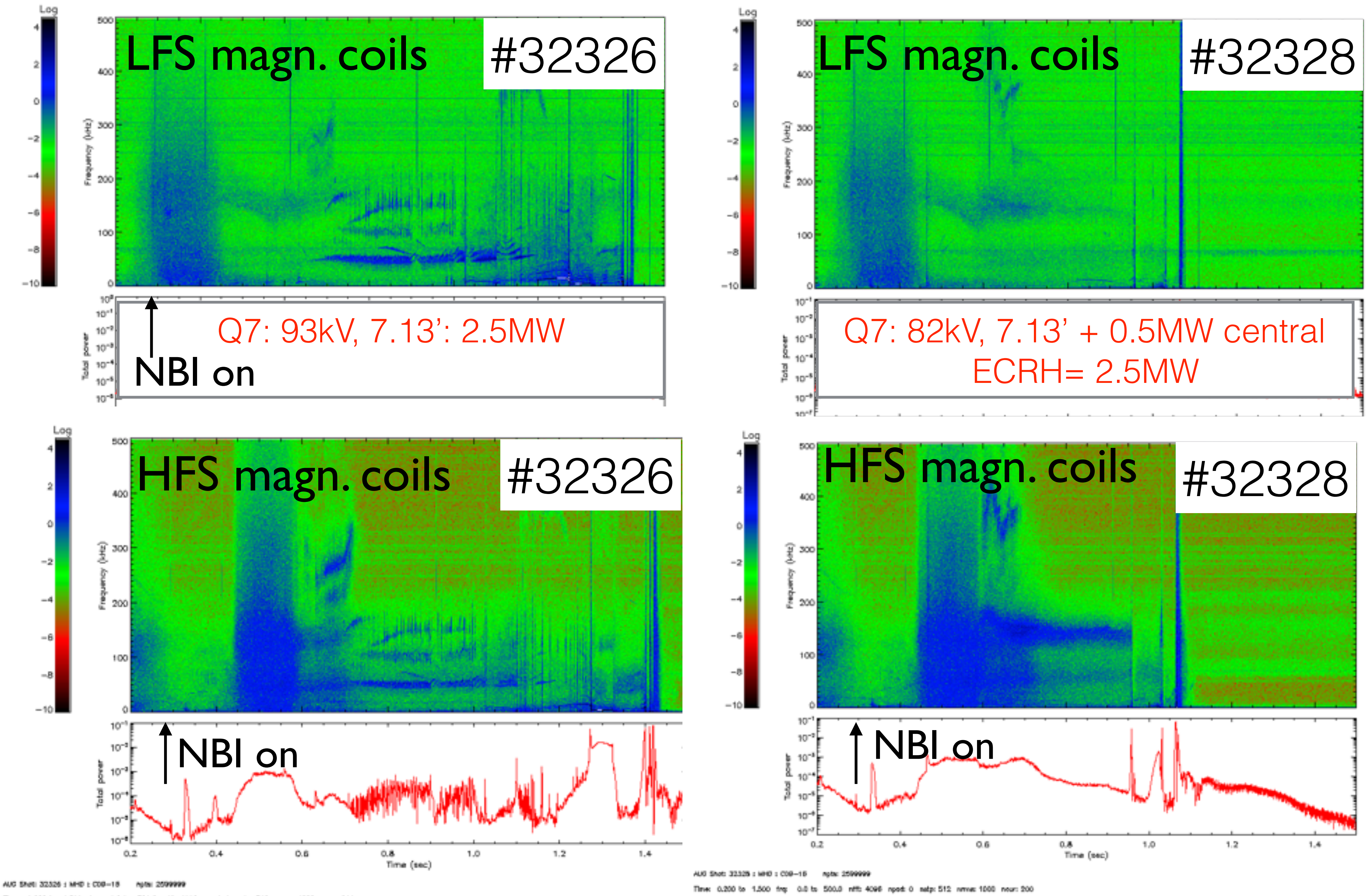

32326(NB) vs 32328 (NB+ECRH) : profiles

ASDEX Upgrade

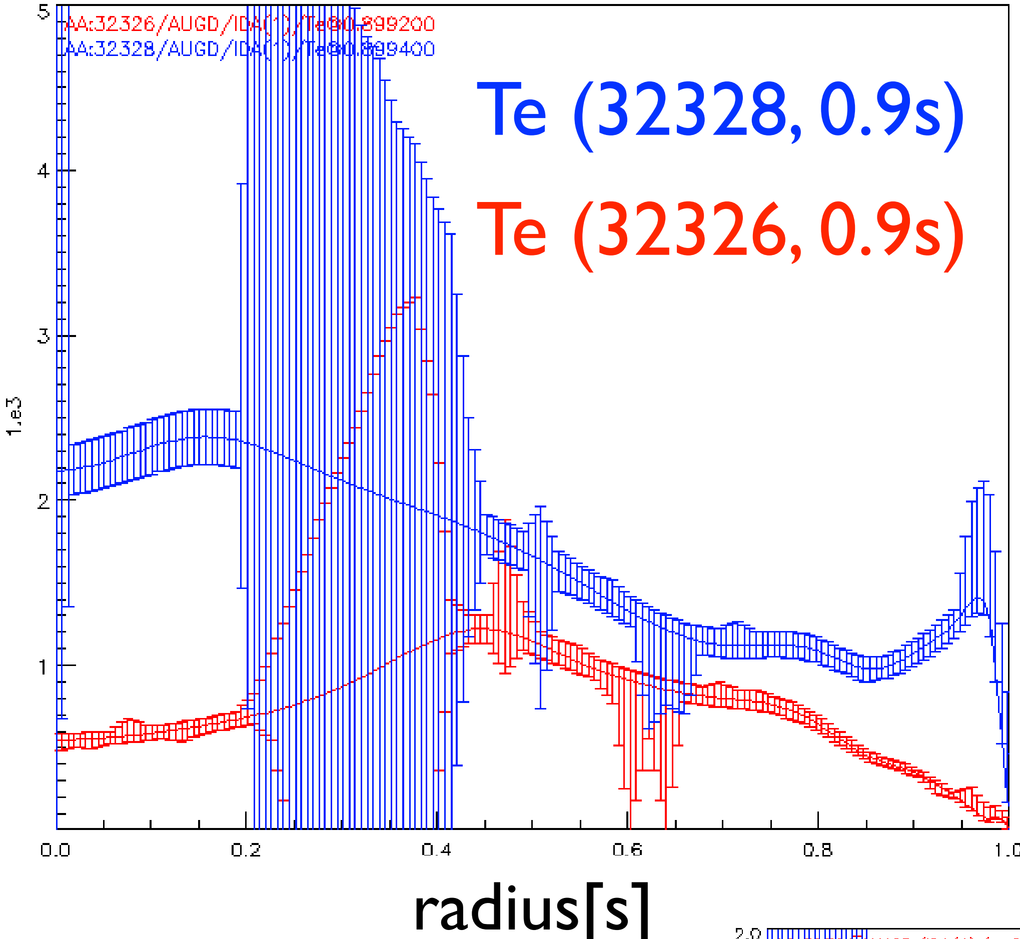

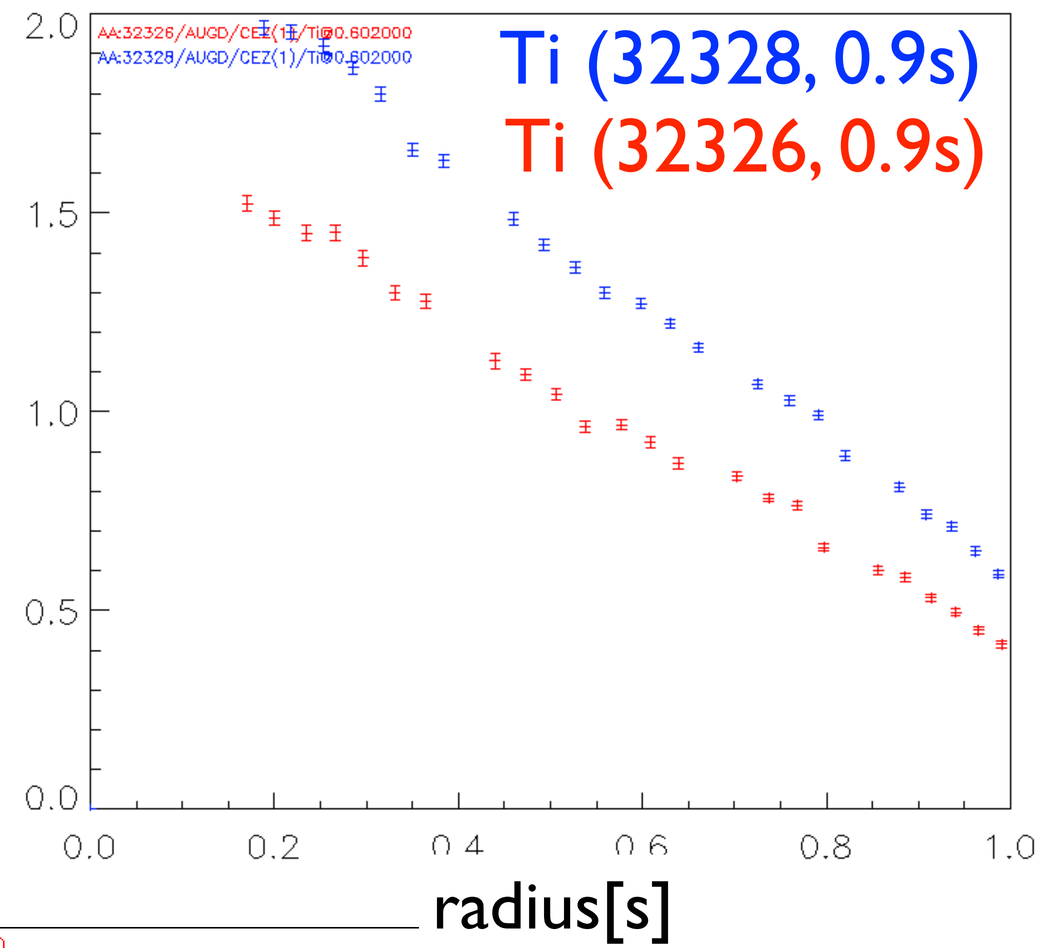

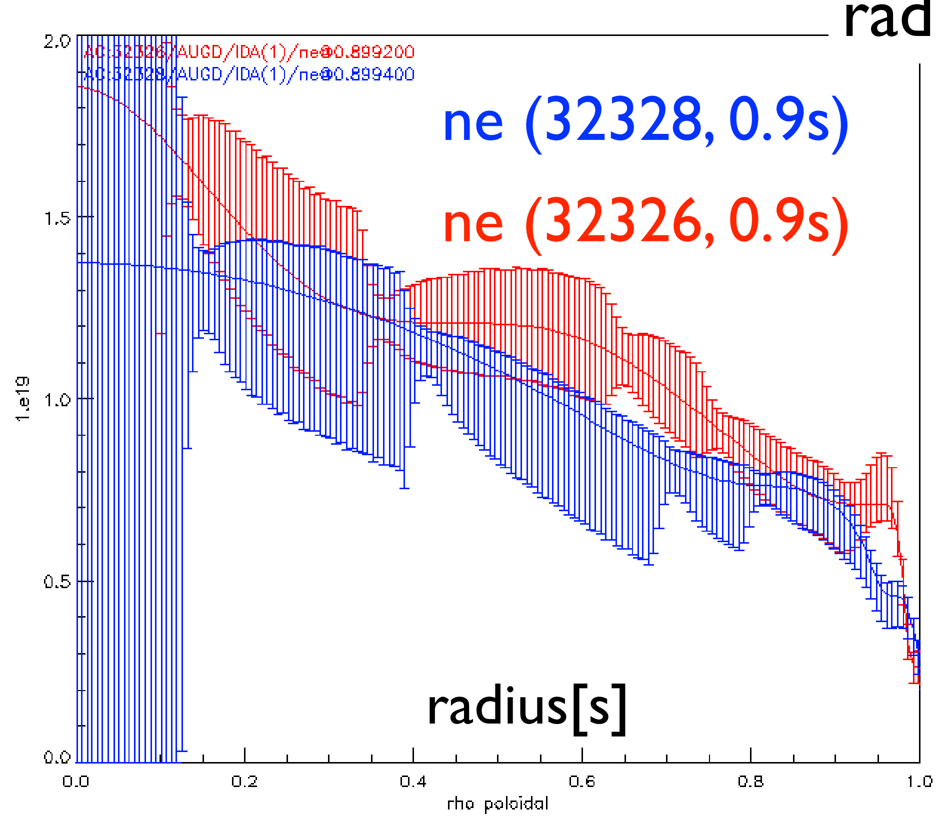

opportunity to investigate plasmas with $\beta_{EP} \sim \beta_{back}$

AND

$\nu_{EP}/\nu_{back} \sim 100!$

Comparison of:

discharge with and without EGAM/TAE/ W accumulation

very different turbulent spectrum magnetic coils HF side

although R/L_{Ti} is quite similar

is this due to modes?

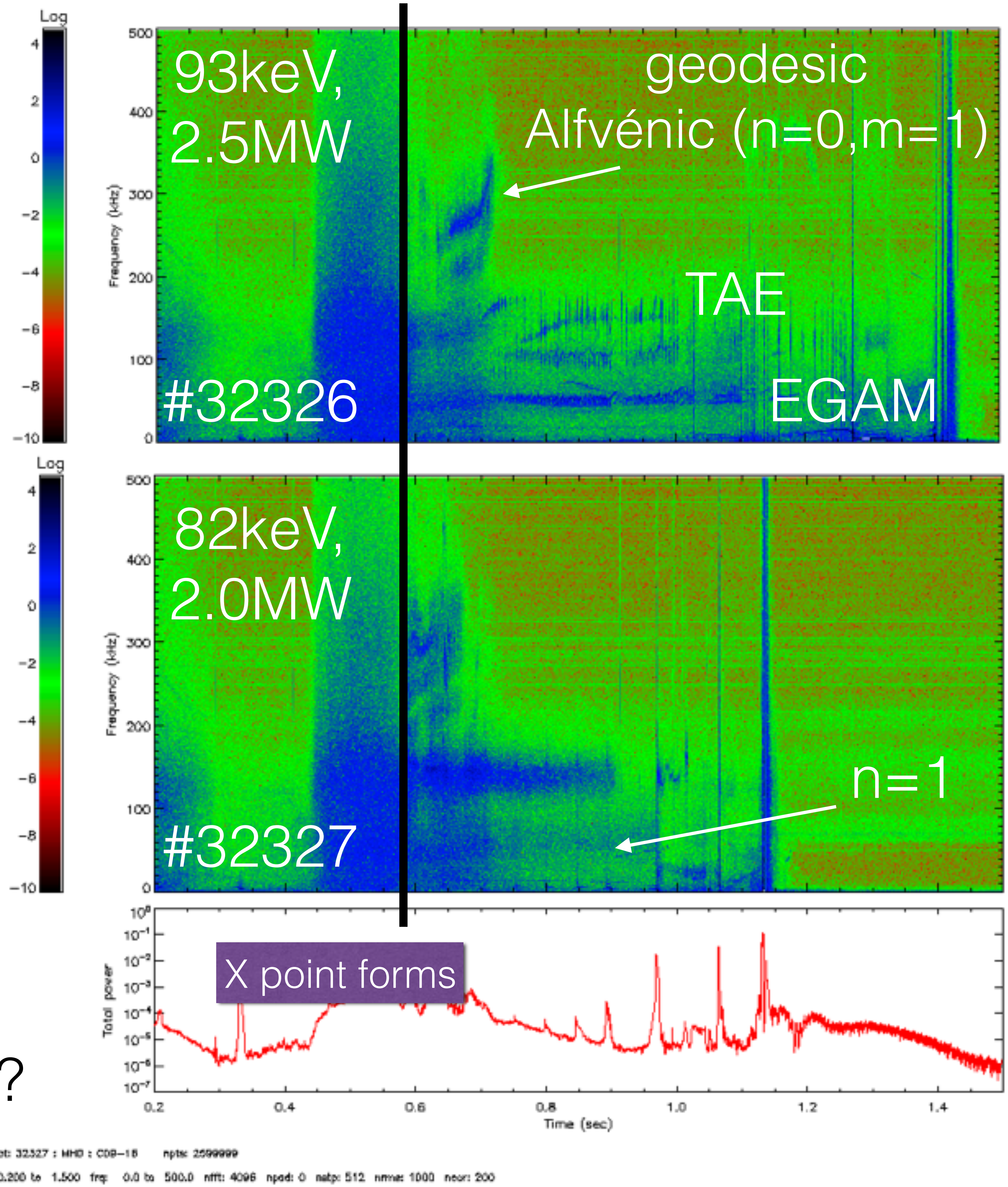

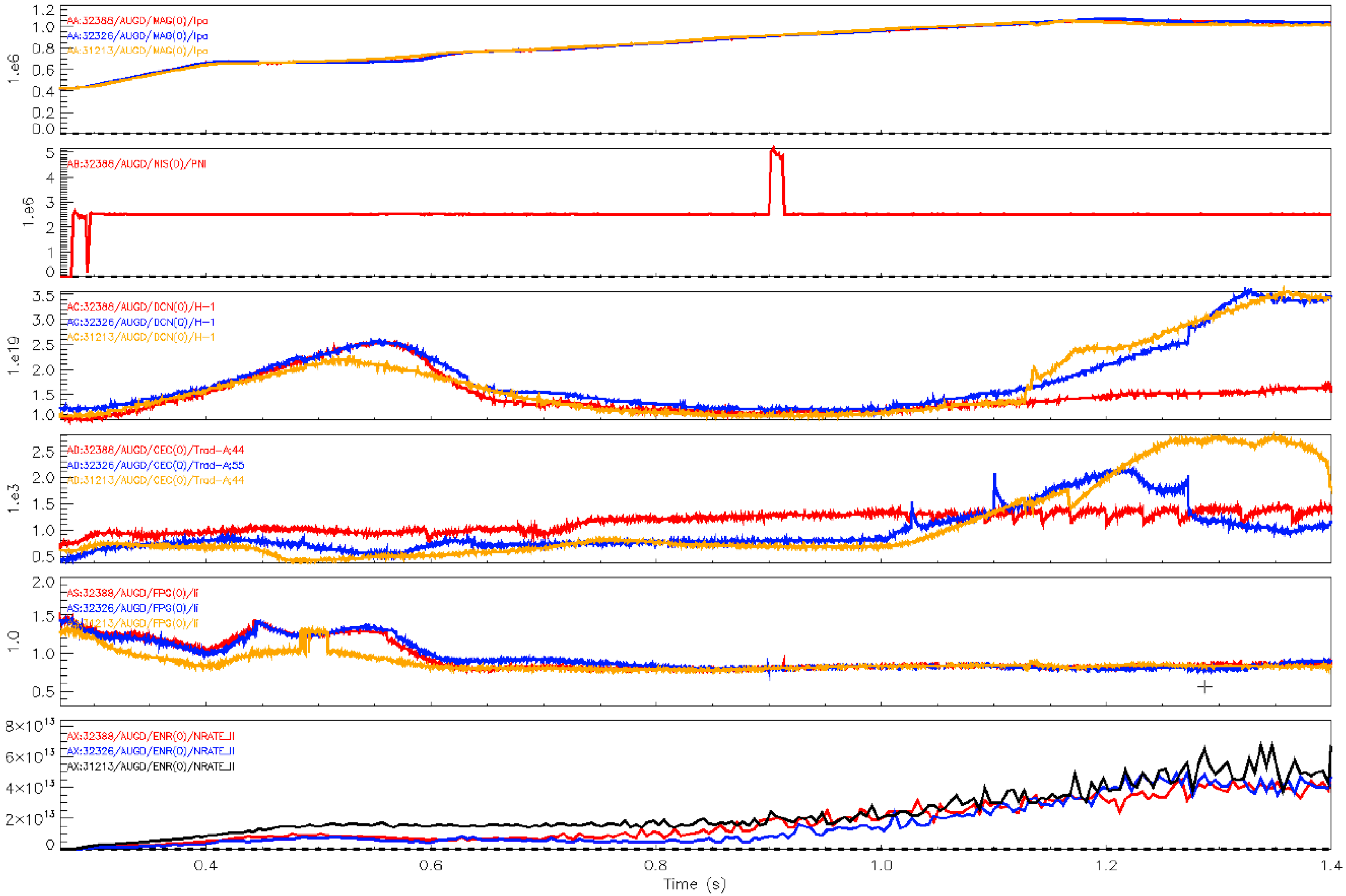
AA:32388/AUGD/MAG(0)/Ipa
AA:32326/AUGD/MAG(0)/Ipa
AA:31213/AUGD/MAG(0)/Ipa
1.e6
AB:32388/AUGD/NIS(0)/PNI
1.e6
AC:32388/AUGD/DCN(0)/H-1
AC:32326/AUGD/DCN(0)/H-1
AC:31213/AUGD/DCN(0)/H-1
1.e19
AD:32388/AUGD/CEC(0)/Trad-A;44
AD:32326/AUGD/CEC(0)/Trad-A;55
AD:31213/AUGD/CEC(0)/Trad-A;44
1.e3
AS:32388/AUGD/FPG(0)/li
AS:32326/AUGD/FPG(0)/li
AS:31213/AUGD/FPG(0)/li
1.0
AX:32388/AUGD/ENR(0)/NRATE_II
AX:32326/AUGD/ENR(0)/NRATE_II
AX:31213/AUGD/ENR(0)/NRATE_II
Time (s)

ASDEX Upgrade

#	EGAM/BAE/	NBI	angle	behav	later heating		I	B
27923	y/y/y/n	2:0.35-0.5;3:0.38-0.59;80.59-0.63;5:0.63-0.76;7:0.76	6,65					
28880	n/y/y/n	2:0.35-0.5;3:0.5-0.6;7:0.6	6,65				I	2,4
28881	y/y/y/n	2:0.35-0.5;3:0.5-0.6;7:0.6	6,65				I	2,4
28883	n/y/n/n	2:0.35-0.5;3:0.5-0.6;7:0.6	6,65					2,4
28884	y/y/y/n	3:0.5-0.6;7:0.6	6,65				I	2,4
28885	y/y/y/n	2:0.35-0.5;3:0.5-0.6;7:0.6	6,65				I	2,4
30383	y/y/y/n	7: 0.26-0.75	6,65	Hmode		FILD FHA FIPM 09	I	2,6
30945	n/y/n/n	2:0.28-0.376;6:0.382-0.697	6,65	dis@4s			I	2,2
30946	y/y/n/y	2:0.28-0.445;6:0.451-0.928	6,65	Lmode	no heating!	later TAE???	I	2,2
30947	y/n/n/y	2:0.28-0.478;6:0.482-0.928	6,65	dis@4s	H mode	EGAM @1s 100kHz	I	2,2
30948	n/y/y/n	2:0.28-0.491;3:0.497-0.789	6,65	dis@1.2s	Q6@0.789		I	2,2
30949	y/y/n/n	2:0.35-0.5;3:0.38-0.79;6:0.79;7:1.0;8:1.2	6,65	dis@1.5		late EGAMs	I	2,2
30950	y/y/y/n	3:0.28-0.295;7:0.312-0.797	6,65	dis@1.5	3:0.8-0.92;6,8@0.9		I	2,2
30951	n/y/n/n	3:0.28-0.295;5:0.312-0.552,8	6,65	dis@1.7	8-0.84;3:-0.99		I	2,2
30952	y/y/y/n	3:0.28-0.295;7:0.312-0.797	6,65	dis@1.18	Q6@0.8		I	2,2
30953	y/y/n/n	3:0.28-0.295;6:0.312-0.753	6,65	dis@1.11	Q2@0.76++		I	2,2
31213	y/y/y/n	3:0.28-0.295;7:0.296-1.033	7,13	dis@1.7	Q6@1.0		I	2,2
31214	y/y/y/n	3:0.28-0.295;7:0.296-1.033	6,05	dis@1.0			I	2,2
31215	y/y/y/n	3:0.28-0.295;7:0.296-1.033	6,65	dis@1.0			I	2,2
31216	y/y/y/n	3:0.28-0.295;7:0.296-3.045+blips	6,65	Lmode		q=2 and qa>4!	I	2,2
31233	y/y/y/n	3:0.28-0.501;7:0.506-3.227	7,13	Hmode	Q6@1.0		I	2,2
31234	y/n/y/n	3:0.28-0.310;7:0.318-0.813	7,13	dis@ 0.8			I	2,2
32326	y/n/y/y	7: 0.28 +blips	7.13	EGAMS, TAEs			I	2.2
32327	y/n/y/n	7: 0.28 +blips: 82kV	7.13	transition			I	2.2
32328	n/n/n/n	7: 0.28 +blips +0.5 ECRH	7.13	only turbulence			I	2.2
32329	n/n/n/n	7: 0.28 + blips+0.5 ECRH	7.13	only Alfvenic turb			I	2.2
32384	y/n/y/n	7: 0.28 +blips 93kV	7.13	too high density			I	2.2
32386	y/n/n/n	7: 0.28 +blips: 65kV	7.13				I	2.2
32387	y/n/y/y	7+6: 0.28 +blips: 65kV	7.13				I	2.2
32388	y/y/y/y	7: 0.28 +blips + higher density 93kV	7.13				I	2.2
33872	y/y/y/y	7: 0.28 +blips + higher density 93kV	7.13		diff breakdown	no Te inversion		2.2
33873	y/y/y/y	7: 0.28 +blips + higher density 93kV	7.13		diff breakdown	no Te inversion		2.5
33874	y/y/y/y	7: 0.28 +blips + higher density 93kV	7.13	dis@1.0	std brkdwn	no Te inversion		2.0
33875	y/y/y/y	7: 0.28 +blips + higher density 93kV	7.13	dis@1.0s	std brkdwn	no Te inversion		2.2
34184	y/y/y/y	7: 0.28 +blips + higher density 93kV	7.13	shape scan t>0.8		Te inversion		2.2
34185	y/y/y/y	7: 0.28 +blips + higher density 93kV	7.13	shape scan t>0.8		Te inversion		2.2
34186	y/y/y/y	7: 0.28 +blips + higher density 93kV	7.13	std		Te inversion		2.2
34187	y/y/y/y	7: 0.28 +blips + higher density 93kV	6.65	std		Te inversion		2.2

comparison to reference discharge (#32388/#34185)

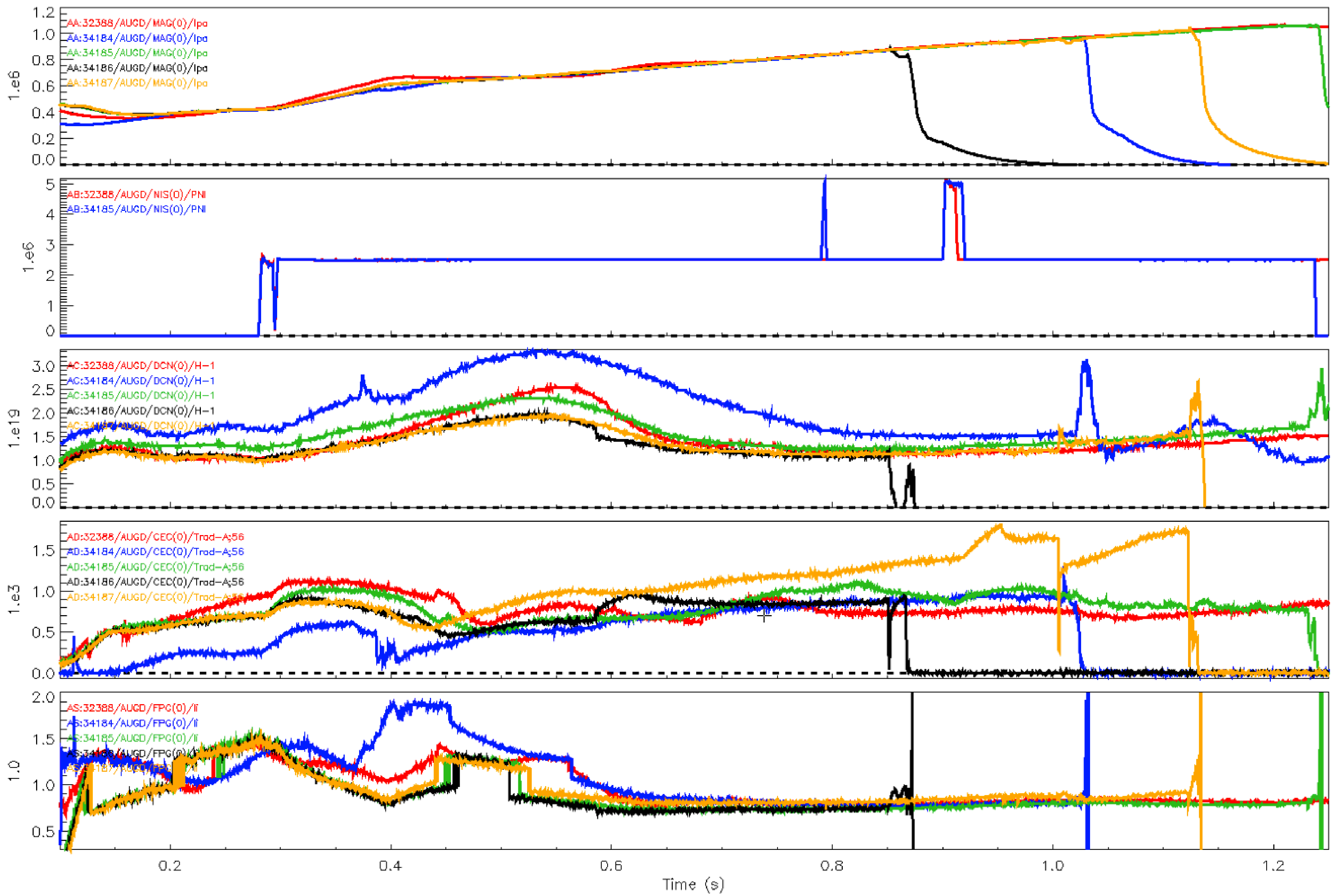

32326(NB) vs 32328 (NB+ECRH)

ASDEX Upgrade